ASPECTS OF BIO-ENGINEERING OF HUMAN SKIN: TOWARDS CLINICAL APPLICATION

DISSERTATION

ZUR

ERLANGUNG DER NATURWISSENSCHAFTLICHEN DOKTORWÜRDE

(DR. SC. NAT.)

VORGELEGT DER

MATHEMATISCH-NATURWISSENSCHAFTLICHEN FAKULTÄT

DER

UNIVERSITÄT ZÜRICH

VON

FABIENNE HARTMANN-FRITSCH

VON

WORB BE

PROMOTIONSKOMITEE

PROF. DR. LUKAS SOMMER (VORSITZ)

PROF. DR. MARTIN HERSBERGER

PROF. DR. ERNST REICHMANN (LEITUNG DER DISSERTATION)

ZÜRICH, 2013

This work has been performed under the supervision of Prof. Dr. Ernst Reichmann at the Tissue Biology Research Unit, Department of Surgery, University Children's Hospital Zurich, Zurich, Switzerland.

TABLE OF CONTENTS

1. SUMMARY

Skin is the largest organ of the human body and protects it from detrimental effects of the surrounding environment. As skin is directly exposed to the outer environment, it frequently occurs that it is destroyed by accidents. Large full-thickness skin defects may result from burns but also from the surgical excision of congenital giant nevi or scar tissue. The treatment of large (> 40% total body surface area) full-thickness wounds represents a major challenge, as donor sites for autologous skin transplantation often are very limited, and transplantation of autologous split-thickness skin (the present gold standard of treatment) can lead to severe scarring, especially in children. These problems could be significantly reduced applying a bio-engineered autologous dermo-epidermal skin substitute. The Tissue Biology Research Unit (TBRU) has shown that collagen type I hydrogels are a promising scaffold for skin tissue engineering in pre-clinical models. As collagen hydrogels show weak mechanical properties, the first part of my work aimed on engineering human dermo-epidermal skin substitutes based on collagen type I hydrogels which were stabilised by both, plastic compression (established by a postdoctoral fellow in our team) and incorporated biodegradable meshes (established by me). I applied two different meshes of synthetic polymers to mechanically stabilise the collagen hydrogel. I was able to generate skin substitutes which developed into a near normal skin with a dermal compartment and a stratified epidermis *in vitro* and *in vivo* using a rat model.

Another aspect of skin tissue engineering and the second part of my work concerns the youngest patients possible, the unborn human fetus. Fetal surgery to treat spina bifida has been convincingly demonstrated to markedly improve the perspectives of the patients. However, closure of skin defects of a fetus is a challenge, and in such cases engineered autologous fetal skin might help. In a first step towards engineering fetal skin, I could successfully apply human amniotic fluid derived cells in the dermal compartment of dermo-epidermal skin analogues, instead of the usually used human dermal fibroblasts, and succeeded in obtaining a well stratified, near normal epidermis.

Bio-engineered dermo-epidermal skin substitutes could serve, additionally to their clinical application, for pre-clinical testing of newly designed medicinal products.

I therefore aimed in a third part of this work to evaluate whether the engineered skin substitutes can be used for pre-clinical testing of products designed for dermal regeneration.

As clinical application of bio-engineered dermo-epidermal skin substitutes is a major goal of the TBRU, we last but not least aimed to fulfil all pre-clinical studies required for clinical trials. As the rat animal system only allows the transplantation of small, circular skin substitutes, we aimed in establishing a large animal model to proof the principle also in clinical relevant size and shape. Porcine skin shows the highest similarities to human skin and with this newly designed pig model transplantation of large, square autologous skin substitutes are possible.

2. ZUSAMMENFASSUNG

Die Haut ist das grösste Organ des menschlichen Körpers und schützt ihn vor schädlichen Umwelteinflüssen. Da die Haut direkt der Umwelt ausgesetzt ist, sind Verletzungen der Haut durch Unfälle häufig. Grossflächige tiefe Hautwunden können bei Verbrennungen entstehen, oder aber auch bei der chirurgischen Entfernung von grossen angeborenen Nävi oder Narbengewebe. Die Behandlung von grossflächigen (> 40% der gesamten Körperoberfläche) tiefen Hautwunden stellt eine grosse Herausforderung dar, da Donorstellen für die Transplantation von autologer Haut häufig sehr limitiert sein können. Zudem kann die Transplantation von autologer Spalthaut, dem heutigen Goldstandard zur Behandlung, zu starker Narbenbildung führen. Dies wird vor allem bei Kindern häufig beobachtet. Diese Probleme könnten mit der Anwendung eines bio-engineerten autologen dermo-epidermalen Hautersatzes signifikant vermindert werden. Die Tissue Biology Research Unit (TBRU) hat gezeigt, dass Hydrogele aus Kollagen Typ I eine vielversprechende Grundlage für die Herstellung von Hautsubstituten für präklinische Modelle sind. Da Hydrogele aus Kollagen aber schwache mechanische Eigenschaften haben, war das Ziel des ersten Teiles meiner Arbeit die Herstellung eines humanen dermo-epidermalen Hautsubstitutes basierend auf einem Kollagen Typ I Hydrogel, welches sowohl durch plastische Kompression (entwickelt von einen Postdoktoranden aus dem Team) als auch mit einem biodegradierbaren Netz (von mir entwickelt) mechanisch stabilisiert wird. Ich habe zwei verschiedene Netze aus synthetischen Polymeren angewandt, um die Kollagengele zu stabilisieren. Damit konnte ich Hautsubstitute herstellen, welche sich sowohl *in vitro* als auch *in vivo* in einem Rattenmodell zu einer fast normalen Haut mit einem dermalen Kompartiment und einer stratifizierten Epidermis entwickelt haben.

Ein weiterer Aspekt der Hautersatzforschung, und der zweite Teil meiner Arbeit, betrifft die jüngst möglichen Patienten, nämlich die ungeborenen menschlichen Feten. Es wurde überzeugend gezeigt, dass fetale Chirurgie für die Behandlung von Spina bifida die Aussichten der Patienten enorm verbessert. Das Schliessen eines Hautdefektes eines Fetus ist jedoch häufig eine Herausforderung und in solchen Fällen würden Hautsubstitute aus fetalen Zellen helfen. In einem ersten Schritt in Richtung eines fetalen Hautsubstitutes konnte ich erfolgreich

humane Zellen aus Amnionflüssigkeit in das dermale Kompartiment eines dermo-epidermalen Hautsubstitutes einbringen, anstelle der üblicherweise verwendeten humanen dermalen Fibroblasten. Auch diese Hautsubstitute entwickelten eine gut stratifizierte Epidermis mit Eigenschaften ähnlich einer normalen Epidermis.

Bio-engineerte Hautsubstitute aus dem Labor könnten, zusätzlich zu einer klinischen Anwendung, auch für präklinische Studien für neu entwickelte Medizinalprodukte genutzt werden. Deshalb habe ich in einem dritten Teil dieser Arbeit evaluiert, ob die hergestellten Hautsubstitute für präklinische Tests für Produkte verwendet werden können, welche für die dermale Rekonstruktion entwickelt wurden.

Die klinische Anwendung der bio-engineerten dermo-epidermalen Hautsubstitute ist ein Hauptziel der TBRU. Daher war ein weiteres Ziel dieser Arbeit alle präklinischen Studien abschliessen zu können. Mit dem Rattenmodell können nur kleine, zirkuläre Hautsubstitute transplantiert werden. Unser Ziel war deshalb ein neues Tiermodell zu etablieren, welches die Transplantation von Hautsubstituten in klinisch relevanter Grösse und Form erlaubt. Die Haut von Schweinen weist die grösste Ähnlichkeit zu humaner Haut auf und mit dem neu etablierten Schweinemodell können grosse, rechteckige autologe Hautsubstitute transplantiert werden.

3. INTRODUCTION

3.1 Human skin

Human skin is the boundary of the human body to the environment. As such, skin has the most important role in protecting the body from environmental influences and maintaining the internal milieu, and therefore needs to resist the potentially harmful environmental influences. Amongst its wide range of functions, there are very diverse functions such as:

- Anatomical barrier against irradiation, chemicals, physical forces, pathogens and microorganisms
- Mediator of immune reactions via Langerhans cells that take up antigens and provide immunity by interacting with T cells
- Help in thermoregulation via sweat secreting sweat glands and dilatation or contraction of blood vessels as response to heat/cold
- Sensory function
- Production of vitamin D via its synthesis from 7-dehydrocholesterol with the help of UV light

In mammals, skin represents the largest organ. In adult humans it measures between 1.5 m^2 and 2 m^2 and weighs approximately 15% of the total body weight. Depending on the area of the body, the skin shows different characteristics which are adapted to the special needs of the local area, e.g. the thickness of the skin, which varies from 1 mm to 4 mm, and the distribution of skin appendages such as hairs, sweat glands and sebaceous glands (1). The outermost layer of the skin (Figure 1), which is in direct contact with the environment, is the stratified and keratinised epidermis. This layer contains no blood vessels and the cells of the epidermis, mainly keratinocytes, are nourished and supported by the underlying dermis, which is a collagen-rich connective tissue. The dominant cell type in the dermis is the fibroblast. The skin appendages such as hair follicles and sweat glands derive from the ectoderm, but reach down deep into the dermis. Underneath the dermis, the

subcutaneous tissue mainly consists of adipose tissue. This tissue serves as a protection from injuries with its function as a cushion, serves as energy supply and insulates the body (2-3).

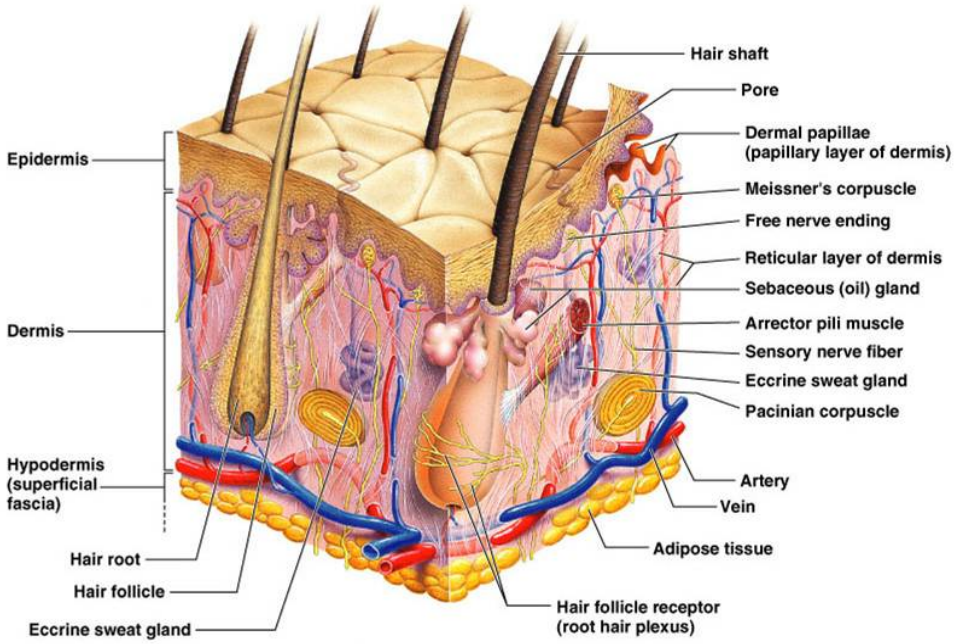

Figure 1: The composition of human skin. Schematic view of the composition of the human skin, showing the two main layers as well as the most important skin appendages. (4)

3.1.1 Epidermis

The epidermis is a stratified epithelium. The main cell type of the epidermis, constituting about 90-95% of it, is the keratinocyte. Other cell types in the epidermis are melanocytes, Langerhans cells and Merkel cells. The epidermis undergoes constant renewal by the keratinocytes. Keratinocyte stem cells in the basal cell layer of the epidermis give rise to new keratinocytes which then, while undergoing additional steps of differentiation, migrate through the different epidermal layers towards the epidermal surface, until they reach the outermost layer as flattened, dead cells that are shed from the surface (1). The average thickness of the epidermis is about 100 µm, but high variations can be seen depending on their location in the body. The epidermis of palms and soles can be up to 1 mm thick, whereas the epidermis of the eyelid is only 50 µm thick.

Keratinocytes

Keratinocytes (Figure 2) are the main cell type of the epidermis. They originate from the ectoderm and are arranged in the epidermis in continuous layers.

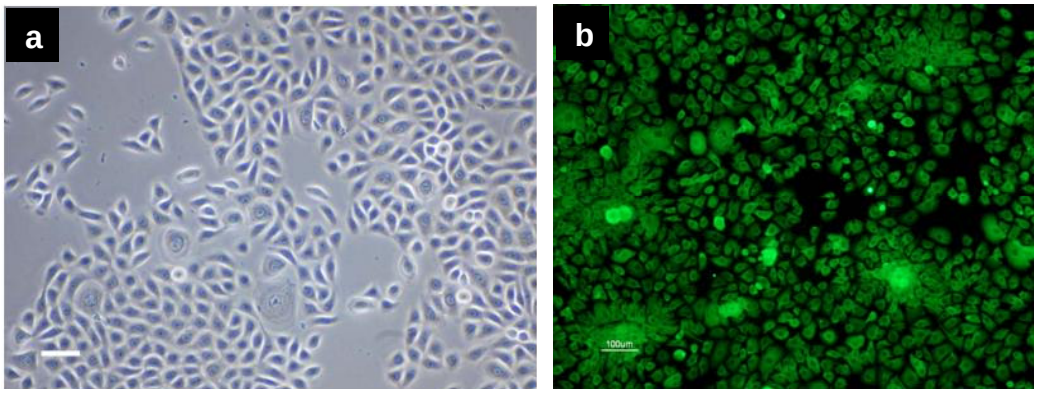

Figure 2: Human keratinocytes in culture. The typical appearance of human primary epidermal keratinocytes on cell culture plastic visualised by

a) light microscopy and

b) immunofluorescence staining. The cells are positive for the human cytokeratin marker K5 (green). Scale bars 50 µm (a), 100 µm (b). (Figure b from L. Pontiggia)

They show specific differentiation characteristics and morphology depending on their exact location within the different layers of the epidermis (Figure 3). Keratinocytes from the basal layer show a columnar morphology with an average size of 6-10 µm and a large nucleus, whereas keratinocytes from the stratum spinosum are larger with a size of 10 - 15 µm and polygonal in shape. The flattened keratinocytes from the granular layer have a diameter of 25 µm and are arranged parallel to the skin surface. The keratinocytes of the stratum corneum lost their nucleus, show a hexagonal shape when viewed from above and have a diameter of 30-40 µm. (1,5)

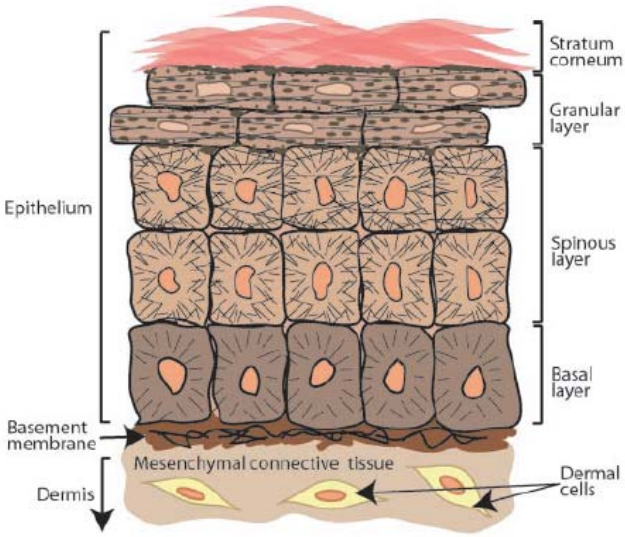

Figure 3: Schematic overview on the strata of the human epidermis. (6)

Other cell types of the epidermis

Melanocytes are neural crest-derived cells that reside in the basal layer of the epidermis at a ratio of about one melanocyte per five keratinocytes. They produce the skin pigment melanin, which is stored in melanosomes. The melanosomes are transported via dendrites and transferred to keratinocytes of the upper strata. One melanocyte supplies about 36 keratinocytes with melanin. In the keratinocytes, the melanin is located supra-nuclear to protect the nucleus from UV-light. Interestingly, the different skin colours seen in different ethnic groups do not result from different melanocyte numbers, but are a result of variations in melanocyte activity and most importantly variations in the ratio between the two main forms of melanin, the eumelanin and pheomelanin. (7)

3-6% of the cells of the epidermis are the mobile **Langerhans cells** which are constituents of the immune system. They originate from haematopoietic precursors of the bone marrow and show a rounded morphology with dendrites. They reside in the epidermis as immature cells, which mature upon contact with an exogenous antigen. They take up the antigen, process it and present it in regional lymph nodes to naive T-cells (8).

Merkel cells reside in the basal layer of the epidermis and are involved in sensory transduction. Their density is highly variable with a maximum in palmo-plantar skin. They form synaptic junctions with dermal sensory axons (9).

Keratins

Keratins constitute up to 85% of a fully differentiated keratinocyte. These proteins are a type of intermediate filaments. Intermediate filaments are one class of the three major cytoskeletal proteins of eukaryotic cells (Table 1). They give structure and stability to the keratinocytes and are responsible for the mechanical strength of the vertebrate epidermis (10). In addition to their importance as cytoskeletal elements, recent studies showed that some keratins also have regulatory functions in intracellular signalling pathways, such as stress protection, wound healing and apoptosis, which suggest that they are involved in the refinement of epithelial functions (11-14). To fulfil all these functions, the cytoskeletal network they form is very dynamic and in a constant cycle of keratin intermediate filament assembly and disassembly (15-17). Certain mutations in keratin intermediate filaments are known to lead to blistering diseases (18).

Table 1: Cytoskeletal proteins. Overview on the three main groups of cytoskeletal proteins found in eukaryotic cells. (19)

Cytoskeleton class	Fibre diameter	Main function	Examples
Actin filaments	6 nm	Cell motility	Actin
Intermediate filaments	10 nm	Cell structure	Keratins, vimentin, nuclear laminins
Microtubules	23 nm	Intracellular transport, mitotic spindle	α-tubulin, β-tubulin

Keratins can be divided in two families based on their pH value. The acidic keratins type I include the keratins K9-K20 and four hair keratins (Ha1-Ha4). The group of the basic keratins type II includes the eight epithelial proteins K1-K8 and four hair keratins (Hb1-Hb4) (18). All the keratins share common protein-structural characteristics. The central α-helical rod domain (~310 amino acids) is flanked by non-helical head and tail domains of variable lengths. The first step in the assembly of keratin intermediate filaments is the formation of heterodimers, built from a type I keratin and a type II keratin, where the central rod domains are arranged in a parallel way. Two of these dimers assemble into a protofilament, and two protofilaments

interact to form the protofibril. Finally, four protofibrils form the 10 nm intermediate filament (Figure 4) (14,18).

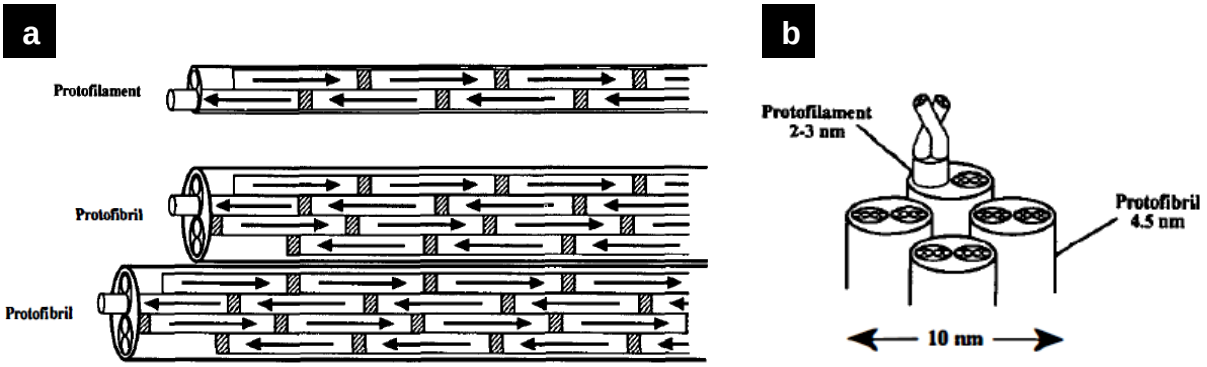

Figure 4: Intermediate filaments. Schematic representation of the alignment of the subunits of an intermediate filament.

a) The arrows indicate the direction of the polypeptides. (20)

Pairs of type I and type II keratins are expressed in most epithelial cells, whereas the type of pair is specific for the stages of development, differentiation and the body location. A summary of the most important keratins that can be found in human skin with their expression site is shown in Table 2. The keratins K8 and K18 are the first keratins that appear in embryogenesis and they only can be found in the single-layered epithelium in a mammal embryo but not in adult, fully stratified human epidermis. (14,18,20)

Table 2: Keratins. Overview of the most important keratins in human skin and their expression site. (14,18,20)

Keratin	Expression site	Main partner
K1	Suprabasally in most body regions	K10
K2e	In granular keratinocytes	K11
K5	In basal cells that maintain their proliferative capacity	K14
K6	Transiently expressed during wound healing in suprabasal cells	K16
K9	Restricted to suprabasal palmar and plantar skin	K1
K10	Suprabasally in most body regions	K1
K14	In basal cells that maintain their proliferative capacity	K5
K15	In a subpopulation of basal cells	K5
K16	Transiently expressed during wound healing in suprabasal cells	K6
K19	In a subpopulation of K15 positive cells in the basal layer	K7

Structure of the human epidermis

The epidermis of the human skin shows four or five distinct layers, depending on the body location. A schematic overview on the different strata of the epidermis is shown in Figure 3.

The **stratum basale** (basal layer) is the layer of the epidermis in contact with the basement membrane. It mainly consists of one layer of tall, columnar, mitotically active keratinocytes. Cells from this layer proliferate to give rise to new keratinocytes that “migrate” upwards through all strata and eventually will be shed from the stratum corneum. The most important keratin filaments in the basal keratinocytes are fine bundles of K5 and K14, which allow enough flexibility for cell division and migration, but also K15 and K19 can be found (18,21). In contrast to many reports, we found that only K15 is exclusively expressed in basal keratinocytes of adult human skin, whereas K5 and K14 are also expressed in suprabasal layers (21). This may be different in mouse skin. In addition to keratinocytes there are also melanocytes in the stratum basale. Both cell types can be found in a ratio of about one (melanocyte) to five (keratinocytes). There are also Langerhans cells and Merkel cells (3,6). The basal keratinocytes are connected to the basement membrane via hemidesmosomes

(Figure 5) (22-23). In hemidesmosomes, the $\alpha_6\beta_4$ integrin heterodimer can be found with several other associated proteins (22,24).

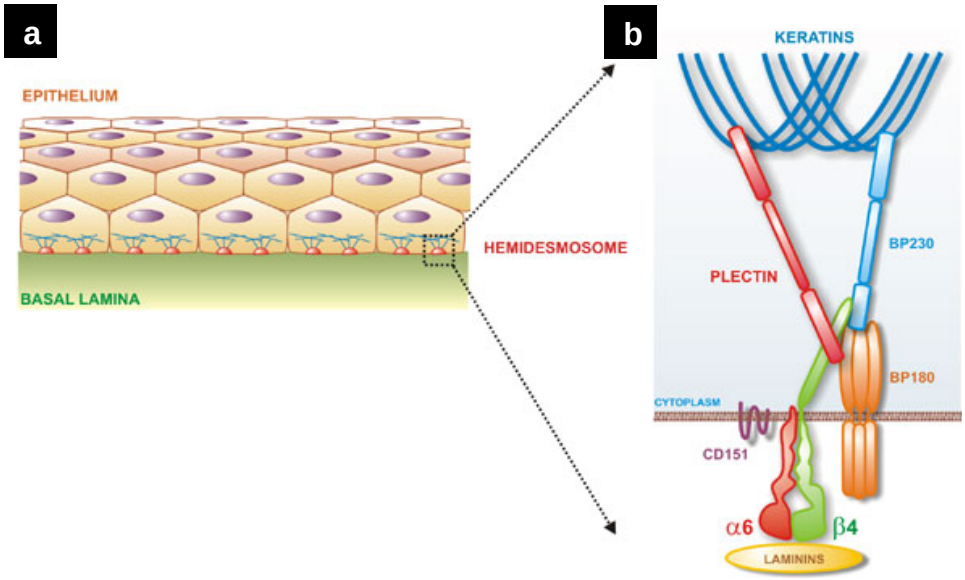

Figure 5: Hemidesmosomes.

a) Schematic overview on the location of hemidesmosomes in epithelia.

b) Schematic model of the organisation of a hemidesmosome showing the protein-protein interactions of the main components. (23)

The layer that gives structure and stability to the epidermis is the **stratum spinosum** (spinous layer). The suprabasal keratinocytes show a polyhedral morphology, whereas the keratinocytes in the upper layers of the stratum spinosum show a larger, flattened morphology. Additionally, the upper keratinocytes can already contain lamellar granules. The keratins in this stratum are present in thick bundles, which are organised concentrically around the nucleus and connect to the cytoplasmic plaques of the desmosomes (3). Cells in this layer adhere to each other via desmosomes (Figure 6) (22). These calcium-activated structures are composed of desmogleins and desmocollins, both belonging to the superfamily of cadherins (25). The types of desmogleins and desmocollins expressed in a desmosome depend on the localisation of the desmosome within a stratified epithelial sheet. In the lower spinous layers desmoglein 3 and desmocollin 3 can be found, whereas in the upper spinous layers the desmoglein and desmocollin types 1 are most expressed. Basal cells express mainly desmoglein 2 and desmocollin 2 (22). Desmosomes connect inside the cell to the keratin filaments through a series of

adaptor molecules. Desmogleins and desmocollins connect to plakoglobin. Plakoglobin binds to desmoplakin which associates with the intermediate filaments (Figure 6). For maximal stability and cohesion, the desmogleins of a given cell attach to the desmocollins of the neighbouring cells (22,25).

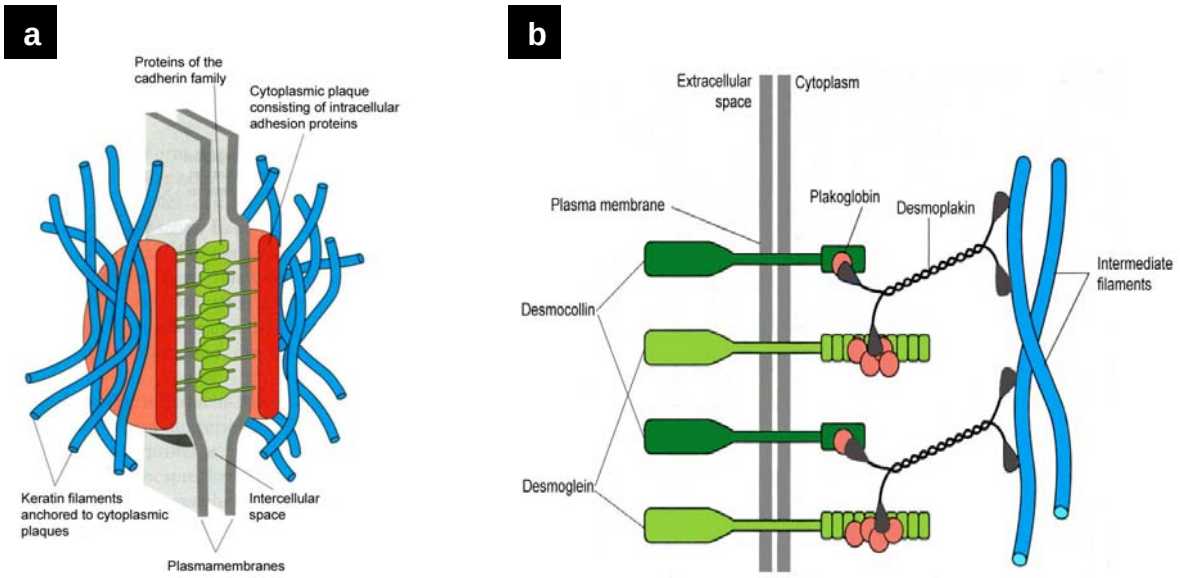

Figure 6: Desmosomes.

a) Structural elements of a desmosome. The cytoplasmic plaques (red) consist of intracellular anchor proteins. Keratin intermediate filaments (blue) are shown at the surface of the plaques. Transmembrane anchor proteins of the cadherin family (green) attach to the plaques and join cells to one another.

b) Scheme of a desmosome showing the protein-protein interactions of its main components. Desmogleins (light green) and desmocollins (green) associate with plakoglobins (red) in the cytoplasm. Plakoglobins bind to desmoplakins (black), which in turn bind to intermediate filaments (blue). Modified from (19)

The **stratum granulosum** (granular layer) consists of keratinocytes that are stratified and squamous. The cells are arranged in one to three layers and they contain the name-giving lamellar granules, organelles with a diameter of 100-300 nm. The lamellar granules contain precursors of the stratum corneum lipids, enzymes, and components needed for desquamation. They fuse with the plasma membrane and release the content to form a lipid-containing membrane that helps to maintain the impermeable skin barrier. The stratum granulosum is prominently formed in the skin of palms and soles. (3,26)

Only in the thicker skin of palms and soles, the transparent **stratum lucidum** can be found, which is built by three to five layers of dead, flat keratinocytes. These keratinocytes are filled with the clear protein eleidin, an intermediate form of keratin. This stratum serves as an additional barrier at these most exposed sites and enhances the impermeability of skin. (27)

The outermost layer, facing the environment, is the **stratum corneum** (cornified cell layer). This stratum of about 15-20 cell layers mainly consists of dead, flattened terminally differentiated keratinocytes (corneocytes) (28). The stratum corneum prevents water loss through its structure and the lipid matrix, and serves as a barrier to prevent harmful micro-organisms, such as bacteria, from entering the body (29). The thickness of the stratum corneum varies, depending on its localisation on the body. Areas more prone to injuries such as the sole of the feet and the palms of the hands exhibit a thicker stratum corneum, which may consist of up to hundreds of layers (30). 20% of the total mass of this stratum consist of a continuous lipid matrix, in which the terminally differentiated keratinocytes are embedded (31). The major lipid components are ceramides, fatty acids and cholesterol (31-32). 70-80% of the protein mass in these keratinocytes consists of loricrin and involucrin. The cells of the stratum corneum are continuously shed from the surface by a stringently controlled process, and are replaced by new keratinocytes derived from the lower strata (3,29,33). The time a basal cell needs to get up into the stratum corneum is up to four weeks (18). In the stratum corneum, desmosomes are modified to form the corneodesmosomes (34). These structures connect neighbouring corneocytes in the same layer, but also in adjacent layers. They are composed of desmoglein 1 and desmocollin 1 and additionally they contain specialised proteins such as corneodesmosin (35-36). For desquamation, corneodesmosomes are degraded by several hydrolytic enzymes in a specific pattern. (33)

Development of the epidermis

The first ectodermal covering of a human embryo early in gestation is the single-layered structure called periderm (Figure 7). The periderm appears to have a barrier function as tight junctions can be found. Additionally it is suggested that the periderm interacts with the amniotic fluid, as it has surface microvilli. Cells of the periderm are positive for keratin 8 and 18, but also for keratins 6, 16 and 17, which

normally are associated with wound healing and keratinocyte migration (37). During the first six weeks of development the coverage changes into a two-layered structure that consists of the outer periderm and the inner epidermis by receiving signals from the underlying mesenchyme which triggers and defines the program of differentiation. The ectoderm starts to proliferate and stratify. During gestational weeks nine and ten, expression of keratin 1 and keratin 10 can be detected in the epidermal cells. During the same time, other cell types migrate into the skin (38). In particular melanocytes from the neural crest, Langerhans cells from the thymus and bone marrow, and Merkel cells, believed to originate from epidermal keratinocytes (39-40).

Soon after the stratification, during weeks 11-14 of gestation specialised mesenchymal cells called dermal placode cells form a dotted pattern beneath the basal layer. At the positions where these cells have contacted the basal layer of the epidermis, basal cells start to move downwards into the dermis and eventually form a hair follicle (25). Acceleration of the formation of the stratum corneum can be detected during week 20 - 40 of gestation, mainly in specific body sites such as the face, scalp, palms and soles (37-38). During the phase of rapid skin expansion, proliferation can be found suprabasally and not only restricted to basal cells. (25,41).

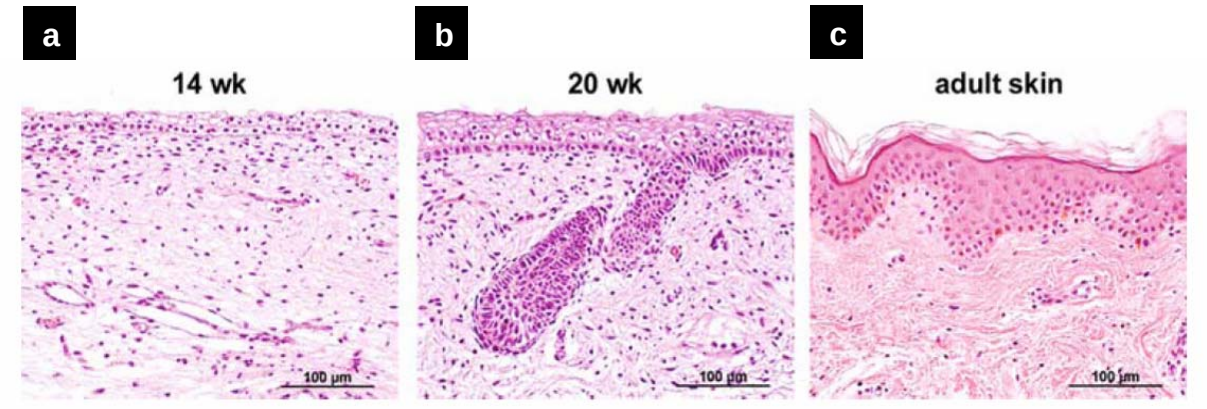

Figure 7: Haematoxylin&Eosin staining of fetal and adult human skin.

a) At week 14 of gestation, a basal layer can be detected as well as an intermediate cell layer and a periderm.

b) The number of intermediate cell layers is increased at week 20 of gestation. Additionally, developing hair follicles are detectable.

c) The adult epidermis is composed of a basal cell layer, followed by the spinous and granular cell layers and the stratum corneum which is the outermost layer. Scale bars 100 µm. (42)

3.1.2 Dermis

The layer of the skin underneath the epidermis is the dermis. This skin layer consists of connective tissue that gives the elasticity and flexibility to the skin via its components, such as collagens, elastin and proteoglycans. This connective tissue is mainly composed of collagen types I and III (7). The dermis is compressible, and rich in blood vessels. It undergoes a continuous change of synthesis and degradation. The space between the fibres and the dermal cells is filled with macromolecules such as glycoproteins and proteoglycans.

The most important cell type of the dermis is the fibroblast. But also cells of the immune system such as macrophages, T and B cells can be found. In addition there are blood vessels, lymphatic vessels and nerves (3). The dermis is innervated by two types of nerves; Parasympathic nerves release acetylcholine to the sweat glands via cholinergic neurons and nerves of the sympathicus nerves release norepinephrine to sweat glands, arteriolar smooth muscles and erector pili muscles (3).

Two main layers of the dermis are identified, namely the papillary and reticular dermis (Figure 8) (43). The papillary dermis is the layer closest to the epidermis and has a variable thickness of approximately 300 - 400 µm, depending on age and anatomical localisation. The papillary dermis forms the dermal papillae, conical projections towards the epidermis. These dermal papillae alternate with the downward projections of the epidermis, the rete ridges. Together these structures markedly increase the area of contact between dermis and epidermis and increase the stability of the dermo-epidermal junction. The collagen fibre bundles in the papillary dermis are thin, poorly organised, and mainly consist of collagen type I and III (44). Elastic fibres found in the papillary dermis are thin and in a vertical orientation to the dermo-epidermal junction. In the papillary dermis of the finger tips, tactile corpuscles can be found which act as mechanoreceptors (1).

The underlying reticular dermis shows collagen bundles which are thick and well organised. These bundles show a parallel orientation to the skin surface. The elastic fibres of the reticular dermis are thicker compared to the elastic fibres of the papillary dermis. The reticular dermis overlies the subcutaneous fat layer. The papillary and reticular dermis are separated by a vascular plexus, the rete subpapillare (45).

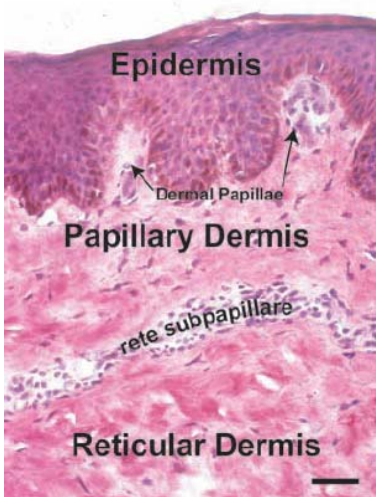

Figure 8: Haematoxylin and Eosin staining of normal human skin. Haematoxylin & Eosin staining of normal human skin. The dermis is divided into the papillary and reticular dermis. These two layers are separated by the rete subpapillare. Scale bar 45 µm. (44)

Extracellular matrix

The main class of molecules in the extracellular matrix are collagens. Additionally, other macromolecules such as fibronectin, elastin, laminins and proteoglycans can be found. The different macromolecules of the extracellular matrix assemble into a network. The composition and architecture of this network contributes to the properties of the tissue (46). Components of the extracellular matrix are synthesised by dermal fibroblasts in response to diverse growth factors and cytokines. Metalloproteinases are involved in the degradation of these components (47).

The different collagen types all share the same basic structure. Three polypeptide chains form a left-handed triple helix, which is held together by hydrogen and covalent bonds (48-49). In normal human skin, collagen type I is with ~90% the most abundant collagen type. Collagen type III has a content of ~10%. Collagen type V has a small content of only ~2% (50).

Fibroblasts

The main cell type found in the dermis is the fibroblast. These mesenchymal cells can also be found in many other organs as they are the most prominent cell type in connective tissues. Independently of the organ in which they are located, they share their spindle-shaped morphology (Figure 9), but it has been shown that they differ in their gene-expression profile, depending on the anatomical location (51). The main function of fibroblasts is the synthesis and deposition of the different types of fibres and macromolecules that constitute the extracellular matrix. But they also have a crucial role in supporting growth and stratification of the epidermis and in wound healing.

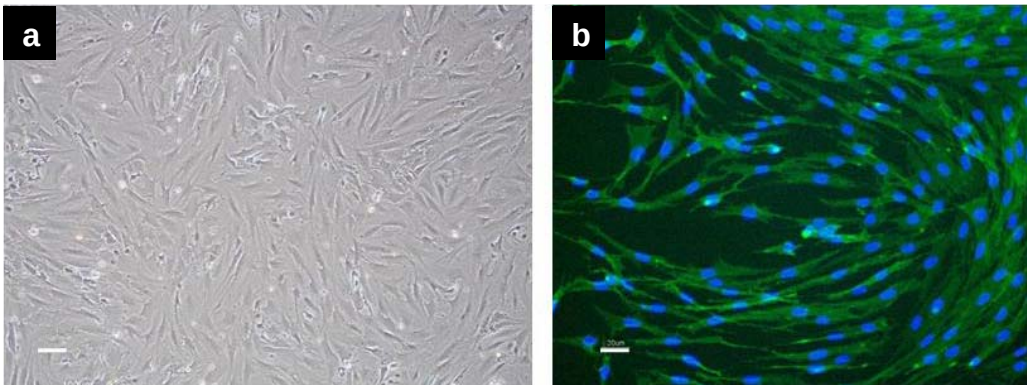

Figure 9: Human fibroblasts in culture. Morphology of human primary fibroblasts on cell culture plastic as seen in

a) light microscopy and with

b) immunofluorescence staining. The cells are positive for the human fibroblast marker CD90 (green). Nuclei are stained with Hoechst (blue). Scale bars 20 µm.

Although fibroblasts are the dominant and essential cell type in the dermis, their population is highly heterogeneous, depending on the exact location within the dermis, but also within the body (45,52). Papillary fibroblasts show a higher proliferation rate and when cultured in monolayers reach a higher cell density because they are not completely contact inhibited (45,53). When seeded into a collagen type I hydrogel, reticular fibroblasts contract the hydrogel faster than papillary fibroblasts (54). Differences can also be observed regarding their production of matrix molecules. It was shown that papillary fibroblasts produce only low levels of versican. In contrast, reticular fibroblasts produce high levels of this protein (44-45).

Other differences between different types of fibroblasts can be seen regarding their capacity to support basement membrane formation. It was shown that myofibroblasts isolated from a wound site do not support keratinocyte differentiation and basement membrane deposition as well as fibroblasts isolated from an unwounded site do (55). Small quiescent fibroblasts, the fibrocytes, which do not show any obvious metabolic activity, can be found in mature connective tissue. Fibroclasts are fibroblasts with phagocytic activity (1,56).

Fibroblasts are essential for the proliferation and differentiation of keratinocytes. One of the first factors identified to be secreted by fibroblasts and to regulate keratinocyte proliferation and differentiation was keratinocyte growth factor 1 (KGF-1). This factor is exclusively produced by mesenchymal cells; however, only epithelial cells express the according receptor and therefore are able to respond to KGF-1 (57-58). KGF-1 overexpression leads to a certain hyperplasia of the epidermis, which might be a result of increased proliferation of basal keratinocytes and suppression of their terminal differentiation (59). Other factors that are secreted by fibroblasts and that regulate the biology of keratinocytes and are involved in wound healing include epidermal growth factor (EGF) (60), interleukin 6 (61), granulocyte colony-stimulating factor (GCSF) (62), and hepatocyte growth factor/scatter factor (HGF) (63).

Basement membrane

The basement membrane separates the epithelial cells from the underlying connective tissue. It can not only be found in the skin but also in diverse organs such as in the digestive tract, lung, kidney and cornea. It is a multi-molecular sheet-like structure that consists of different glycoproteins and proteoglycans such as collagens, laminins, integrins, entactin, and dystroglycans (64). The formation and organisation of the basement membrane needs the interaction of both, basal keratinocytes and stromal fibroblasts (65-66). The basement membrane has several important roles: 1) It is essential for the adhesion of the epidermis to the dermis. 2) It is involved in the regulation of exchange of metabolic products between dermis and epidermis, and 3) it functions as a support for keratinocyte migration in wound healing (1).

The basement membrane is composed of four layers (Figure 10), which were identified by electron microscopy. The uppermost layer is composed of the cell membranes of the basal keratinocytes, where the intracellular keratin filaments are anchored to hemidesmosomes. Below these cell membranes, the lamina lucida can be found, which is approximately 40 nm thick and consists of various macromolecules such as laminin 5. Anchoring filaments, composed of collagen type VII, reach from hemidesmosomes through the lamina lucida to the lamina densa, which is 50-70 nm thick and mainly composed of collagen type IV and laminin 5. The sub-basal lamina filamentous zone is mainly composed of anchoring fibrils (Figure 10a) (67).

Laminin 5 (also named laminin 332 according to its chains α3, β3, and γ2) can only be found in the basement membranes of stratified epithelia such as the skin and mucosa (64). It is essential for the anchoring of the epidermis to the dermis.

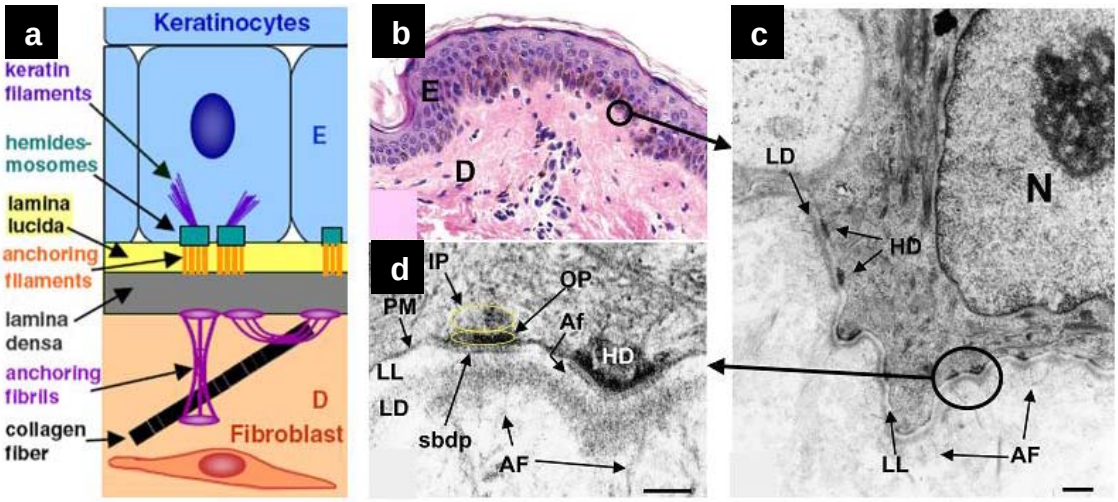

Figure 10: Characteristics of the basement membrane.

a) Schematic view of the organisation of the anchoring elements between the epidermis (E) and the dermis (D).

b) Haematoxylin and Eosin staining of human skin. (E) Epidermis, (D) dermis.

c) Electron micrograph of the basement membrane, showing lamina densa (LD), lamina lucida (LL), hemidesmosomes (HD), anchoring fibrils (AF) and the nucleus of a basal keratinocyte (N).

d) High magnification of the region shown in (c) encircled. Additionally to the components observed in c), a subbasal dense plate (sbdp) can be seen. The hemidesmosome can be structured into an inner plaque (IP) and an outer plaque (OP) in contact with the plasma membrane (PM).

d) Schematic representation of the architecture of the epidermal anchorage. Scale bars 0.1µm. Modified from (68-70)

Development of the dermis

During the first six weeks of gestation of a human embryo, the embryo is covered by the single-layered periderm and thereafter by a two-layered epidermis. During this time, the dermis has not yet developed. Instead of the dermis, a subepidermal cellular layer is found and collagen type IV and laminin 5 can be detected (37-38). Already at eight weeks, the development of the vasculature starts. During weeks nine and ten of gestation, the basement membrane develops with cell adhesion and expression of integrin α6 and integrin β4. Also during this time, the extracellular matrix is deposited. Merkel cells that first can be found in the epidermis are then also detectable in the dermis. (38)

3.1.3 Skin appendages

Hair follicles

The development of hair follicles (Figure 11) starts at the end of the first trimester of pregnancy in humans. They are mainly formed by ectodermal epidermal cells and reach deep into the dermis (3). For their formation in the fetus, fibroblasts play a significant role and the crosstalk between the fibroblasts and keratinocytes is essential (71-72). The formation of a hair follicle starts with mesenchymal cells signalling to the overlying epidermal cells to form small epidermal invaginations into the dermis, the so called hair placodes (left part of Figure 11) (73). The dermal papilla cells then signal to the cells in the hair placode to grow downwards, with the matrix cells at its leading front, and to form the hair follicle. Further crosstalk between the mesenchyme and epithelium leads to the maturation of the hair follicle (72,74).

The hair is surrounded by seven concentric layers of terminally differentiated matrix cells. The outer root sheath is composed of several layers. The outermost layer is the one showing the least differentiation. The outer root sheath always stays in contact with the basement membrane. The inner root sheath consists of three cell layers (72,75). The mature hair follicle can be divided into several segments; these differ in their structure and also in their behaviour during the hair cycle. The uppermost part of the hair is the intraepidermal part. From there, the infundibulum reaches down to the opening of the sebaceous gland. The isthmus extends from the

sebaceous gland down to the bulge, which is where the arrector pili muscle attaches. The structure between the bulge and the hair bulb is called lower follicle. The hair bulb is responsible for the growth of the hair and contains melanocytes. The bulb forms a cavity which contains stromal cells and is highly vascularised and innervated. This mesenchymal cavity is referred to as the dermal papilla. (1,76)

The upper parts of the hair are differentiated and do not change markedly during the hair cycle. In contrast, the structures of the lower parts vary depending on the state of the cycle. The hair grows in the anagen phase by proliferating keratinocytes located above the dermal papilla. In the regression phase, the catagen, the lower parts of the hair follicle undergo apoptosis (Figure 11) (77). During the telogen phase (Figure 11), in humans the hair follicle rests up to several months, before the anagen phases starts again upon activation of the hair follicle stem cells (75). The bulge of a hair follicle is an important stem cell niche of the skin (75,78). In the anagen phase of the hair follicle, stem cells migrate off the bulge, proliferate and differentiate into the cell lineages of the hair follicle, which can be distinguished by the expression patterns of different keratins, which are characteristic for the different concentric layers of the hair follicle (79-80). In addition to their function in the normal hair cycle, keratinocyte stem cells of the bulge are involved in the process of skin wound healing. Upon wounding of the surrounding epidermis, they migrate out of the bulge and contribute to the closure of the epidermis (81-84).

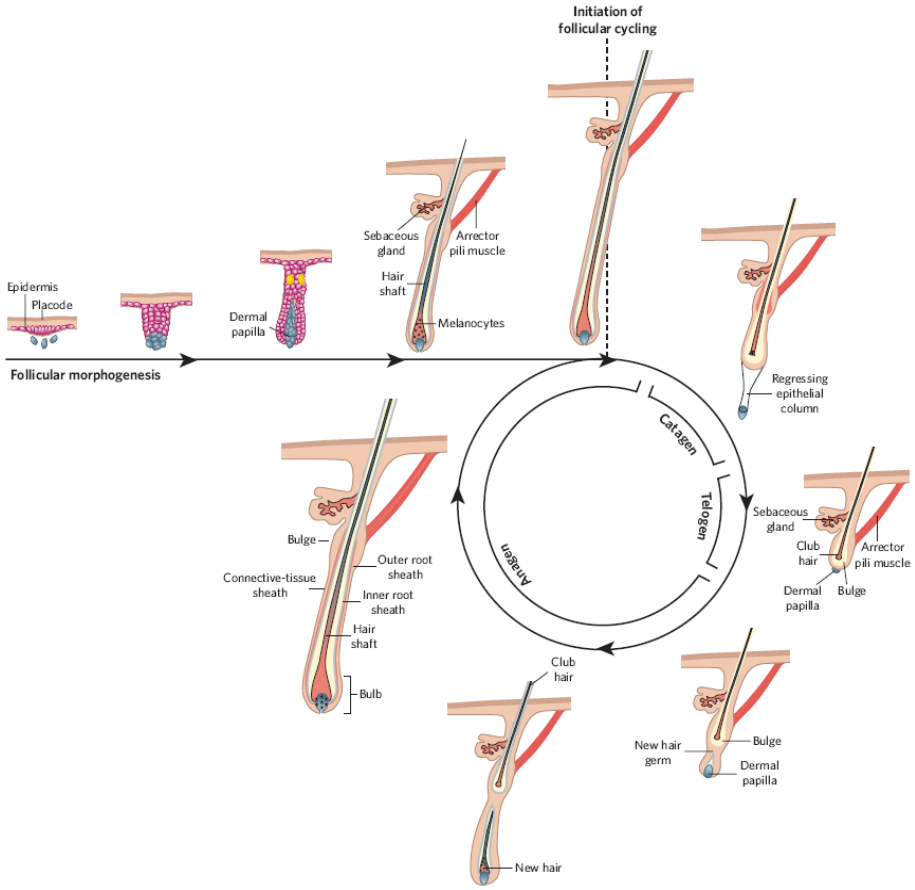

Figure 11: Schematic view of the hair cycle in humans. The hair cycle starts with the regression phase, the catagen. During the catagen, the lower hair undergoes apoptosis and regresses. At the end of this phase, the dermal papilla can be found directly under the bulge region. After the resting phase, the telogen, the stem cells of the hair are activated and growth of the hair starts again. (75)

Sebaceous glands

Sebaceous glands (Figure 11) are mainly associated with hair follicles, therefore they can be found in all areas of the body, except in hairless skin. They are located between the skin surface and the arrector pili muscle. Higher numbers of sebaceous glands, and also larger gland sizes, can be found in regions exhibiting small vellus hairs, which is the case in facial skin (3).

Progenitor cells of the sebaceous gland constantly proliferate and give rise to cells that differentiate into terminally differentiated sebocytes. These cells produce lipids and sebum. For the secretion, the sebocytes disintegrate and the release their content into the hair canal. The oils and sebum function as protection for the hair against bacterial infections and as lubrication. Hormones play an important role in the control of sebaceous gland secretion. (1,3)

Sweat glands

In humans, two types of sweat glands (Figure 12) can be distinguished, namely eccrine sweat glands and apocrine sweat glands. Both types consist of a secretory coil and an excretory duct. Eccrine sweat glands are the dominant type in humans and can be found almost all over the body. They have a major role in thermoregulation by producing an odourless, hypotonic clear fluid (85). Their highest density can be observed over the palms, soles, axillae and forehead, with up to 300 sweat glands per square centimetre. The secretory coil reaches deep into the dermis and consists of one cell layer composed of myoepithelial cells and dark and clear secretory cells. The excretory duct is composed of two cell layers, the peripheral cell layer and the inner cell layer (1).

Apocrine sweat glands are less abundant in humans, they can be found in the axillae, anogenital region and nipples. They produce an odourless, milky fluid, which after puberty produces a viscous secretion that is acted on by bacteria to produce a characteristic odour (86).

It has been shown that eccrine sweat gland cells can contribute to epidermal wound healing by stem cells that migrate out of the sweat gland, similar to stem cells found in the hair follicle bulge (87-89).

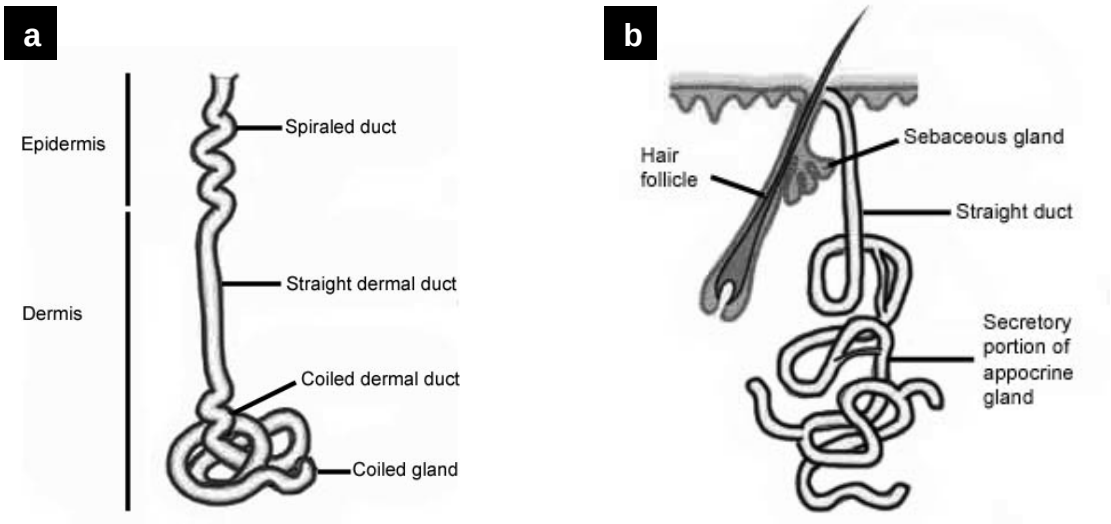

Figure 12: Schematic view of the two types of sweat glands in humans.

a) Eccrine sweat gland.

b) Apocrine sweat gland. Modified from (90)

3.2 Skin injury and wound healing

3.2.1 Thermal injuries

Extensive skin loss can result from many reasons such as acute soft tissue trauma, genetic disorders, chronic wounds, skin diseases, or tumours. Thermal trauma, such as scalds and burns, is one of the most common causes for major skin loss. It is estimated that in Switzerland annually 70'000 burn accidents occur. 1000 of these victims need to be hospitalised, and 200 are treated in a specialised burn care centre. One third of these patients are children (91). Hospitalisation is needed when the burn area exceeds more than 10% of the total body surface area in adults, and 5% of the total body surface area of children (92).

Burn injuries are categorised into four classes according to the depth of the wound (Table 3). Using the self-healing capacity of the skin, skin wounds of the classes I-III can regenerate. In such wounds, keratinocytes from the borders of the wound but also from hair follicles and sweat glands in the remaining dermis change into a proliferating migratory cell type and contribute to the healing and re-epithelialisation process (81,84,88,93). Deep partial-thickness skin wounds show a greater dermal damage, which leads to slower healing because fewer skin appendages can contribute to the healing process. Additionally, scarring is severe in this class of injury compared with superficial partial-thickness wounds. After a class IV injury, all the components of the skin that could contribute to the regeneration are completely destroyed, leaving a wound that only can heal from the wound edges and by contraction. This leads to an unsatisfactory outcome with regard to function and cosmetics. In these cases, the wound size is critical, as full-thickness wounds with a diameter of more that 1 cm would heal with extensive scar formation (94).

Table 3: Skin defects. Overview on the categories of skin defects. Modified from (92)

Skin defect class	Depth of injury	Clinical description
Class I	Epidermal	No blisters, dry, red, painful
Class II a	Superficial partial-thickness	Blisters, moist, red, painful
Class II b	Superficial partial-thickness	Blisters, less moist, dotted pink, painful
Class III	Deep partial-thickness	Dry, white, painless
Class IV	Full-thickness	Charred, painless

3.2.2 Wound healing

The process of wound healing is very similar all over the human body; the process differs little whether it is a myocardial infarction, an injured lung or a skin wound, and it consists of three overlapping phases, namely 1) inflammation, 2) new tissue formation and 3) remodelling (Figure 13).

As a first step of the inflammation-phase of skin wound healing and immediately after injury, platelets aggregate to form a haemostatic plug and blood coagulates, forming together a clot that serves as a temporary barrier to the wounded area and as a provisional repair matrix. This matrix is mainly made of cross-linked fibrin fibres, derived from thrombin cleavage of fibrinogen, and smaller amounts of plasma fibronectin, vitronectin and thrombospondin (95). The clot also serves as a substrate for cell adhesion and migration. Activated platelets degranulate and release growth factors and adhesive proteins, leading to an inflammatory response and cell migration into the wound area. Neutrophiles arrive at the wound site within minutes; they react to changes in the surface of the endothelial cells lining the blood vessels at the wound site. Monocytes arrive 2-3 days after injury and differentiate into macrophages and together with the neutrophiles they clean the wound by phagocytosing and solubilising cell- and matrix debris and pathogenic organisms. The neutrophiles are also involved in producing pro-inflammatory cytokines that are used as very early signals to activate local fibroblasts and keratinocytes (Figure 13a).

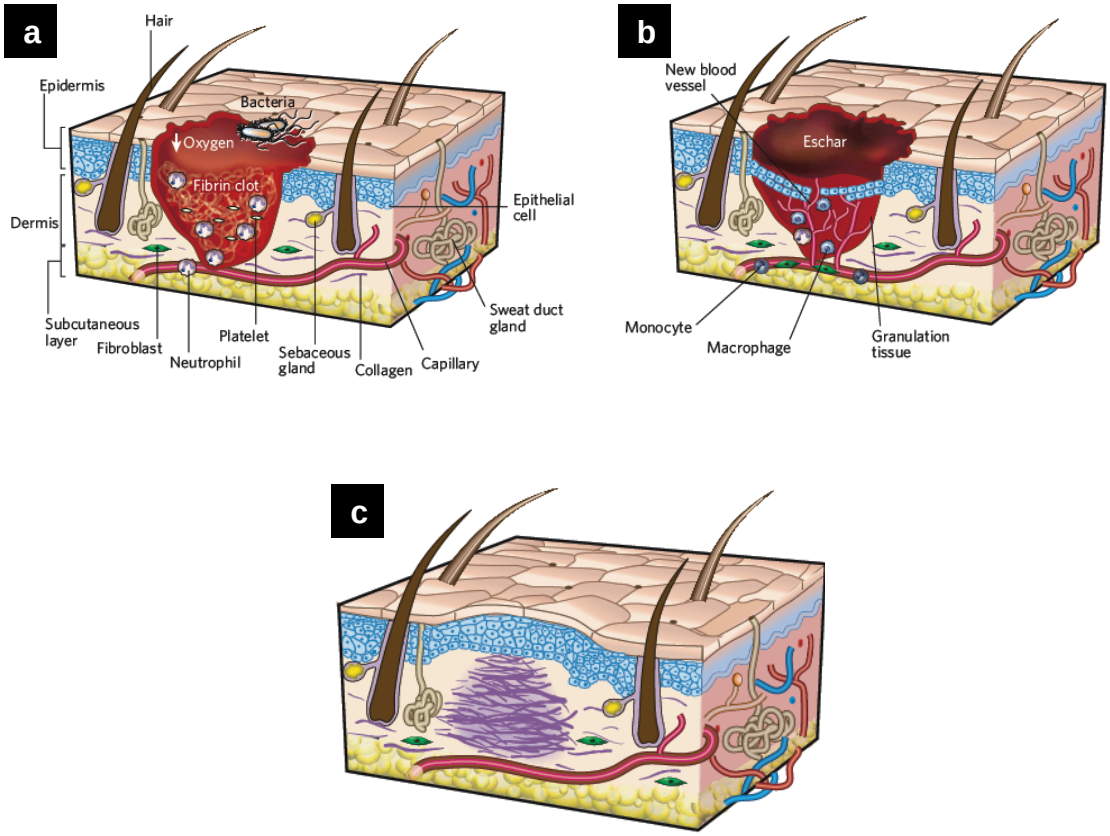

Figure 13: Schematic view of the three classical wound healing stages.

a) Characteristic for wounds in the first stage, the inflammation phase, is the formation of a fibrin clot and the presence of bacteria, platelets and neutrophiles in the wound area.

b) During the phase of new tissue formation an eschar has formed, most cells of the previous phase are not anymore present and blood vessels grow into the area. Under the eschar, keratinocytes migrate to close the wound.

c) During the third phase, tissue remodelling occurs. Fibroblasts deposit collagen in dense parallel bundles (violet lines) and the wound contracts. The reconstituted scar tissue does not contain any skin appendages. (96)

In the second phase, during days 2-10 after wounding, haematopoietic as well as mesenchymal cells from the circulation and the surrounding tissues are attracted to the wound site. Fibroblasts and capillaries invade the temporary fibrin matrix to replace it with a contractile granulation tissue, which is mainly composed of collagen type III. This new tissue has a pink granular appearance that results from numerous capillaries growing into the provisional matrix. Usually now the wound margins are concentrically contracted, with the help of fibroblasts that had differentiated into contractile myofibroblasts. Keratinocytes from the wound margins migrate to close the wound area. Keratinocytes from hair follicles and sweat glands migrate off these

skin appendages to participate in wound closure. First, the keratinocytes form a monolayer, then a new basal lamina is formed and the cells stratify. In the wound area, an oxygen gradient is created by the diffusion of oxygen from the blood vessels at the wound edges. Fibroblasts at the wound borders produce collagen type III, a process supported by the high-oxygen concentration in this area. The hypoxic environment in the centre of the wound is essential for the macrophages, which release cytokines that stimulate chemotaxis and mitosis (Figure 13b).

2-3 weeks after injury, the last phase of the wound healing process starts, and most of the processes of the first two phases are terminated. After wound closure, the cells in the granulation tissue undergo apoptosis and during the following months, the collagen-rich scar tissue is re-modelled. During 6-12 months after injury, matrix metalloproteases secreted by fibroblasts, macrophages and endothelial cells, transform the matrix from a matrix mainly composed of collagen type III to one that is largely composed of collagen type I. This re-modelling phase can last for more than one year (Figure 13c). (96-98) Figure 14 shows an overview of the time course of these wound healing processes in mammals.

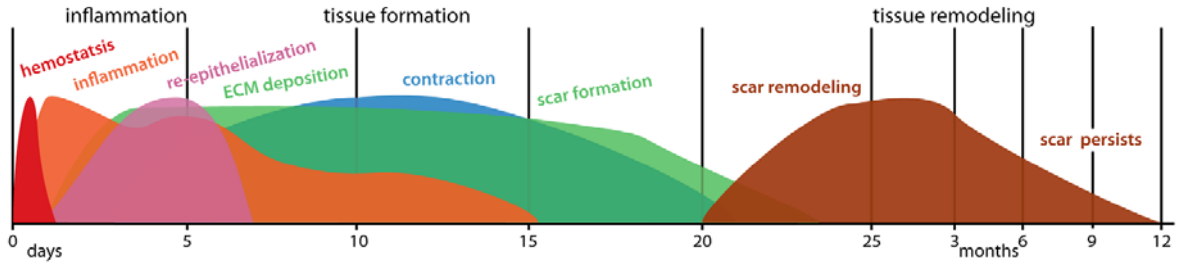

Figure 14: Time course of the wound healing process in mammals. The x-axis in this scheme represents the time, whereas the y-axis represents the strength of the response for each process. The colours highlight the individual overlapping processes during the three main wound healing phases inflammation, new tissue formation and tissue remodelling. (99)

3.2.3 Scarring

Ideally, wound repair would result in a tissue showing the same structure, function and aesthetics as the uninjured skin. But in most cases, the outcome of wound healing in mammals is fibrotic scar tissue. The consequences of this scar repair often include loss of function, movement restriction and disfigurement (Figure 15) (38,100). Scarring results from excessive accumulation of unorganised extracellular matrix, mainly collagen, deposited by myofibroblasts which, under the influence of TGFβs 1 and 2, show characteristics of smooth muscle cells (101). In intact non-wounded dermis, the collagen shows a mechanically efficient basket-weave meshwork. In contrast, the collagen in scar tissue is deposited in dense parallel bundles (95). Additionally, modifications in the vascularisation can often be found together with changes in cell proliferation of the cells in the originally injured area. If the injury is deep, no remnants of hair follicles and sweat glands are left; hence, the repaired skin will fail to regenerate those. Time is a critical component in wound healing and scarring. The faster a wound heals, the better the outcome is with respect to scar formation (38).

However, although today the treatment of skin defects includes scar prevention, the revision of scars remains a major challenge of reconstructive surgery (100).

Figure 15: Disfiguring scars in three burn patients. (a, c, e) lateral view, (b, d, f) frontal view.
(a, b) 16 year old adolescent.
(c, d) 12 year old patient.
(e, f) 12 year old patient. Modified from (100)

Fetal wound healing

Complete regeneration is found in lower vertebrates (e.g. salamanders) and invertebrates (102). Scar less wound healing can only be found in early mammalian embryos (103). In mammals, the fetal dermis reacts to tissue damage with generating a non-disrupted collagen matrix that is identical to the unwounded dermis. However, this scar less repair mechanism is only observable until a certain transition time point, after which also in fetuses skin injury results in scar formation. This transition point from scar less wound healing to scarring is found approximately in week 24 of gestation in humans. During the period a mammal fetus shows scar free wound healing, the fetus has an immature endocrine system as well as an immature immune system and the cells of the fetus exist in a hypoxic environment (104). During this phase, the fetus can restore normal tissue architecture and reconstitute even the appendages.

The mechanisms why wounds can heal without any scar formation until a certain transition point still are not completely understood. Many studies investigated the differences between human fetal and adult skin. Differences detected include a higher ratio of collagen type III to collagen type I in fetal skin, a higher level of glycosaminoglycans in the extracellular matrix (ECM) in fetal skin, and the absence of the ECM component elastin in fetal dermis (42). Amongst the many differences that were found in fetal wound healing compared to wound healing in adults are the missing conversion of fibroblasts into myofibroblasts and the absence of a significant angiogenic response (95,105).

3.2.4 Current treatment of burn injuries

Any skin injury that exceeds 4 cm^2 in diameter will not show good spontaneous healing. In these cases a skin graft can significantly improve the outcome (106). The today's gold standard of treating severe and large skin defects is the early debridement of the destroyed tissue and the transplantation of autologous split-thickness skin grafts harvested from an unaffected body area, the so called donor site (107-112).

Split-thickness skin is consists of the epidermis and only a thin layer of dermis (Figure 16a). Split-thickness skin is harvested from the donor site with the help of a dermatome and transplanted to the wound site, where the capillaries of the split-thickness skin graft will anastomose with the capillary network of the wound site. The donor site will heal properly within a week, as a sufficient number of keratinocytes remains in the skin appendages located in the dermis, hence the donor site can be re-used three to four times to harvest split-thickness skin (110).

Transplantation of autologous full-thickness skin grafts (Figure 16b) can only be performed in patients with injured areas of less than 2% of the total body surface area (113). With full-thickness skin grafts the contraction at the wound site will be minimal and there will be almost no scar. However, the donor site will take longer to heal. An additional disadvantage of full-thickness skin grafts is that donor and recipient sites should match well because of potential skin mismatches due to the very diverse skin specialisations seen over the total body area (38).

A major drawback of the use of split-thickness skin grafts may be that donor sites are extremely limited when large areas of the body (e.g. 80% TBSA) are severely injured, or the physical condition of the patient will not allow the harvesting of skin. When using split-thickness skin grafts, the area that is available to cover the defect can be enlarged by meshing the graft. However, meshing of the split-thickness skin leads to a suboptimal deprived cosmetic result and poor functional outcome, due to the lack of dermal and epidermal components in the gaps of the meshed graft (94). Skin expansion *in vivo*, i.e. in the patient itself, can be reached by subcutaneous insertion of inflatable devices (expanders) (114), which can be enlarged stepwise, resulting in expansion of the overlying skin by cell proliferation. The advantage of such an expanded skin is that it is composed of all skin layers and that it shows the characteristics of the donor site (38,115).

The best surgical results can be obtained when the split-thickness skin graft is transplanted in combination with a dermal template (116), such as Integra Dermal Regeneration Template® (100,107,113,117-119) or Matriderm® (116,120-124). It has been shown that the use of such off the shelf, acellular templates can improve wound healing and reduce scar contraction (125-126). In the following, I will consider three different templates for skin reconstruction in more detail.

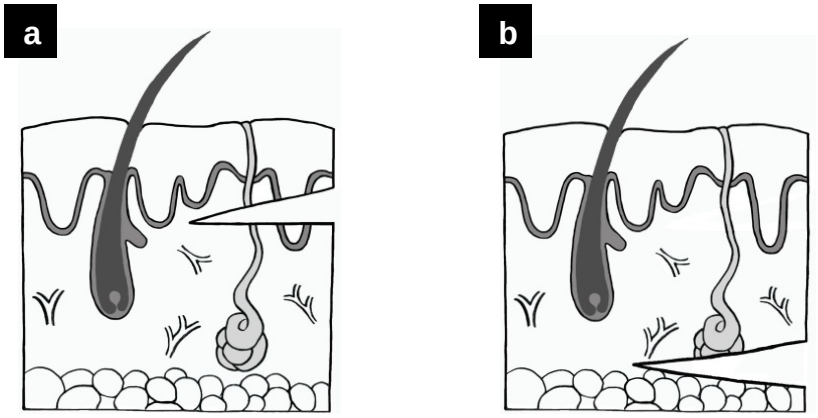

Figure 16: Split-thickness and full-thickness skin. Schematic representation of the composition of
a) split-thickness skin and
b) full-thickness skin.

Integra Dermal Regeneration Template

The product Integra Dermal Regeneration Template® 2 mm (Integra, Integra Life Science Corp., Plainsboro, NJ, USA) (Figure 17a) is composed of two different layers: The dermal layer is composed of bovine cross-linked tendon collagen and glycosaminoglycans from shark cartilage. The second layer consists of a temporary silicone sheet (94). It is applied in a two-step procedure: after initial transplantation of Integra, cells from the patient will grow into the dermal layer and will permanently colonise it to form a neo-dermis. In a second surgery 15-20 days after the initial transplantation of Integra, the silicone sheet will be peeled off, and the now vascularised neo-dermis will be covered with an autologous split-thickness skin graft (127). As it is an acellular product, it can be applied off-the-shelf and has no limitations in availability. The indication for the use of Integra is post-excisional treatment of deep-partial thickness or full-thickness skin defects, but it can also be applied for scar revision and other reconstructive surgeries at almost all body sites (128). The results obtained with Integra show regeneration of near normal skin with only minimal scarring. Disadvantages are the long repopulation time and the necessity of two successive operations (100,129-130).

Matriderm

The product Matriderm® (Matriderm, Dr. Suwelack Skin and HealthCare AG, Billerbeck, Germany) (Figure 17b) is a matrix of bovine non-cross-linked lyophilised dermis. The surface is coated with α-elastin hydrolysate. Matriderm is intended to substitute for the dermis and it can be applied simultaneously with split-thickness skin in a single surgical intervention (131). It is an off-the-shelf product that therefore has no limitations in availability and serves as a permanent dermal substitute. However, since it is rapidly degraded, it is not clear whether Matriderm has a true advantage in applications other than hand surgery (121,132).

Apligraf

The product Apligraf® (Apligraf, Organogenesis, Inc., Canton, MA, USA) (Figure 17c) is, in contrast to Integra and Matriderm, a cellular product. It is based on a bovine collagen type I gel matrix, combined with allogenic fibroblasts and keratinocytes form neonatal foreskin (127). As it is a living product, it has a shelf-life of only five days at room temperature, and the allogenic cells contained in Apligraf make it only a temporary wound dressing. These allogenic cells are efficient for pain relief and support for wound healing, but it has been shown that they do not survive in the patient longer than one to two months (133-134). Apligraf is licensed for use in the treatment of venous leg and diabetic foot ulcers, but there are no reports of large clinical trials for its use in burns treatment (94).

Figure 17: Examples for commercially available products for skin reconstruction.

a) Integra Dermal Regeneration Template.

b) Matriderm.

c) Apligraf. (135-137)

3.3 Bio-engineering of skin

3.3.1 Definition of tissue engineering

An article published in 1992 by Robert M. Nerem describes the working definition of the term “tissue engineering” as follows:

> *“Tissue engineering is the application of the principles and methods of engineering and the life sciences toward the fundamental understanding of structure/function relationships in normal and pathological mammalian tissues and the development of biological substitutes to restore, maintain or improve functions.”* (138)

This definition is today, 20 years later, still valid. Tissue engineering has the ultimate goal of creating living replacements for tissues and organs of the body (139). The field of tissue engineering has developed, and researchers all over the world are working on engineering different tissues and organs such as skin, nerves, heart valves (140), and bone (141), to supply the constantly growing need for tissue and organ transplantations (142). Independently of the tissue or organ that is to be engineered, two major points have to be considered. Firstly, there is the need for a cell source that can provide cells capable of differentiating and/or forming the desired tissue or organ. Secondly, for these cells an appropriate growth and differentiation factors have to be used, and an appropriate extracellular matrix has to be provided. This ECM ideally exhibits both, excellent biological properties and convenient handling by the surgeon.

For tissue engineering, the understanding of the physiology of the tissue or organ to be reconstructed is fundamental, but at the same time the exact needs for clinical application have to be specified in detail. Therefore the collaboration between different disciplines such as basic research, translational research and clinicians is essential.

3.3.2 Historic perspectives

A first essential step towards tissue engineering of skin was achieved in 1975, when successfully cultured keratinocytes were reported by Rheinwald and Green. They were able to generate small sheets consisting of about two to three layers of human keratinocytes. These keratinocytes were grown on a feeder layer of lethally irradiated 3T3 murine fibroblasts, and with this Rheinwald and Green were the first to describe the complex relationship between mesenchymal fibroblasts and epithelial keratinocytes (143). Based on the success of these researchers, cultured epidermal autografts were tested worldwide at many different burn centres. A major shortcoming of this method was the very variable take of the cultured epidermal autografts (144-151). Only some years after the first successful cultivation of keratinocytes a dermo-epidermal skin substitute was developed in 1981 and later refined as the above described product Apligraf, containing allogenic fibroblasts and keratinocytes (152). Also in 1981, Burke and Yannas reported the development of an artificial skin based on an acellular collagen-glycosaminoglycan matrix. This product, since 1996 commercially available in the USA, and now known as Integra, today still is very important for the treatment of severe skin defects in combination with split-thickness skin. In 1995, cultured autologous fibroblasts and keratinocytes were transplanted onto Integra in burn patients (153). However, it appeared that this did not lead to any success as neither case reports of treated patients, nor follow-up reports or any results of clinical trials of these experiments were published.

3.3.3 The bio-engineering of skin: “Skingineering”

The necessity for bio-engineered skin

The coverage of large skin wounds with autologous split-thickness skin is the current gold standard. However, in severely injured patients, if the defect exceeds 50-60% of the total body surface area, the availability of donor sites is very limited, and these donor sites would add to the total injured area which represents and additional risk for these patients (154). Patients in which even meshing of the split-thickness skin grafts does not allow to cover all skin areas, wound dressings or

cadaver skin are used as temporary coverage to prevent fluid loss and microbial contaminations, and delayed serial grafting of split-thickness skin is performed (155). Such wounds which cannot heal over a long period of time represent a high risk for complications and will not result with a satisfactory outcome (156). Additionally, harvesting of split-thickness skin can result in scarring, in particular in children who frequently may suffer from disabling and disfiguring hypertrophic scars, or keloid formation (157). Alternative treatment methods without the need for large donor sites for harvesting split-thickness skin may considerably improve the perspectives of patients with severe skin defects.

Chronic wounds associated with old age and diabetes are increasing in the developed world. These wounds significantly increase health care costs and are a major problem for the affected patients. In these patients, tissue engineered skin substitutes may significantly support wound healing (158-159).

Other fields with increasing potential for the use of bio-engineered skin are scar revisions, reconstructive surgery, correction of pigmentation defects such as vitiligo, and congenital nevi (160).

Materials for bio-engineering of skin

Tissue engineering depends on the use of an appropriate material. The material serves as a substitute for the extracellular matrix, in which cells can be integrated in a three-dimensional way. Additionally, factors can be included into it which serve as stimuli to direct the growth and differentiation of the incorporated cells (161). The ideal material for skin bio-engineering must not induce an immune response, excessive inflammation, or toxic reaction. If possible there should be no or only a very low risk for disease transmission for materials composed of animal derived components. Furthermore, it should degrade over time but support the tissue reconstruction and show similar properties as the normal skin (162). FDA-approved polymer materials include animal derived substances such as bovine collagen but also synthetic materials such as poly(lactic-*co*-glycolic acid). They can either be solid, but alternatively hydrogels, composed of hydrophilic polymer chains, can be used showing good characteristics. Also the materials for hydrogels can either be synthetic or natural (163). The choice of material that is used highly depends on the tissue of

interest and its application. In the following, a natural as well as a synthetic polymer for skin tissue engineering will be discussed exemplarily in more detail.

Natural polymer – Collagens:

For bio-engineering of human skin, one of the most important scaffold materials for hydrogels is the naturally derived collagen type I. In mammals, collagen is the main protein of the extracellular matrix and contributes with 25% to the total protein mass (19,48). Collagen itself can create stable fibres, but the mechanical properties and stability of the fibres can additionally be enhanced by cross-linking with chemicals (164), physical treatments such as UV irradiation (165), or, by blending with other polymers (132). The requirements for a collagen type I hydrogel used in skin tissue engineering are divers. For example, when cells should be integrated into the collagen hydrogel, the hydrogel must polymerize without damaging the cells and must allow appropriate diffusion of nutrients. Additionally, it should provide enough mechanical integrity for that it can be handled in the laboratory as well as in the operation theatre (142). Collagen type I hydrogels are not only used for skin tissue engineering (21,88-89), they also have been used for tissue engineering of skeletal muscle (166), adipose tissue (167), and blood vessels (168). As collagen is an animal derived material, it carries the risk of disease transmission (169). However, for the production of skin substitutes under GMP (Good Manufacturing Practice) guidelines for clinical application, collagen type I is available that fulfils all regulatory and quality regulations, i.e. collagen type I with certificate of origin, certificate of analysis, and certificates for testing for sterility, endotoxines and mycoplasma. Therefore the actual risk for disease transmission from animal to human can be minimised.

Synthetic polymer – PLGA:

Many biodegradable and biocompatible synthetic polymers have been studied to serve as material for tissue engineering. Poly(lactic-*co*-glycolic acid) (PLGA) is widely used for tissue engineering (170), as this material is FDA approved and not expensive. PLGA can be processed easily and the microstructure and morphology can be controlled. The mechanical strength as well as the degradation time of PLGA can be adjusted to different needs by changing the ratio of lactide and glycolide (171). As lactide is more hydrophobic than glycolide, PLGA polymers composed of

more lactide are less hydrophilic, therefore absorb less water and degrade slower compared to PLGA polymers with higher glycolide contents (172). *In vivo*, PLGA polymers will degrade into lactic acid and glycolic acid. Lactic acid is metabolised and eliminated from the body as carbon dioxide and water. Glycolic acid is either directly excreted in the kidneys or it is metabolised similar to lactic acid and eliminated from the body as carbon dioxide and water (173). With electro-spinning, ultra-fine PLGA fibres can be formed using a high-voltage electrostatic field which charges a suspended drop of PLGA. With this technique, scaffolds can be generated that have a high surface area-to-volume ratio and provide a good substrate for cell attachment (174). Additionally, PLGA sheets can be produced to incorporate them into other matrices to give additional support. Scaffolds are usually no ideal substrate for cells, thus they mostly have to be combined with ECM components, such as collagens, fibrin, or hyaluronic acid.

Quality criteria for bio-engineered skin substitutes

The major requirements that need to be fulfilled by all bio-engineered skin substitutes, whether they are dermal, epidermal, or, dermo-epidermal skin substitutes, are: safety for the patient, clinical effectiveness and convenience in handling and application (124). A transplanted skin substitute needs to adhere to the wound bed and be incorporated and supported by the vasculature. The critical thickness for sufficient ingrowths of blood vessels that a skin graft cannot exceed is 1 mm (175). When using dermal substitutes, sufficient vascularisation can often only be achieved with a two-step procedure to provide sufficient time for the needed vascularisation, though this leads to an additional stress for the patient. Moreover, the skin substitute has to be accepted by the patient's immune system, and it has to serve as a permanent graft (160). Additionally, an engineered skin substitute should exhibit similar properties as normal skin with regard to elasticity and pigmentation, and it should not contract upon transplantation.

The bio-engineered products for skin reconstruction that are currently available do not yet fulfil all the above mentioned requirements to a completely satisfactory extent and therefore there is still a high necessity for novel, more functional dermo-epidermal skin substitutes (94,113).

Plastic compression of collagen hydrogels

Collagen hydrogels have been shown to have high potential for tissue engineering purposes (21,88-89,166-168). To generate large, more stable collagen hydrogels for skin tissue engineering, Braziulis et al. (176) modified a method previously published by Brown et al. (177) to create 7x7 cm compressed collagen hydrogels. Plastic compression of a collagen hydrogel in a compression chamber (Figure 18) densifies the collagen fibres. This leads to reduced gel contraction and degradation and therefore to a more stable, functional collagen hydrogel.

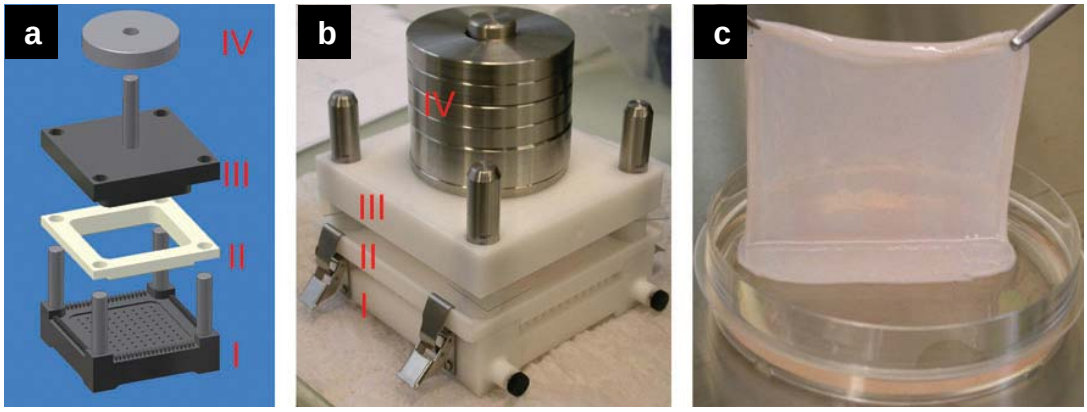

Figure 18: Plastic compression of collagen hydrogels (7x7 cm).

a) Schematic drawing of the compression chamber.

b) Picture of the assembled compression chamber. (I) perforated base plate, (II) casting frame, (III) compression stamp, (IV) weights.

c) Large square 7x7 cm compressed collagen hydrogel. (176)

Novel skin grafts developed by the Tissue Biology Research Unit

Phase I clinical trials are currently being prepared with two skin substitutes developed and produced by the TBRU.

Firstly, denovoDerm (Figure 19a) is a tissue-engineered, autologous dermal substitute. It consists of a compressed collagen type I hydrogel with incorporated autologous dermal fibroblasts. After a short cultivation phase *in vitro* of about 6-8 days, this dermal substitute will be transplanted onto the wound bed. As denovoDerm has no epidermal compartment, autologous split-thickness skin will be used to cover this dermal substitute at the same surgical intervention. On the patient, this dermal substitute will develop into a fully functional dermis greatly supporting the split-

thickness skin that it is tightly connected to. In phase I clinical trials, it will be applied on acute as well as on elective patients with not more than 25% TBSA affected.

Secondly, denovoSkin (Figure 19b) is a tissue-engineered, autologous dermo-epidermal skin substitute. It consists of a compressed collagen type I hydrogel with incorporated autologous dermal fibroblasts and autologous epidermal keratinocytes seeded on top of this hydrogel. This dermo-epidermal skin substitute will be transplanted after a cultivation phase of 18-21 days *in vitro*. It will be applied directly onto the wound bed. As it also has an epidermal compartment, no additional coverage of this skin substitute with split-thickness skin will be needed. On the patient, this dermo-epidermal skin substitute will develop into a functional skin analogue. For this product, there are no limitations for the patient's TBSA affected, as it is independent of split-thickness skin. (178)

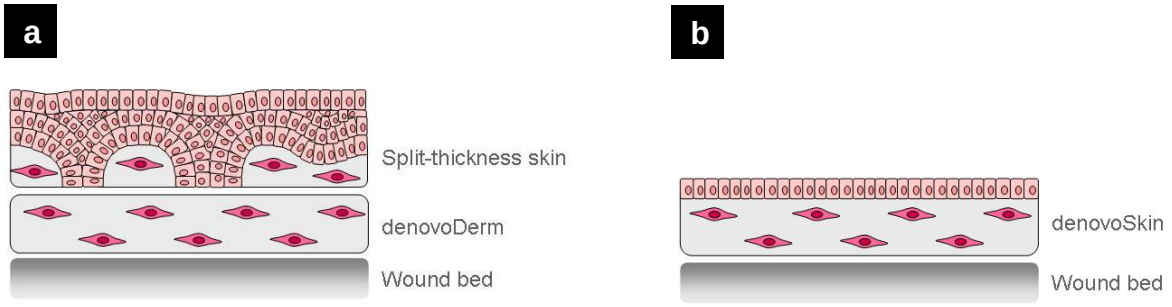

Figure 19: denovoDerm and denovoSkin.

a) The dermal graft denovoDerm will be applied directly onto the wound bed and covered with autologous split-thickness skin.

b) The dermo-epidermal graft denovoSkin will be applied directly onto the wound bed and requires not further covering with split-thickness skin.

3.4 Outline of this dissertation

In the following, a short background and the experimental outline of each of the publications included in this dissertation is presented.

3.4.1 Publication I

Collagen hydrogels strengthened by biodegradable meshes are a basis for dermo-epidermal skin grafts intended to reconstitute human skin in a one-step surgical intervention:

Collagen hydrogels are widely used for tissue engineering purposes. Also at the TBRU, collagen type I hydrogels are used for the generation of most skin substitutes. However, collagen hydrogels tend to be fragile and handling is often difficult. Therefore we aimed in generating dermo-epidermal skin substitutes based on collagen type I hydrogels with incorporated biodegradable scaffolds. The scaffolds should stabilise the hydrogels for better handling characteristics and should be fully biodegradable and biocompatible especially with regard to epidermal growth and stratification.

Therefore we generated dermo-epidermal skin substitutes with different incorporated biodegradable scaffolds. The skin substitutes were analysed *in vitro* as well as *in vivo*, with special focus on epidermal stratification (Figure 20).

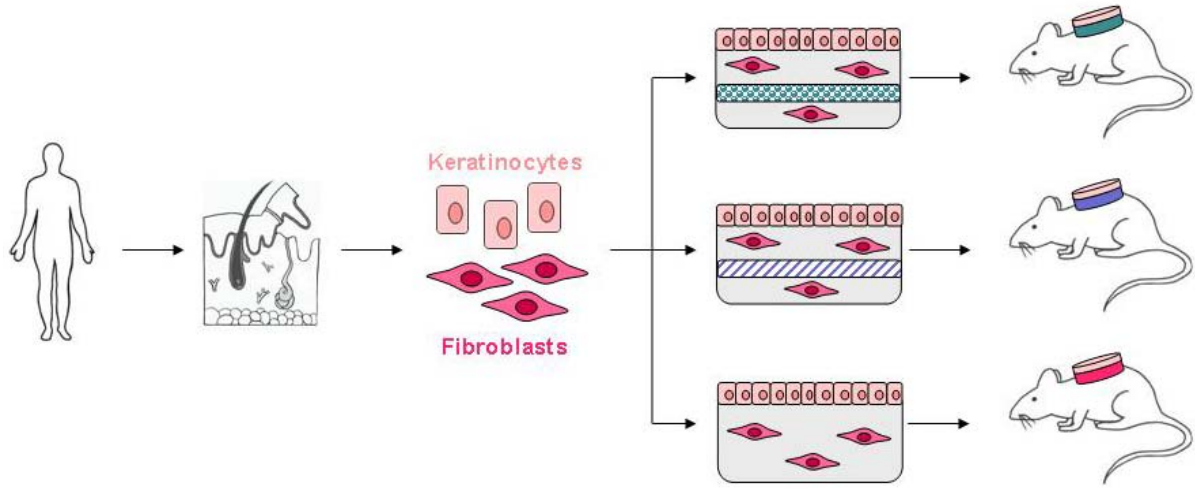

Figure 20: Experimental outline of publication I. Schematic overview on the experimental design of the manuscript entitled: *Collagen hydrogels strengthened by biodegradable meshes are a basis for dermo-epidermal skin grafts intended to reconstitute human skin in a one-step surgical intervention*.

3.4.2 Publication II

Human amniotic fluid derived cells can competently substitute dermal fibroblasts in a tissue engineered dermo-epidermal skin analogue:

Today, fetal surgery for spina bifida is performed at a few centres worldwide and also at the University Children's Hospital Zurich in Switzerland. The skin defects resulting from spina bifida operation often are huge, compared to the small size of the fetus. Closure of these skin defects is often difficult, and in these cases fetal skin tissue engineering might help. We therefore raised the question whether we can engineer a fetal skin from cells contained in the amniotic fluid. This would be very appealing, as the amniotic fluid represents an easily accessible cell source not only after birth, but also already during pregnancy. In a first step towards engineered fetal skin, we wanted to evaluate whether human amniotic fluid derived cells (amniocytes) can take over the function of dermal fibroblasts, in particular with regard to supporting epidermal growth and stratification (Figure 21).

To address this question, we used our procedure to generate dermo-epidermal skin analogues based on a collagen type I hydrogel. From a human skin biopsy, we isolated human dermal fibroblasts and human epidermal keratinocytes. These cells we used to generate a dermo-epidermal skin substitute with incorporated fibroblasts and keratinocytes seeded on top of these hydrogels. The skin substitutes

were transplanted onto the back of immuno-incompetent rats and analysed three weeks thereafter. As control, we generated skin substitutes with an acellular dermal compartment. Human amniocytes were isolated from samples of human amniotic fluid. These cells were then, instead of the usually used fibroblasts, incorporated into collagen hydrogels. As epidermal layer, the usually used epidermal keratinocytes were used. Also these grafts were transplanted onto immuno-incompetent rats and analysed after three weeks. All types of grafts were analysed macroscopically, histologically and with immunofluorescence stainings.

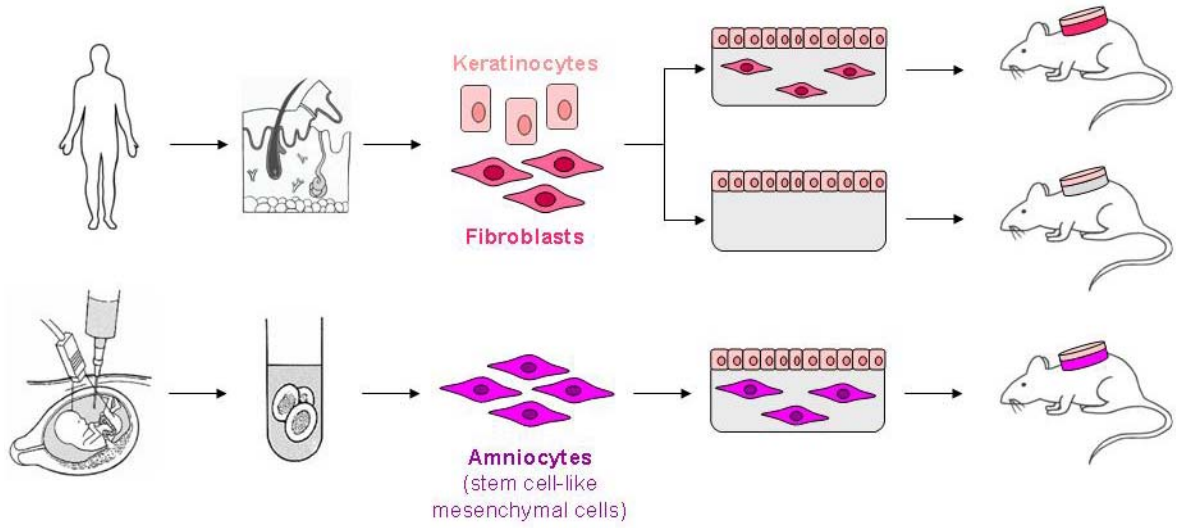

Figure 21: Experimental outline of publication II. Schematic overview on the experimental design of the manuscript entitled: *Human amniotic fluid derived cells can competently substitute dermal fibroblast in a tissue engineered dermo-epidermal skin analog*. Scheme of amniocentesis modified from (179).

3.4.3 Publication III

A new model for preclinical testing of dermal substitutes for human skin reconstruction:

The treatment of severe skin defects such as burns and congenital giant nevi often requires skin reconstruction. The today's gold standard in such cases is the transplantation of autologous split-thickness, either directly onto the wound bed, or it

can be transplanted onto a dermal substitute such as Integra or Matriderm. The development of such dermal substitutes requires intensive preclinical testing for its biological behaviour and compatibility with split-thickness skin. As human split-thickness skin is very limited for research purpose, we aimed in generating a model to test newly designed dermal substitutes in a humanized animal system, without the need for human split-thickness skin.

We combined different dermal substitutes with different human coverage grafts and transplanted them onto the back of immuno-incompetent rats (Figure 22). Grafts were analysed 21 days thereafter. As gold standard we used Matriderm and human split-thickness skin. This we compared to an engineered human coverage graft. To generate human engineered grafts, we isolated dermal fibroblasts and epidermal keratinocytes from a human skin biopsy. We incorporated the fibroblasts into a collagen type I hydrogel, and seeded keratinocytes on top of these gels. We transplanted the split-thickness skin, consisting of the epidermis and some parts of the dermis, directly onto the fascia, on Matriderm, and onto an acellular collagen type I hydrogel. The same three groups we used for neonatal rat epidermis, which only consists of about 1 layer of keratinocytes, and no dermal components. The human engineered grafts, consisting of dermal and epidermal compartments, we transplanted as well directly onto the fascia, onto Matriderm and on the acellular collagen hydrogel. All combinations of grafts were analysed three weeks post transplantation macroscopically, histologically and with immunofluorescence stainings.

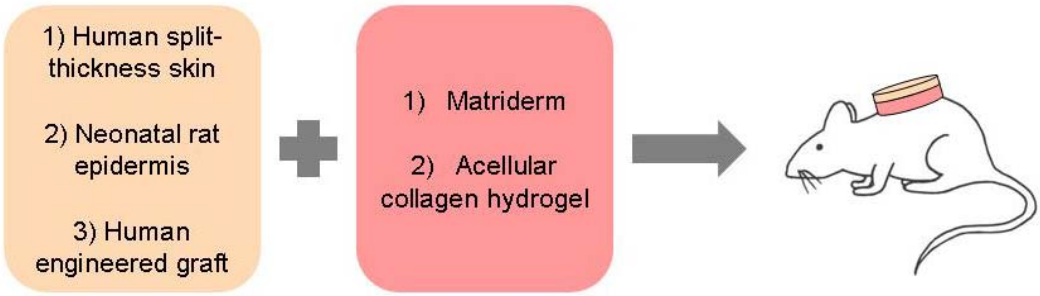

Figure 22: Experimental outline of publication III. Schematic overview on the experimental design of the manuscript entitled: *A new model for preclinical testing of dermal substitutes for human skin reconstruction.*

3.4.4 Publications IV + V

Skingineering I: Engineering porcine dermo-epidermal skin analogues for autologous transplantation in a large animal model
Skingineering II: Transplantation of large-scale laboratory-grown skin analogues in a new pig model:

One major disadvantage of the rat model is the small size of these animals. The skin substitutes transplanted onto the rats can only have a diameter of about 3 cm. But considering envisioned future clinical trials, the engineered dermo-epidermal skin substitutes also have to be pre-clinically evaluated in a size and shape relevant for clinical application. Therefore, to circumvent the shortcoming of the rat model, we aimed in establishing a large animal model that allows the transplantation of large engineered skin substitutes. As porcine skin has shown to be the closest relative to human skin with regard to anatomy and physiology (180-181), we decided aiming for a porcine model.

The pig allows to test skin substitutes of 49 cm^2, but requires autologous porcine skin substitutes as these immuno-competent animals otherwise would reject the transplants (Figure 23). To set up a new animal model requires several steps:

- Establishing a protocol to isolate and propagate porcine dermal fibroblasts and keratinocytes in the laboratory.
- Investigate the potential of these cells to generate a dermo-epidermal skin substitute *in vitro*
- Establishing a protocol for the transplantation of autologous skin substitutes to pigs, with regard to transplantation site, graft protection, and suitable wound dressing for these animals.

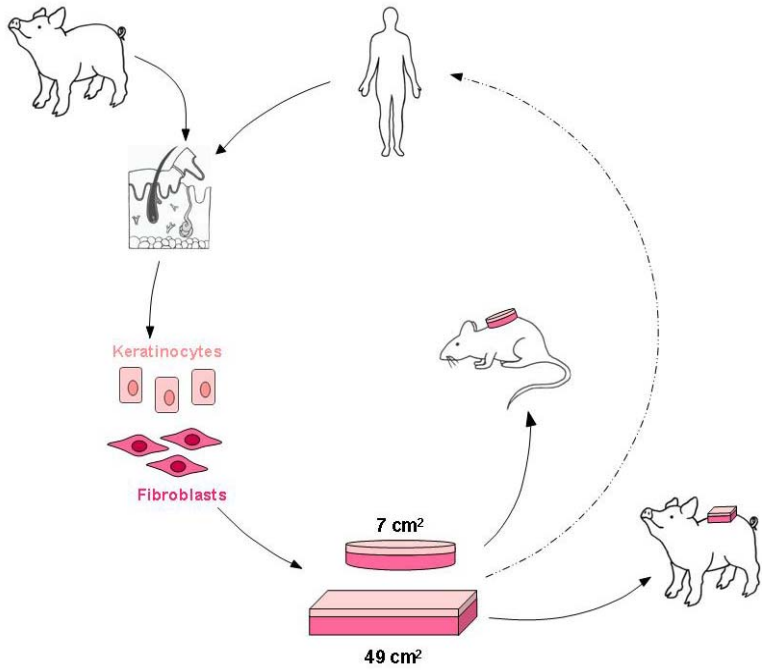

Figure 23: Experimental outline of publications IV and V. Schematic overview on the experimental design of the manuscripts entitled: *Skingineering I: Engineering porcine dermo-epidermal skin analogues for autologous transplantation in a large animal model*, and *Skingineering II: Transplantation of large-scale laboratory-grown skin analogues in a new pig model.* When working with the rat animal model, round skin substitutes of ~7 cm^2 can be transplanted with cells of human origin, as the rats are immuno-incompetent. When working with the porcine animal model, square skin substitutes of 49 cm^2 can be transplanted, but in contrast to the rat model, here the cells must be autologous cells for each animal.

4. RESULTS

4.1 Collagen hydrogels strengthened by biodegradable meshes are a basis for dermo-epidermal skin grafts intended to reconstitute human skin in a one-step surgical intervention

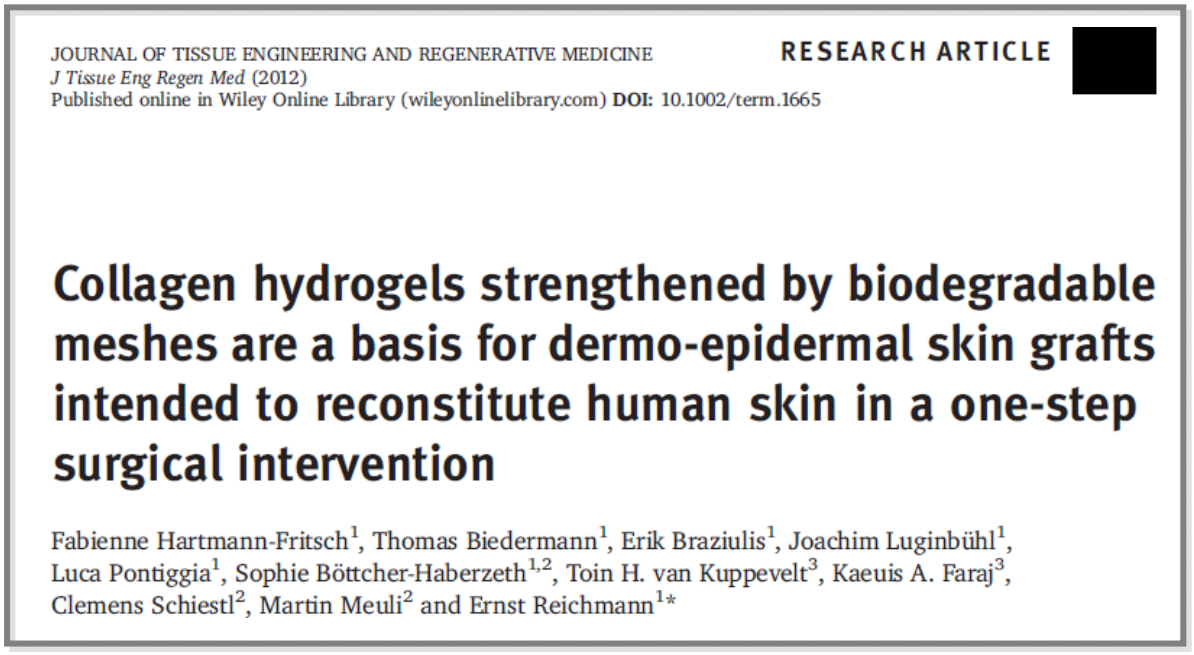

JOURNAL OF TISSUE ENGINEERING AND REGENERATIVE MEDICINE
J Tissue Eng Regen Med (2012)
Published online in Wiley Online Library (wileyonlinelibrary.com) **DOI:** 10.1002/term.1665

RESEARCH ARTICLE

Collagen hydrogels strengthened by biodegradable meshes are a basis for dermo-epidermal skin grafts intended to reconstitute human skin in a one-step surgical intervention

Fabienne Hartmann-Fritsch[1], Thomas Biedermann[1], Erik Braziulis[1], Joachim Luginbühl[1], Luca Pontiggia[1], Sophie Böttcher-Haberzeth[1,2], Toin H. van Kuppevelt[3], Kaeuis A. Faraj[3], Clemens Schiestl[2], Martin Meuli[2] and Ernst Reichmann[1]*

Abstract

Extensive full-thickness skin loss, associated with deep burns or other traumata, represents a major clinical problem that is far from being solved. A promising approach to treat large skin defects is the use of tissue-engineered full-thickness skin analogues with nearly normal anatomy and function. In addition to excellent biological properties, such skin substitutes should exhibit optimal structural and mechanical features. This study aimed to test novel dermo-epidermal skin substitutes based on collagen type I hydrogels, physically strengthened by two types of polymeric net-like meshes. One mesh has already been used in clinical trials for treating inguinal hernia; the second one is new but consists of a FDA-approved polymer. Both meshes were integrated into collagen type I hydrogels and dermo-epidermal skin substitutes were generated. Skin substitutes were transplanted onto immuno-incompetent rats and analyzed after distinct time periods. The skin substitutes homogeneously developed into a well-stratified epidermis over the entire surface of the grafts. The epidermis deposited a continuous basement membrane and dermo-epidermal junction, displayed a well-defined basal cell layer, about 10 suprabasal strata and a stratum corneum. Additionally, the dermal component of the grafts was well vascularised.

Introduction

Treatment of patients with extensive skin loss resulting from burns, soft tissue trauma, removal of congenital giant naevi and skin diseases still represents a major clinical problem that is far from being solved. None of the current therapeutic strategies, based on autologous split-thickness skin or cultured keratinocyte sheets transplanted onto dermal templates, such as Integra® or Matriderm®, yield truly satisfactory long-term functional and cosmetic results (Böttcher-Haberzeth et al., 2010; Gobet et al., 1997; Pandya et al., 1998; Schneider et al., 2009).

Hypothetically, a significant improvement may be reached by the use of a tissue-engineered, autologous full-thickness skin analogue to replace the missing skin.

Apart from exhibiting superb biological features, the skin substitute should possess adequate mechanical properties to allow easy handling by surgeons, permit sewing to the wound site and resist, to a certain extent, shear forces exerted on the area of transplantation (e.g. joint areas) (van der Veen et al., 2009). Due to its advantageous properties, collagen type I proved to be an ideal matrix for skin tissue engineering in preclinical models (Böttcher-Haberzeth et al., 2012; Braziulis et al., 2010; Faraj et al., 2007; Kinikoglu et al., 2009; Schiestl et al., 2010). This is in contrast to collagen sponges, such as Integra Dermal Regeneration Template® (Schiestl et al., 2011; Stiefel et al., 2010) and Matriderm® (Ryssel et al., 2008; van Zuijlen et al., 2000), into which and onto which it is difficult, if not impossible, to seed and grow skin cells. In contrast, collagen hydrogels mimic the natural extracellular matrix (ECM) of dermal fibroblasts, thereby significantly supporting their proliferation, migration and differentiation (Drury and Mooney, 2003; Elisseeff, 2008; Oh et al., 2012). In addition, fibroblasts can be submerged and evenly distributed within such a hydrogel. Markedly supported by the underlying fibroblasts, keratinocytes will proliferate on such gels and develop into a stratified epidermis (Bell et al., 1981; Parenteau et al., 1992; Stark et al., 2004). Due to the excellent biological properties of collagen hydrogels, dermo-epidermal grafts can be generated. Most importantly, these can be applied in only one surgical intervention (instead of two successive operations). Since in this procedure skin cells are massively expanded, the donor site for the biopsy is very small. In large burns, the availability of large enough donor sites is frequently a serious problem.

Major disadvantages of collagen hydrogels, however, are their physical weakness, contraction and degradation in combination with cells (Krishnan et al., 2004). However, it has been shown that these problems can be circumvented by varying collagen concentrations (Helary et al., 2010, 2011, 2012). Even more importantly, significantly improved stability of collagen hydrogels was reached by plastic compression (Hu et al., 2010; Levis et al., 2010), even allowing the construction of large, clinically relevant (49 cm^2) dermo-epidermal skin substitutes (Braziulis et al., 2012) and collagen gel tubes (Micol et al., 2011). Nevertheless, additional increased mechanical stability of skin substitutes is desirable to be able to fix them on the patient by sewing or stapling and to provide optimal handling characteristics. This can be achieved by the incorporation of a net-like mesh.

A long-term, resorbable, net-like fabric (TIGRW Surgical Mesh) was developed by the Swedish company Novus Scientific (Hjort et al., 2012). Based on its mechanical properties and its successful outcome in clinical trials, we assume that it also has high potential with regard to reinforcing our tissue-engineered skin substitutes. The fabric is a knitting of two types of fibres: fibre 1 consists of a co-polymer of trimethylene carbonate and lactide; fibre 2 consists of a co-polymer of trimethylene carbonate, lactide and glycolide. For the present study, the fibres of type 2 of this mesh were removed (leading to a modified TIGRW Surgical Mesh, referred to below as knitted mesh), as mainly stability over a longer time period was desired.

A second material showing high potential for application in skin tissue engineering is poly(lactic-*co*-glycolic acid) (PLGA). This co-polymer can be seeded with human skin fibroblasts (Chen et al., 2005) and is FDA-approved. It is synthesized by means of random ring-opening copolymerization of two different monomers, viz. glycolic acid and lactic acid, and has good biodegradability, suitable biodegradation kinetics, good mechanical properties and a certain ease of processing (Kumbar et al., 2008; Lu et al., 2009). A mesh-like PLGA sheet has been produced by aap Bioimplant. This electrospun mesh (as it is referred to below) exerts good biological characteristics and mechanical stability.

The goal of this study was to develop skin analogues exhibiting optimal biological and, in particular, also mechanical properties. The latter should be realized by including a biodegradable, net-like scaffold into the collagen hydrogel that eventually makes up the dermal part of a dermo-epidermal skin substitute. The scaffolds used are supposed to easily incorporate into a collagen hydrogel and

provide a maximum of stability for the time point of transplantation and the first period after transplantation, but thereafter should start to degrade without harming the surrounding tissue by their degradation products.

Materials and Methods

Biodegradable matrices: knitted mesh

The biodegradable knitted mesh (TIGRW Surgical Mesh) used in the study was kindly provided by Novus Scientific (Uppsala, Sweden). The mesh was originally made from two different multifilaments: multifilament 1 was made from a co-polymer of trimethylene carbonate and lactide and showed slow degradation kinetics, with good stability over a 9 month period; multifilament 2 was made from a co-polymer of trimethylene carbonate, lactide and glycolide, showed relatively fast degradation kinetics and was completely degraded after 6 months. The mesh was tested for biocompatibility according to the requirements found in standard ISO 10993-1. As the fibres of type 2 comprise about 40 wt% of the mesh, these fibres were removed for the present study by incubation of the mesh in an aqueous solution of 34.85 g/l dipotassium phosphate, pH 12, for 5 days, leaving a mesh composed only of fibres of type 1, viz. fibres of a co-polymer of trimethylene carbonate and lactide behind (Figure 1a). The knitted mesh consists of a co-polymer of trimethylene carbonate and lactide, with good stability over a period of at least 9 months (unpublished data from Novus Scientific). It has been shown that full resorption of the fibres is reached after 36 months (Hjort et al., 2012). Additionally, it has been shown that 4 months post implantation the mesh was surrounded by a moderate grade of fibrous tissue and induced an inflammatory reaction, similar to the reaction observed with a control mesh. At 15 and 24 months, the mesh induced a higher inflammatory reaction than the control mesh, with mainly higher recruitment of phagocytic cells, which is part of the degradation process, as evidenced by fibres displaying signs of degradation (Hjort et al., 2012). At 4, 9, 24 and 36 months after implantation the mesh was well integrated, without signs of encapsulation (Hjort et al., 2012).

Biodegradable matrices: electrospun mesh

The biodegradable electrospun mesh used in the present study was kindly provided by F. Yang (Department of Biomaterials, Radboud University Nijmegen Medical Centre, Nijmegen, The Netherlands). The biodegradable electrospun mesh (Figure 1b) is made of poly(lactic-*co*-glycolic acid) (PLGA; PURAC Biochem bv, Gorinchem, The Netherlands). Detailed procedures are described in Supplementary materials and methods (see Supporting information).

The ratio glycolide:lactide determines the degradation time of a poly(lactic-*co*-glycolic acid) polymer, with increasing percentages of lactide increasing the degradation time. However, the fastest degradation time was seen in PLGA with a ratio of 50:50 (Makadia and Siegel, 2011). The material used for this study was composed of PLGA in a ratio of 52:48 (52% D,L-lactide and 48% glycolide). Therefore, it was expected that this material exhibited a somewhat slower degradation than the 50:50 PLGA material, with an in vitro half-life of about 3-4weeks (Lu et al., 2000).

Cell isolation and culture

Human full-thickness skin biopsies were obtained after informed consent of the patient or parents. Human primary fibroblasts and keratinocytes were isolated and cultured as previously described (Biedermann et al., 2010; Kiowski et al., 2012; Pontiggia et al., 2009). Detailed procedures are described in Supplementary materials and methods (see Supporting information).

Engineering of dermo-epidermal skin substitutes

Organotypic cultures for a dermo-epidermal skin substitute were prepared as earlier described (Pontiggia et al., 2009), using a previously established transwell system (six-well cell culture inserts with membranes of 3 mm pore size; BD Falcon, Basel, Switzerland). Briefly, membranes were covered with either the knitted mesh (Figure 2a) or the electrospun mesh (Figure 2b). Subsequently, a solution of bovine collagen type I (BD Biosciences, Basel, Switzerland) was mixed with $1x10^5$ human primary dermal fibroblasts and neutralized with a buffer containing NaOH (Costea et al., 2003) just before pouring the solution on the scaffolds. Additionally, constructs were engineered without any scaffold incorporated as internal control (Figure 2c). After performing compression according to Braziulis et al. (Braziulis et al., 2012; Brown et al., 2005), the hydrogels were cultured for 5 days in fibroblast growth medium before seeding $7.5x10^5$ keratinocytes onto the complete surface of the hydrogels. After initial submersed cultivation in Rheinwald and Green keratinocyte differentiation medium (RGM) (Rheinwald and Green, 1975) for 3 days, the medium level was lowered to expose the developing epidermis to air (air–liquid interface; Gauvin et al., 2012) for an additional 3 days before transplantation of the constructs onto immuno-incompetent rats. Medium changes were performed every 2–3days.

Fluorescein diacetate live cell staining

Fluorescein diacetate (FdA; Sigma, Buchs, Switzerland) staining was performed to determinate cell viability, as previously described (Armour et al., 2008; Jones and Senft, 1985). Briefly, the cell culture medium was removed and replaced with a dilution of 5 mM FdA in PBS (Invitrogen) for 2 min. FdA solution was removed by washing twice with PBS and was replaced by RGM. Fluorescein fluorescence was evaluated using microscopy (Nikon SMZ1500 fluorescent stereo microscope, FITC filter, Nikon DXM1200F camera).

Transplantation of dermo-epidermal skin substitutes

All animal experiments were approved by the local Committee for Experimental Animal Research. Dermo-epidermal skin substitutes were transplanted onto full-thickness skin defects created surgically on the backs of immuno-incompetent female nu/nu rats, aged 8–10 weeks (Harlan, Horst, The Netherlands), as previously described (Biedermann et al., 2010; Kiowski et al., 2012). The animal numbers were: skin substitutes with knitted mesh, n=7 (Figure 2a); skin substitutes with electrospun mesh, n=7 (Figure 2b); skin substitutes without mesh, n=7 (Figure 2c). All animals survived the procedure and the 3weeks post transplantation. A steel ring, 27 mm in diameter, was used as a modified Fusenig chamber (Fusenig et al., 1983) and the transplants were covered with silicon foil. Three weeks after transplantation, all the animals were sacrificed and the grafts excised and processed for cryo- and paraffin sections. For that, samples were halved and either embedded in OCT compound (Tissue-Tek®, Sakura Finetek, Japan) or fixed in 4% paraformaldehyde (Medite Medizintechnik AG, Nunningen, Switzerland) and embedded in paraffin (McCormick, Richmond, USA).

Histology and immunofluorescence

Paraffin-embedded tissue was sectioned by microtome (Leica, Wetzlar, Germany), and 10 mm sections were stained with haematoxylin and eosin (H&E; Sigma) and imaged by light microscopy. OCT compound-embedded tissue was used for cryosections (Leica) and 10 mm sections were used for indirect immunofluorescence. Detailed procedures are described in Supplementary materials and methods (see Supporting information).

Fluorescence microscopy

Immunofluorescence stainings were analyzed using a Nikon Eclipse TE2000-U inverted microscope with Hoechst, FITC and TRICT filter sets connected with a DXM1200F digital camera (Nikon AG, Egg, Switzerland). Images were processed with Photoshop 7.0 (Adobe Systems, Munich, Germany).

Scanning electron microscopy

Scanning electron microscopy (SEM) was performed at the Centre for Microscopy and Image Analysis (University of Zurich, Switzerland). Detailed procedures are described in Supplementary materials and methods (see Supporting information).

Results

Knitted and electrospun meshes integrate into collagen type I hydrogels

We investigated two different polymer meshes and their integration into plastically compressed collagen type I hydrogels. One of these meshes consisted of a slow degrading multifilament produced using a co-polymer of trimethylene carbonate and lactide (Figure 1a). Scanning electron microscopy (SEM) revealed interwoven bundles of about 20 polymer fibres, creating a physically resistant porous mesh (Figure 1c). The second mesh was an electrospun fabric consisting of 52% D,L-lactide and 48% glycolide, with a molecular weight of 153 000; poly(lactic-*co*-glycolic acid) (PLGA) (Figure 1b). SEM showed that the individual fibres of this mesh were arranged in a nonwoven manner and mostly orientated unidirectionally (Figure 1d).

SEM of both fibres incorporated in collagen type I hydrogels showed solid incorporation of the polymer meshes into the collagen hydrogels (Figure 1e, f). The hydrogels surrounded the fibres in all directions; fibres were only visible at the borders of the samples where the samples were cut (Figure 1e, f, white arrowheads).

Dermo-epidermal skin grafts strengthened by biodegradable meshes

Our goal was to develop highly functional dermo-epidermal skin substitutes that can be optimally applied onto the patient. Cell survival, proliferation, differentiation and epidermal stratification in vitro were evaluated by fluorescein diacetate (FdA) live-cell staining and additional histological analyses.

FdA stainings of a dermo-epidermal skin substitute with knitted mesh incorporated into its dermal part were performed at two different time points. These stainings showed that the keratinocytes seeded on this hydrogel do not form a confluent layer 1 day after seeding (Figure 3a), but during a cultivation phase of 2–3 days they proliferate and develop into a confluent cell layer
(Figure 3c).

Similar FdA stainings were performed with collagen type I hydrogels containing fibroblasts and the incorporated electrospun mesh. Here also, the keratinocyte layer was not confluent 1 day after keratinocyte seeding (Figure 3b). After an additional 2–3 day cultivation phase, the keratinocytes proliferated and formed a confluent cell layer, as FdA staining confirmed (Figure 3d).

The presence of an epidermis, consisting of two or three layers of keratinocytes, on the dermo-epidermal skin substitute with incorporated knitted mesh was also confirmed using H&E staining (Figure 3e). In the dermal part, fibroblasts and remnants of the knitted mesh were detectable (Figure 3e, black arrowheads). On H&E stained cryosections of the skin substitutes with incorporated electrospun mesh, similar results were obtained, showing a two- or three-layered epidermis on top of a fibroblast-containing dermal part with remnants of the electrospun mesh (Figure 3f, black arrowheads).

In addition to the suitability of the mesh to allow cell survival and proliferation, the collagen hydrogel containing the knitted mesh also showed excellent handling properties and smoothly adapted to a given underlying shape, as both round patches of 2.5 cm diameter and square skin substitutes of 7x7 cm (Figures 3g, h, 4a).

Testing dermo-epidermal skin substitutes in vivo

The dermo-epidermal skin substitutes were tested in an animal model on full-thickness skin defects of approximately 5 cm^2. Substitutes containing the two different types of scaffolds (Figure 4a, c) were transplanted onto the backs of immuno-incompetent (nu/nu) rats. A modified Fusenig chamber was used to prevent wound closure by the ingrowth of adjacent rat skin (Figure 4b, d). Three weeks after transplantation, the grafts were excised and the specimens were examined histologically. Macroscopic analyses revealed a homogeneous skin-like appearance on the entire grafted area (Figure 4b, d). H&E staining confirmed the macroscopic impression and revealed that dermo-epidermal skin substitutes with either of the meshes exhibited a well-stratified, continuous epidermis that had developed over the entire surfaces of the grafts, including a stratum corneum (Figure 4e–h). The results were comparable to grafts without any reinforcing mesh (Figure 4i). Remnants of both meshes were detected for both scaffold types in correspondence with the degradation times of these scaffolds. The development of the epidermis was supported by ingrowing blood vessels originating in the underlying dermal tissue, as revealed by higher magnification pictures (Figure 4g, h). Blood vessels not only grew into the dermo-epidermal skin substitutes, but were also found in close proximity to remnants of the mesh (Figure 4g, h), thus underlining the non-toxic properties of the scaffolds.

Characterization of dermo-epidermal skin substitutes

To evaluate the quality of the skin developed from the transplanted dermo-epidermal skin substitute, immunofluorescence staining was performed using a set of established markers for wound healing and skin homeostasis.

Cytokeratin 1 (K1) is expressed in all suprabasal keratinocyte layers in normal homeostatic skin. This was also observed in both types of transplants, as well as in the control, 3weeks after transplantation (Figure 5a–c). Deposition of the basal lamina was detected by using an antibody to laminin 5 (Figure 5a–c). In combination, these stainings revealed that a state close to homeostasis was reached, showing a stratum basale typically not expressing K1 (just the blue nuclei stained by Hoechst dye are visible) and the suprabasal, K1-positive keratinocyte layers (Figure 5a-c). Just as in healthy human skin, cytokeratin 15 (K15) was exclusively expressed in basal keratinocytes anchored to a functional basal lamina (Figure 5d–f). In healthy skin of very young children (up to 1.5 years), a subpopulation of K15-expressing basal cells is positive for cytokeratin 19 (K19) (Pontiggia et al., 2009). In accordance with this, 3weeks after transplantation, a subset of K15-positive cells were found to express K19 (Figure 5d–f), indicating a young and self-renewing subset of keratinocytes in the stratum basale. As seen in Figures 5d, e, some of the K19-positive keratinocytes were still detectable in suprabasal layers, indicating that the final homeostatic state was not yet established. This, however, was not surprising at such an early stage after transplantation. Double staining using a human-specific fibroblast marker (CD90) and a rat-specific blood vessel marker (CD31) revealed that blood vessels of rat origin grew into the dermal part of the grafted skin substitute within 21 days, thereby ensuring proper humoral support of the epidermis (Figure 5g–i). Notably, employing the melanosome marker HMB45 proved that human melanocytes, co-cultured with human keratinocytes in both matrix-supported collagen hydrogels, not only survived in the three-dimensional (3D) skin substitutes but were maintained in physiological numbers within the basal cell layer for the period of investigation (Figure 5j–l).

Taken together, it can be said that the included net-like scaffolds only moderately, if at all, slowed down the development of epidermal homeostasis in the tested dermo-epidermal substitutes. In summary, these results revealed that the developed epidermis was well stratified but, nevertheless, was not yet in a completely homeostatic situation.

Scanning electron microscopy analysis

Scanning electron microscopy (SEM) was performed with specimens of the grafted dermo-epidermal skin substitutes 21 days after transplantation. Punch biopsies were taken after excision of the grafts and cross-sections of the biopsies were processed for SEM.

An overview showing the general appearance of the skin substitute with the knitted mesh is shown in Figure 6a. Fibres of this mesh were quite prominent in the dermal part of this skin substitute and an intact epidermis was evident (Figure 6a, white arrow). Skin substitutes containing the electrospun mesh exhibited scaffold remnants that appeared as melted bulbs, which are artefacts due to the SEM preparation procedure (Figure 6b and insert). Nevertheless, the electrospun mesh required less space than the knitted mesh (Figure 6a, b). Higher magnifications of the skin substitutes with the incorporated knitted mesh revealed the high content of collagen fibres in the dermal part. Interestingly, collagen fibres were found not only around the fibre bundles of the knitted mesh but also in close association with the individual mesh fibres, providing evidence for a very good incorporation of the mesh into the substitute (Figure 6c). Higher magnification of the skin substitute with electrospun mesh showed a well-structured epidermis, including a tight basal cell layer, several suprabasal layers and the squamous stratum corneum (Figure 6d). In accordance with the data presented in Figures 4g, h, 5g, h, SEM also revealed that blood vessels were located in close proximity to both types of mesh fibres (Figure 6e, f and inserts in 6e, f).

Discussion

The treatment of massive full-thickness skin defects with tissue-engineered skin grafts has shown promise in preclinical studies and clinical trials. Most of these skin grafts comprised fibroblasts and/or keratinocytes grown on collagen 'sponges', generated by freeze-drying (Boyce et al., 1995). These sponges, however, hardly permit fibroblasts to reach the inner sponge pores; thus, an even distribution of these cells is almost impossible (Powell et al., 2008). In addition, these porous structures represent a barrier for cells and factors that induce essential signals for the epidermis–dermis crosstalk. This is a significant disadvantage, as fibroblasts are essential to promote epidermal cell survival, proliferation and differentiation (El Ghalbzouri et al., 2002). Thus, a biologically ideal collagen type I hydrogel with incorporated fibroblasts represents a valid dermal template for a skin substitute. Indeed, the living fibroblasts in the substitute create a cell-instructive environment which constantly produces and releases a physiological set of biologically active growth factors, cytokines and matrix components in physiological concentrations (Braziulis et al., 2012; Pontiggia et al., 2009; Schneider et al., 2010). A recently published related approach is based on the same elegant idea of employing a synthetic degradable mesh to stabilize a compressed hydrogel (Ananta et al., 2012). It describes a living allogenic wound dressing. Since this wound dressing will be immunologically removed with time, it will transiently support wound healing. Notably, these authors state that the presence of keratinocyte layers on this dressing may not be essential for skin wound healing (Ananta et al., 2012).

In contrast, our goal was the generation of an autologous skin graft, to be applied as a permanent skin substitute. Clearly, this skin graft requires both a functional dermal and epidermal component. Here we present a method that combines the excellent biological properties of a skin substitute, based on a plastically compressed collagen type I hydrogel, with the mechanical support provided by a degradable mesh, and the possibility of surgically fixing this skin graft on the wound site. We found that an electrospun mesh made of poly(lactic-*co*-glycolic acid), as well as a knitted mesh composed of a co-polymer of trimethylene carbonate and lactide, could easily be incorporated into collagen type I hydrogels. Neither mesh interfered with cell survival and proliferation in vitro and in vivo. Both meshes allowed the development of a normally stratified epidermis with a basal

lamina, several suprabasal cell layers and a stratum corneum in vivo. The substitutes survived for at least 3weeks in vivo, indicating that they were nourished by ingrowing blood vessels of recipient (rat) origin. In an early state of organ reconstitution, the engineered dermo-epidermal skin substitutes expressed a characteristic set of established, skin-specific wound-healing markers (Biedermann et al., 2010; Pontiggia et al., 2009). At later stages, markers indicating the establishment of skin tissue homeostasis became expressed. The pattern of these markers was similar to the one found in well-regenerated skin. An identical pattern of markers was found in hydrogel-based grafts generated without any stabilizing meshes.

The skin graft containing the knitted mesh could be handled more conveniently than the substitute with the electrospun mesh; the first fitted ideally and adhered more smoothly to a given wound surface. This might be a result of the higher flexibility and higher total volume of the mesh inside the graft.

We therefore propose that a knitted mesh is probably the best choice currently available. However, the number of fibres may still be reduced (as compared to the one described herein), so that the ideal timing between the initial tissue reinforcement and the subsequent mesh degradation can be realized.

Conflict of interest

The authors have declared that there is no conflict of interest.

Acknowledgements

We thank Torbjörn Mathisen from Novus Scientific for providing us with the TIGRW surgical mesh and Fang Yang from the Radboud University Nijmegen for producing the electrospun mesh. We thank Klaus Marquardt from the Center for Microscopy and Image Analysis, University of Zurich, Switzerland, for valuable help with SEM. This work was supported by a grant from the European Union (Grant No. EuroSTEC: LSHB-CT-2006-037409) and by the University of Zurich. We are particularly grateful to the Fondation Gaydoul for its significant support. Furthermore, we like to thank the sponsors of Dona Tissue (Thérèse Meier and Robert Zingg), the Vontobel Foundation and the Werner Spross Foundation for their financial support and their interest in our work.

Figures

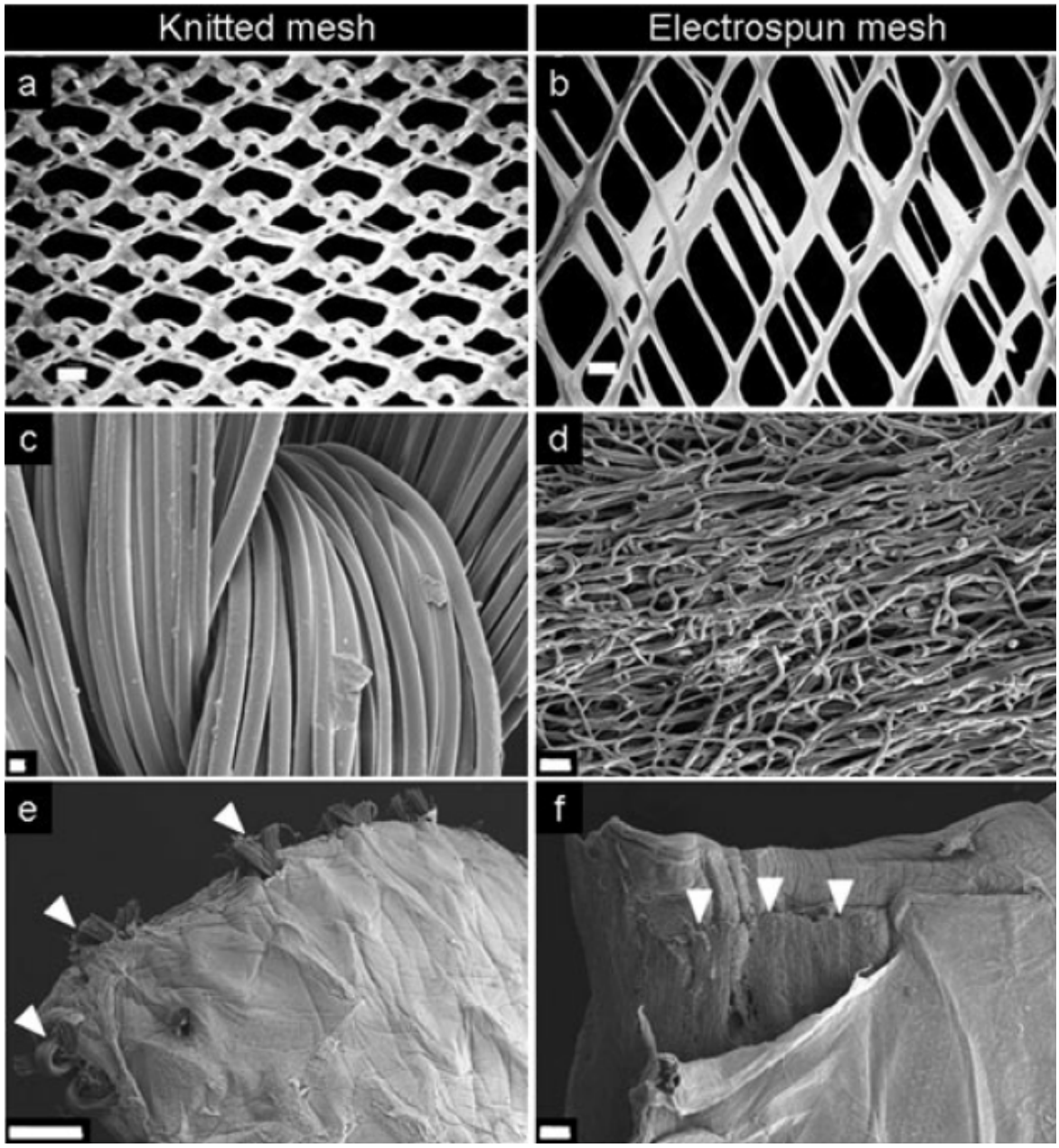

Figure 1. Microscopical analyses of knitted and electrospun meshes: light microscopic view of (a) the knitted and (b) the electrospun meshes; (c) single fibres of the knitted mesh revealed by SEM; (d) the dense network of fibres in the electrospun mesh revealed by SEM; (e, f) SEM micrographs of collagen type I hydrogels surrounding the incorporated meshes. White arrowheads, fibres of the two different scaffolds. Scale bars = 1mm (a, b, e); 10mm (c); 20mm (d); 200mm (f)

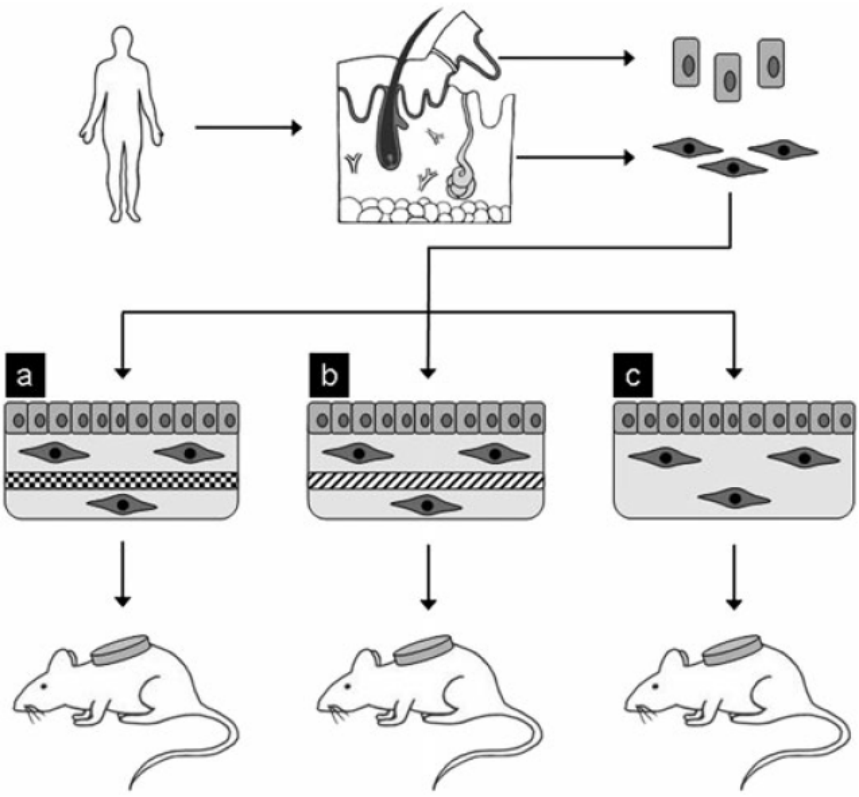

Figure 2. Schematic representation of experimental design. Human full-thickness skin biopsies are used to isolate human primary fibroblasts and keratinocytes. Dermo-epidermal skin substitutes are generated with either: (a) incorporated knitted mesh; (b) incorporated electrospun mesh; or (c) no incorporated scaffold. The dermo-epidermal skin substitutes were transplanted onto the back of immuno-incompetent rats. Three weeks post-transplantation, the grafts were excised and analysed.

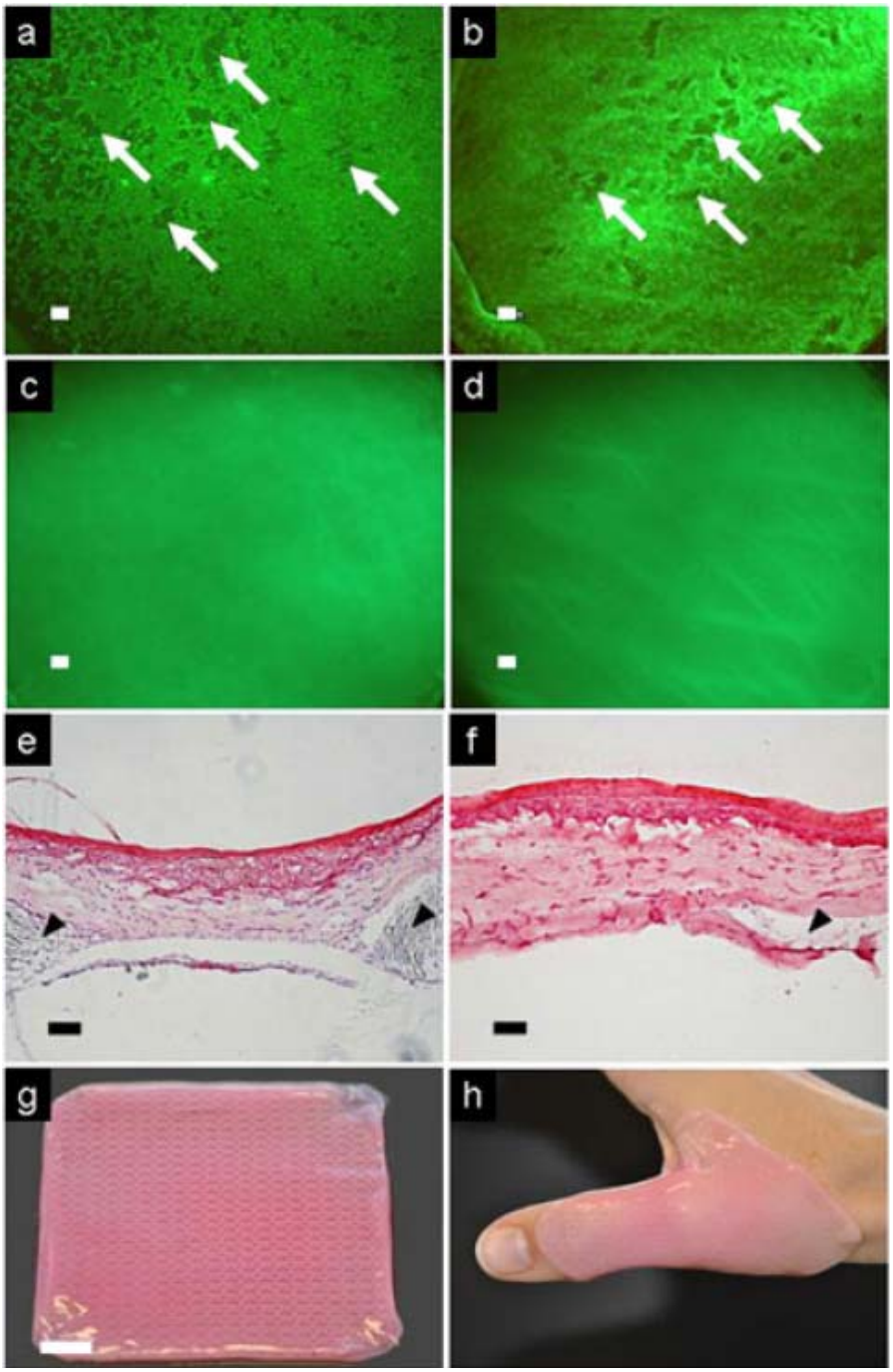

Figure 3. In vitro properties of the dermo-epidermal skin substitutes stabilized by the two different meshes. (a–d) Live cell staining of keratinocyte layers using fluorescein diacetate: (a, b) on both grafts, 1 day after keratinocyte seeding, the keratinocytes did not form a confluent layer; white arrows, areas with holes in the keratinocyte layer; (c, d) on both grafts, keratinocytes have proliferated into confluent cell layers 2–3 days after seeding. (e, f) H&E staining of histological sections of the skin graft containing (e) the knitted and (f) the electrospun meshes, 7 days after keratinocyte seeding. Black arrowheads, remnants of the polymeric fibres. (g, h) Macroscopic views of the construct with the knitted mesh demonstrate its excellent handling properties. Scale bars=1 mm (a–d); 100mm (e); 50mm (f); 1cm(g)

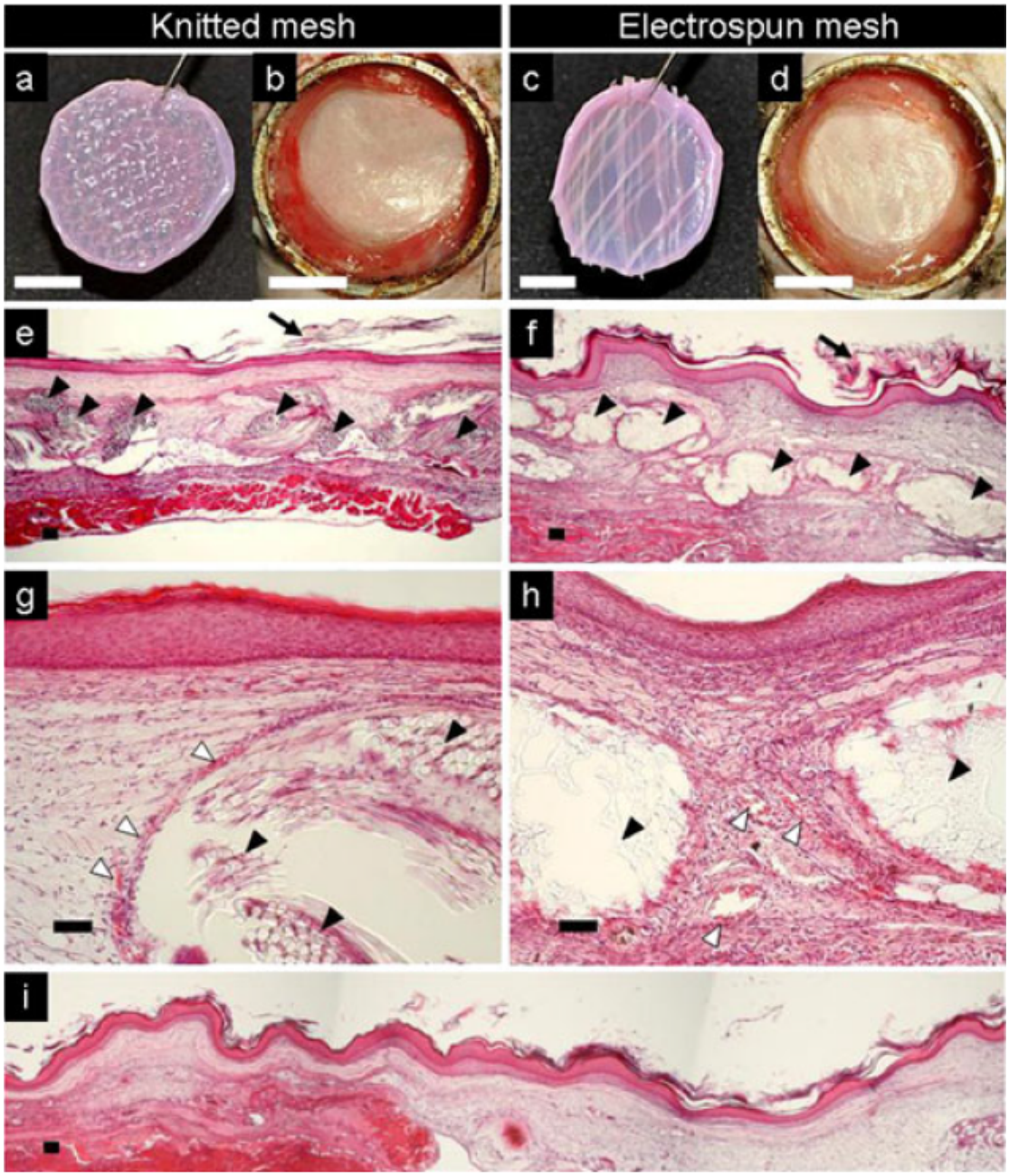

Figure 4. Stabilized dermo-epidermal skin substitutes in vivo. Macroscopic view of the skin substitute containing the knitted mesh (a) before and (b) 3weeks after transplantation onto immuno-incompetent nude rats, showing its highly organotypic appearance. (c, d) Corresponding macroscopic views of the substitute with the electrospun mesh. (e, f) H&E-stained sections of the two types of grafts, 21 days after transplantation, reveals a well-stratified epidermis. Black arrowheads, remnants of the scaffolds; arrows, stratum corneum. (g, h) Higher magnifications showing ingrown blood vessels (white arrowheads) in close proximity to scaffold remnants (black arrowheads). (i) Histology of a control dermo-epidermal skin substitute without any reinforcing mesh reveals a well-stratified epidermis. Scale bars=1cm (a–d); 100mm (e, f, i); 50mm (g, h)

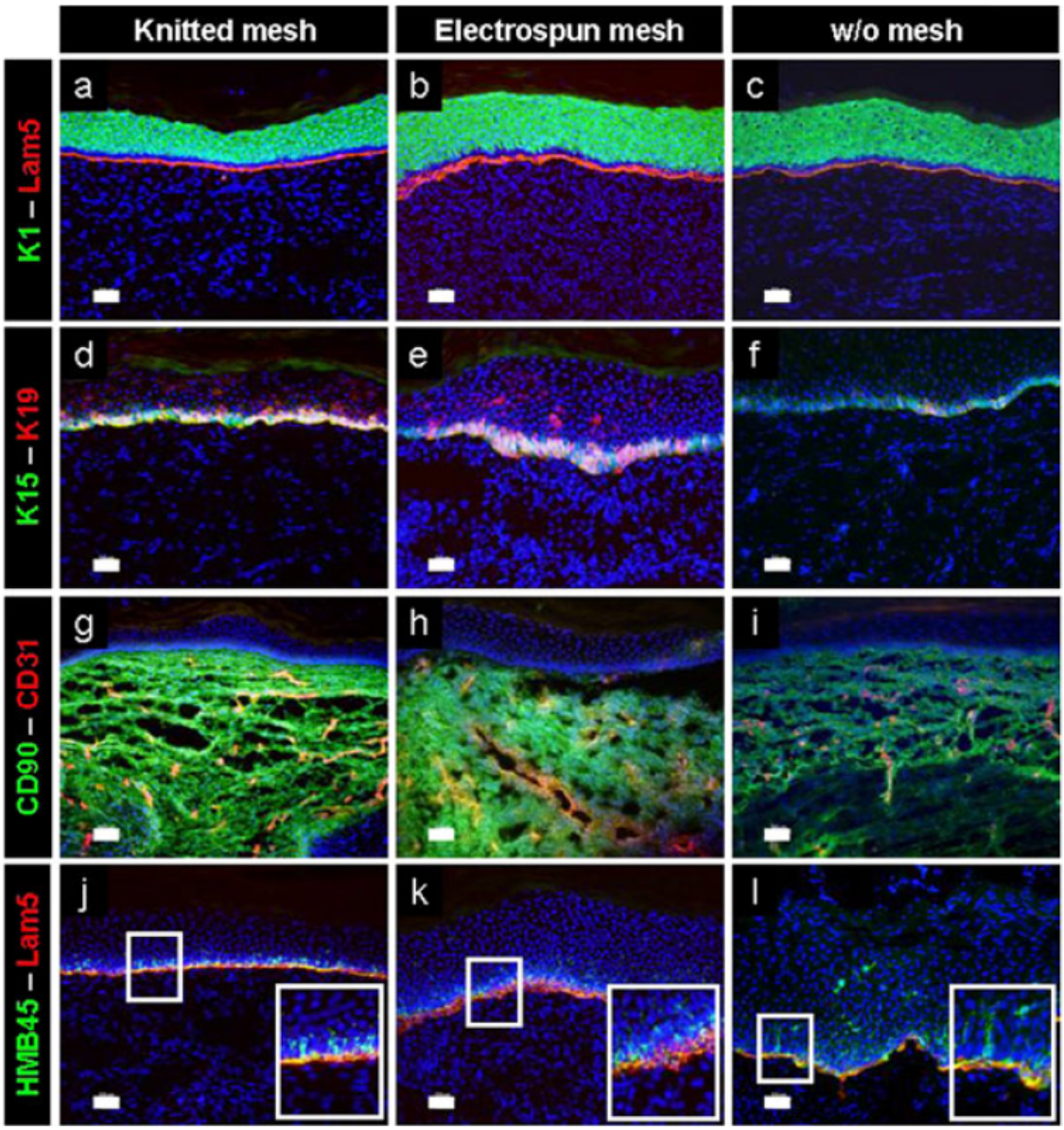

Figure 5. Immunofluorescence analyses of the dermo-epidermal skin substitutes with either knitted or electrospun mesh or without any reinforcing mesh, excised 21 days after transplantation. (a–c) In accordance with the normal physiology, cytokeratin 1 (green) is expressed in all suprabasal layers of the grafts, while the basal layer is excluded. Laminin 5 staining (red) reveals deposition of a continuous basement membrane. (d–f) Staining for cytokeratin 15 (green) reveals restriction of K15 expression to basal cells, whereas cytokeratin 19 (red) expression is mostly found in basal cells but also still in some suprabasal keratinocytes. (g–i) Human dermal fibroblasts (green) are recognized by the human CD90 (Thy-1)-specific antibody, whereas the rat tissue is not stained, CD31 (red) is specifically expressed in blood vessels of rat origin, ingrown into the dermal part of the substitute. (j–l) Staining of human melanocytes withHMB-45 (green) and co-staining of laminin 5 (red) reveals human melanocytes maintained in physiological numbers in the basal cell layer of the substitutes. (a–l) Nuclei are stained with Hoechst dye (blue). Scale bars=50mm (a–f, h–l); 100mm (g)

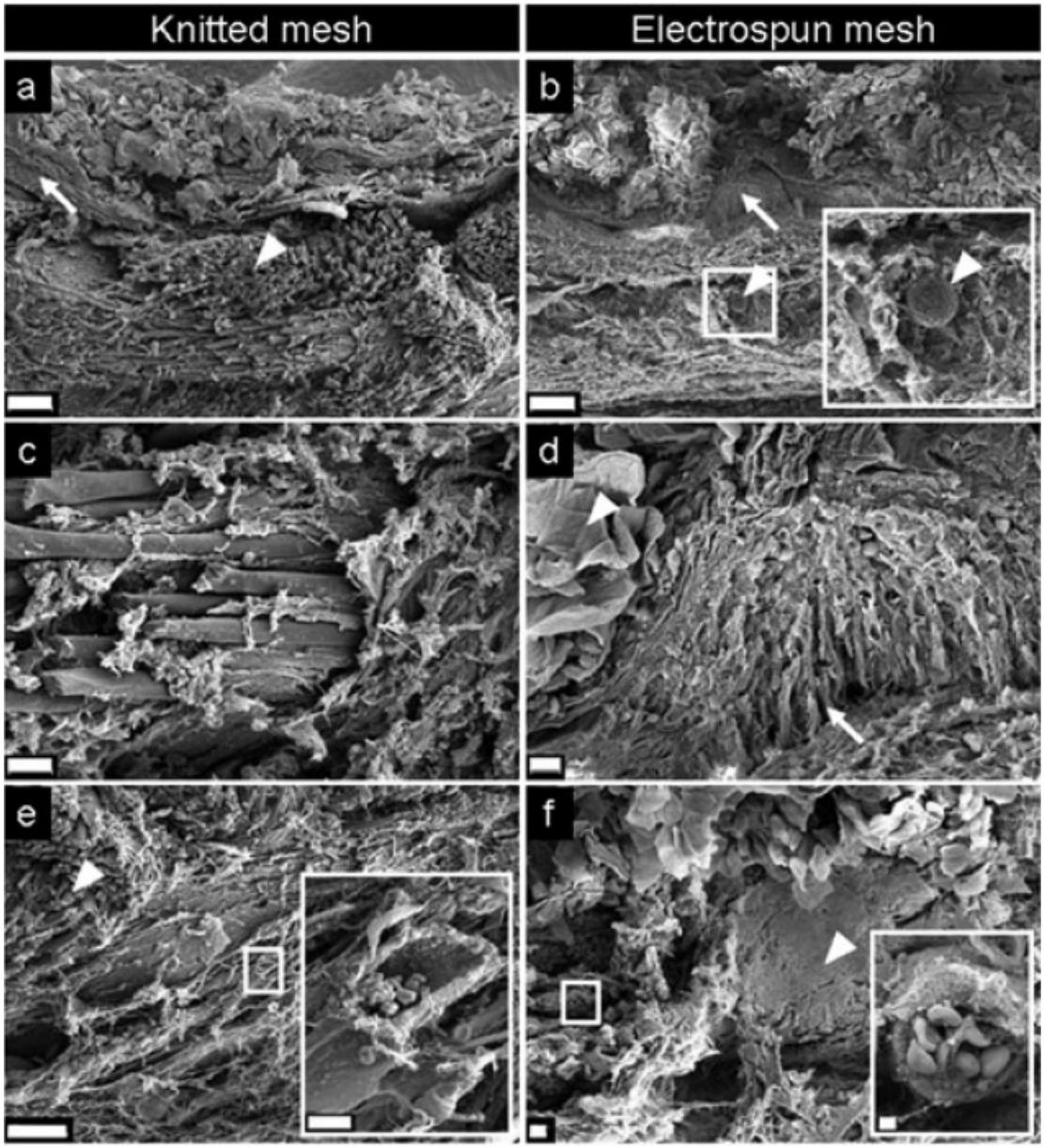

Figure 6. Scanning electron microscopy of dermo-epidermal skin substitutes containing either the knitted or the electrospun mesh, excised 21 days after transplantation. (a) Dermo-epidermal skin substitute containing knitted mesh shows an intact epidermis (white arrow); white arrowhead, fibres of the knitted mesh in the dermal part of the skin substitute. (b) Likewise, the substitute with electrospun mesh shows a well-stratified epidermis (white arrow). Mesh fibres are detectable as melted bulbs, due to preparation artefacts (white arrowhead and insert). (c) Distribution of collagen fibres around and between single mesh fibres. (d) Higher magnification shows organization of the epidermis (white arrow), several suprabasal cell layers and a prominent stratum corneum (arrowhead). (e, f) Higher magnifications show blood vessels in close proximity to the fibres of the knitted and electrospun meshes. Arrowheads, remnants of meshes. Scale bars=100mm (a, b, e); 20mm (c); 10mm (d, e insert, f); and 2mm (f insert)

References

Ananta M, Brown RA, Mudera V. 2012; A rapid fabricated living dermal equivalent for skin tissue engineering: an in vivo evaluation in an acute wound model. Tissue Eng Part A 18(3–4): 353–361.

Armour AD, Powell HM, Boyce ST. 2008; Fluorescein diacetate for determination of cell viability in tissue-engineered skin. Tissue Eng C 14(1): 89–96.

Bell E, Ehrlich HP, Buttle DJ, et al. 1981; Living tissue formed in vitro and accepted as skin-equivalent tissue of full thickness. Science 211(4486): 1052–1054.

Biedermann T, Pontiggia L, Böttcher-Haberzeth S, et al. 2010; Human eccrine sweat gland cells can reconstitute a stratified epidermis. J Invest Dermatol 130(8): 1996–2009.

Böttcher-Haberzeth S, Biedermann T, Reichmann E. 2010; Tissue engineering of skin. Burns 36(4): 450–460.

Böttcher-Haberzeth S, Biedermann T, Schiestl C, et al. 2012; Matriderm® 1mm versus Integra® single layer 1.3mm for one-step closure of full thickness skin defects: a comparative experimental study in rats. Pediatr Surg Int 28(2): 171–177.

Boyce ST, Goretsky MJ, Greenhalgh DG, et al. 1995; Comparative assessment of cultured skin substitutes and native skin autograft for treatment of full-thickness burns. Ann Surg 222(6): 743–752.

Braziulis E, Biedermann T, Hartmann-Fritsch F, et al. 2010; Skingineering I: engineering porcine dermo-epidermal skin analogues for autologous transplantation in a large animal model. Pediatr Surg Int 27(3): 241–247.

Braziulis E, Diezi M, Biedermann T, et al. 2012; Modified plastic compression of collagen hydrogels provides an ideal matrix for clinically applicable skin substitutes. Tissue Eng C 18(6): 464–474.

Brown RA, Wiseman M, Chuo CB, et al. 2005; Ultrarapid engineering of Biomimetic materials and tissues: fabrication of nano and microstructures by plastic compression. Adv Funct Mater 15(11): 1762–1770.

Chen G, Sato T, Ohgushi H, et al. 2005; Culturing of skin fibroblasts in a thin PLGA–collagen hybrid mesh. Biomaterials 26(15): 2559–2566.

Costea DE, Loro LL, Dimba EAO, et al. 2003; Crucial effects of fibroblasts and keratinocyte growth factor on morphogenesis of reconstituted human oral epithelium. J Invest Dermatol 121(6): 1479–1486.

Drury JL, Mooney DJ. 2003; Hydrogels for tissue engineering: scaffold design variables and applications. Biomaterials 24(24): 4337–4351.

El Ghalbzouri A, Lamme E, Ponec M. 2002; Crucial role of fibroblasts in regulating epidermal morphogenesis. Cell Tissue Res 310(2): 189–199.

Elisseeff J. 2008; Hydrogels: structure starts to gel. Nat Mater 7(4): 271–273. Faraj KA, van Kuppevelt TH, Daamen WF. 2007; Construction of collagen scaffolds that mimic the three-dimensional architecture of specific tissues. Tissue Eng 13(10): 2387–2394.

Fusenig NE, Breitkreutz D, Dzarlieva RT, et al. 1983; Growth and differentiation characteristics of transformed keratinocytes from mouse and human skin in vitro and in vivo. J Invest Dermatol 81(1, suppl): 168–175 s.

Gauvin R, Larouche D, Marcoux H, et al. 2012; Minimal contraction for tissue engineered skin substitutes when matured at the air–liquid interface. J Tissue Eng Regen Med [Epub ahead of print].

Gobet R, Raghunath M, Altermatt S, et al.1997; Efficacy of cultured epithelial autografts in pediatric burns and reconstructive surgery. Surgery 121(6): 654–661. Helary C, Abed A, Mosser G, et al. 2011; Synthesis and in vivo integration of improved concentrated collagen hydrogels. J Tissue Eng Regen Med 5(3): 248–252.

Helary C, Bataille I, Abed A, et al. 2010; Concentrated collagen hydrogels as dermal substitutes. Biomaterials 31(3): 481–490.

Helary C, Zarka M, Giraud-Guille MM. 2012; Fibroblasts within concentrated collagen hydrogels favour chronic skinwound healing. J Tissue Eng Regen Med 6(3): 225–237.

Hjort H, Mathisen T, Alves A, et al. 2012; Three-year results from a preclinical implantation study of a long-term resorbable surgical mesh with time-dependent mechanical characteristics. Hernia 16(2): 191–197.

Hu K, Shi H, Zhu J, et al. 2010; Compressed collagen gel as the scaffold for skin engineering. Biomed Microdevices 12(4): 627–635.

Jones KH, Senft JA. 1985; An improved method to determine cell viability by simultaneous staining with fluorescein diacetate-propidium iodide. J Histochem Cytochem 33(1): 77–79.

Kinikoglu B, Auxenfans C, Pierrillas P, et al. 2009; Reconstruction of a full-thickness collagen-based human oral mucosal equivalent. Biomaterials 30(32): 6418–6425.

Kiowski G, Biedermann T, Widmer DS, et al. 2012; Engineering melanoma progression in a humanized environment in vivo. J Invest Dermatol 132(1): 144–153.

Krishnan L, Weiss JA, Wessman MD, et al. 2004; Design and application of a test system for viscoelastic characterization of collagen gels. Tissue Eng 10(1–2): 241–252.

Kumbar SG, Nukavarapu SP, James R, et al. 2008; Electrospun poly(lactic acid-coglycolic acid) scaffolds for skin tissue engineering. Biomaterials 29(30): 4100–4107.

Levis HJ, Brown RA, Daniels JT. 2010; Plastic compressed collagen as a Biomimetic substrate for human limbal epithelial cell culture. Biomaterials 31(30): 7726–7737.

Lu JM, Wang X, Marin-Muller C, et al. 2009; Current advances in research and clinical applications of PLGA-based nanotechnology. Expert Rev Mol Diagn 9(4): 325–341.

Lu L, Peter SJ, Lyman MD, et al. 2000; In vitro and in vivo degradation of porous poly(DL-lactic-co-glycolic acid) foams. Biomaterials 21(18): 1837–1845.

Makadia HK, Siegel SJ. 2011; Poly lactic-coglycolic acid (PLGA) as biodegradable controlled drug delivery carrier. Polymers (Basel) 3(3): 1377–1397.

Micol LA, Ananta M, Engelhardt EM, et al. 2011; High-density collagen gel tubes as a matrix for primary human bladder smooth muscle cells. Biomaterials 32(6): 1543–1548.

Oh SA, Lee HY, Lee JH, et al. 2012; Collagen three-dimensional hydrogel matrix carrying basic fibroblast growth factor for the cultivation of mesenchymal stem cells and osteogenic differentiation. Tissue Eng Part A 18(9–10): 1087–1100.

Pandya AN, Woodward B, Parkhouse N. 1998; The use of cultured autologous keratinocytes with integra in the resurfacing of acute burns. Plast Reconstr Surg 102(3): 825–828; discussion, 829–830.

Parenteau NL, Bilbo P, Nolte CJ, et al. 1992; The organotypic culture of human skin keratinocytes and fibroblasts to achieve form and function. Cytotechnology 9(1–3): 163–171.

Pontiggia L, Biedermann T, Meuli M, et al. 2009; Markers to evaluate the quality and self-renewing potential of engineered human skin substitutes in vitro and after transplantation. J Invest Dermatol 129(2): 480–490.

Powell HM, Supp DM, Boyce ST. 2008; Influence of electrospun collagen on wound contraction of engineered skin substitutes. Biomaterials 29(7): 834–843.

Rheinwald JG, Green H. 1975; Serial cultivation of strains of human epidermal keratinocytes: the formation of keratinizing colonies from single cells. Cell 6(3): 331–343.

Ryssel H, Gazyakan E, Germann G, et al. 2008; The use of Matriderm in early excision and simultaneous autologous skin grafting in burns – a pilot study. Burns 34(1): 93–97.

Schiestl C, Biedermann T, Braziulis E, et al. 2010; Skingineering II: transplantation of large-scale laboratory-grown skin analogues in a new pig model. Pediatr Surg Int 27(3): 249–254.

Schiestl C, Neuhaus K, Biedermann T, et al. 2011; Novel treatment for massive lower extremity avulsion injuries in children: slow, but effective with good cosmesis. Eur J Pediatr Surg 21(2): 106–110.

Schneider J, Biedermann T, Widmer D, et al. 2009; Matriderm versus Integra: a comparative experimental study. Burns 35(1): 51–57.

Schneider RK, Anraths J, Kramann R, et al. 2010; The role of biomaterials in the direction of mesenchymal stem cell properties and extracellular matrix remodelling in dermal tissue engineering. Biomaterials 31(31): 7948–7959.

Stark HJ, Willhauck MJ, Mirancea N, et al. 2004; Authentic fibroblast matrix in dermal equivalents normalises epidermal histogenesis and dermo-epidermal junction in organotypic coculture. Eur J Cell Biol 83(11–12): 631–645.

Stiefel D, Schiestl C, Meuli M. 2010; Integra artificial skin for burn scar revision in adolescents and children. Burns 36(1): 114–120.

van der Veen VC, van der Wal MB, van Leeuwen MC, et al. 2009; Biological background of dermal substitutes. Burns 36(3): 305–321.

van Zuijlen PP, van Trier AJ, Vloemans JF, et al. 2000; Graft survival and effectiveness of dermal substitution in burns and reconstructive surgery in a one-stage grafting model. Plast Reconstr Surg 106 (3): 615–623.

4.2 Human amniotic fluid derived cells can competently substitute dermal fibroblasts in a tissue-engineered dermo-epidermal skin analog

Pediatr Surg Int (2013) 29:61–69
DOI 10.1007/s00383-012-3207-2

ORIGINAL ARTICLE

Human amniotic fluid derived cells can competently substitute dermal fibroblasts in a tissue-engineered dermo-epidermal skin analog

Fabienne Hartmann-Fritsch · Nynke Hosper · Joachim Luginbühl · Thomas Biedermann · Ernst Reichmann · Martin Meuli

Published online: 9 November 2012

Abstract

Purpose Human amniotic fluid comprises cells with high differentiation capacity, thus representing a potential cell source for skin tissue engineering. In this experimental study, we investigated the ability of human amniotic fluid derived cells to substitute dermal fibroblasts and support epidermis formation and stratification in a humanized animal model.

Methods Dermo-epidermal skin grafts with either amniocytes or with fibroblasts in the dermis were compared in a rat model. Full-thickness skin wounds on the back of immuno-incompetent rats were covered with skin grafts with (1) amniocytes in the dermis, (2) fibroblasts in the dermis, or, (3) acellular dermis. Grafts were excised 7 and 21 days post transplantation. Histology and immunofluorescence were performed to investigate epidermis formation, stratification, and expression of established skin markers.

Results The epidermis of skin grafts engineered with amniocytes showed near-normal anatomy, a continuous basal lamina, and a stratum corneum. Expression patterns for keratin 15, keratin 16, and Ki67 were similar to grafts with fibroblasts; keratin 1 expression was not yet fully established in all suprabasal cell layers, expression of keratin 19 was increased and not only restricted to the basal cell layer as seen in grafts with fibroblasts. In grafts with acellular dermis, keratinocytes did not survive.

Conclusion Dermo-epidermal skin grafts with amniocytes show near-normal physiological behaviour suggesting that amniocytes substitute fibroblast function to support the essential cross-talk between mesenchyme and epithelia needed for epidermal stratification. This novel finding has considerable implications regarding tissue engineering.

Introduction

The composition of the amniotic fluid changes with gestational age. Whereas in the first half of gestation most of the fluid comes from active sodium and chloride transport across the amniotic membrane and the fetal skin, most of the fluid in the second half of gestation results from fetal micturition and lung water production [1]. The cells found in this fluid stem from all three germ layers and stem from the fetal skin, the digestive tract, and from the amniotic membranes [2]. Among the heterogeneous population of fetal cells that can be found in the amniotic fluid are mesenchymal, hematopoietic, epithelial, and trophoblastic cells [3].

Previous studies showed that the mesenchymal cells from the amniotic fluid (in this study, referred to as amniocytes) express a phenotypic profile that is consistent with the profile of fetal mesenchymal progenitor cells, i.e., they are negative for CD31 and positive for vimentin, α-smooth muscle actin, keratin 8 and 18, and fibroblast surface protein [4, 5]. They express several, but not all, important markers for embryonic stem cells, i.e., they are positive for Oct-4, Nanog, and SSEA-4, indicating that they represent a new class of stem cells, situated between embryonic stem cells and adult stem cells [3, 6]. It was shown that amniocytes have an expansion capacity four to eightfold higher than bone marrow derived mesenchymal stem cells, and that they differentiate into various mesenchymal lineages, including fibroblasts, osteocytes, and adipocytes [7]. In culture, these cells secrete various cytokines and chemokines important for wound healing, such as IL-6, IL-8, TGF-b, TNFRI, VEGF, and EGF [8]. Culturing of these cells was successful over a period of 8 months with stable karyotype [9]. In addition, it was shown that amniocytes retain their proliferative capacity and differentiation potential also during decades of cryopreservation [10].

Autologous fetal tissue engineering was performed in different animal models for various postnatal surgical interventions such as bladder augmentation, diaphragmatic replacement, tracheal augmentation, and skin defects [11–14]. Of note, in these models, tissue engineering was performed using a biopsy from the respective organ and the engineered tissue was delivered only after birth.

For fetal tissue engineering purposes, the amniotic fluid is a very attractive cell source. Cells can easily be harvested from amniotic fluid aspirated during the frequently performed diagnostic amniocenteses [5]. The goal of this paper was to test

whether amniocytes could be used for tissue engineering of skin. In particular, we wanted to investigate whether these amniocytes finally can assume anatomically and functionally the role of dermal fibroblasts.

Materials and Methods

Cell harvest and culture

Human skin samples were obtained after informed consent from patients and/or parents; all described studies were approved by the Medical Ethical Committee of the Kanton Zurich. Human primary fibroblasts and keratinocytes were isolated and cultured according to the standard protocol as previously described [15].

Confluent back-up human amniocentesis cultures were received after informed consent of the patients from the clinical cytogenetics laboratory of the University Medical Center Groningen. Cells were cultured from healthy fetuses (with a normal karyotype). Cells were harvested and expanded in DMEM (Lonza, Breda, The Netherlands) supplemented with 20 % fetal calf serum (FCS; Perbio Science, Ettenleur, The Netherlands) and 1 % penicillin, 1 % streptomycin (10,000 U/ml, Gibco, Paisley, UK), and 2 mM L-glutamine (Lonza, Breda, The Netherlands).

Engineering of dermo-epidermal skin substitutes

Skin grafts with either normal human dermal fibroblasts or human amniocytes in the dermis were prepared, using a previously established transwell system [6-well cell culture inserts with membranes of 3 µm pore-size (BD Falcon, Basel, Switzerland)] [15–17]. As negative control, skin substitutes with an acellular dermis were produced.

Briefly, bovine collagen type I (BD Biosciences, Basel, Switzerland) was mixed with either 1 x 10^5 human primary dermal fibroblasts or with 1 x 10^5 human amniocytes, or, for the negative control, no cells, and neutralized with a buffer containing NaOH [18]. The solution was poured into the cell culture inserts. The hydrogels were plastically compressed [19] and cultivated in DMEM with 10 % FCS. After 5 days, 7.5 x 10^5 keratinocytes were seeded onto the complete surface of all of the hydrogels. The grafts were cultivated for 3 days under submersed conditions in Rheinwald and Green keratinocyte medium, followed by 3 days cultivation at the air–liquid interface before transplantation onto immuno-incompetent rats. Medium was changed every 2–3 days.

Bright light microscopy

To compare the morphology of amniocytes and fibroblasts, bright light microscopic pictures were taken using a Nikon SMZ1500 stereo microscope with a Nikon DXM1200F camera.

Fluorescein diacetate live cell staining

The viability and morphological shape of the cells incorporated into the collagen type I hydrogels was compared using fluorescein diacetate (FdA) live cell staining [20]. Cell culture medium was removed and the hydrogels were incubated with 5 µM FdA (Sigma, Buchs, Switzerland) in PBS (Invitrogen, Basel, Switzerland). After 2 min, the FdA solution was removed and the hydrogels were washed with PBS. Fluorescein fluorescence was observed using a Nikon SMZ1500 fluorescent stereo microscope (FITC filter, Nikon DXM1200F camera).

Transplantation of dermo-epidermal skin grafts

Animal experiments were approved by the local committee for Experimental Animal Research. Immuno-incompetent nu/nu rats (age 8–10 weeks, Harlan, Horst, The Netherlands) were prepared as previously described [16, 17, 21, 22]. To prevent wound closure by the surrounding skin, steel rings (diameter 26 mm) were implanted into full-thickness skin defects on the back of the rats and served as a modified Fusenig chamber [23]. The transplants were inserted into the ring and covered with a silicon foil (Silon-SES, BMS, Allentown, PA, USA). Animal numbers were: amniocyte-grafts excised 7 days post transplantation (n = 6); amniocyte-grafts excised 21 days post transplantation (n = 6); fibroblast-grafts excised 7 days post transplantation (n = 6); fibroblast-grafts excised 21 days post transplantation (n = 6); grafts with acellular dermal part excised 21 days post transplantation (n = 6). Wound dressing changes and photographic documentations (Nikon D90) were performed every 7 days. Animals were killed 7 or 21 days post transplantation. Transplants were excised, halved, and embedded in O.C.T compound (Tissue-Tek®, Sakura Finetek, Japan), or fixed in 4 % paraformaldehyde (Medite Medizintechnik AG, Nunningen, Switzerland) and embedded in paraffin (McCormick, Richmond, USA).

Histology and immunofluorescence

Paraffin sections (sectioned at 10 µm with a microtome from Leica, Wetzlar, Germany) were deparaffinised and stained with haematoxylin & eosin (Sigma, Buchs, Switzerland) and imaged by light microscopy (Nikon Eclipse TE2000-U inverted microscope connected with a DXM1200F digital camera (Nikon AG, Egg, Switzerland).

O.C.T-embedded tissue was frozen at -20 °C and sectioned at 10 µm (Leica, Wetzlar, Germany). Sections were permeabilised in ice-cold acetone for 5 min, air-dried, and washed three times with phosphate buffered saline (PBS, Invitrogen, Basel, Switzerland). Blocking was performed with PBS containing 2 % bovine serum albumin (Sigma, Buchs, Switzerland) for 30 min at room temperature. Sections were incubated with the pre-labelled antibodies for 1 h at room temperature. After three washing steps with PBS, nuclei were stained with 1 µg/ml Hoechst 33341 (Sigma, Buchs, Switzerland) in PBS for 5 min at room temperature. After two final washing steps with PBS, sections were mounted with Dako fluorescent mounting solution (Dako, Baar, Switzerland).

Antibodies

The following antibodies were used: K1 (clone LHK1, 1:200, Novus Biologicals, Littleton, USA); K15 (clone SMP190, 1:50, Spring Biosciences, Fermont, USA); K16 (clone LL025, 1:100, Chemicon International, Temecula, USA); K19 (clone RCK108, 1:100, Dako, Glostrup, Denmark); Ki67 (clone B56, 1:100, ABD Serotec, Dusseldorf, Germany); Lam5a3 (clone P3H9-2, 1:100, Santa Cruz, Labforce AG, Nunningen, Switzerland) [24].

For immunofluorescence stainings, primary antibodies were pre-labelled with either Alexa488 or Alexa555 conjugated polyclonal goat F(ab')2 fragments, according to the manufacturer's instructions (Zenon Mouse IgG Labelling Kit, Molecular Probes, Invitrogen, Basel, Switzerland).

Fluorescence microscopy

Immunofluorescence stainings were analyzed using a Nikon Eclipse TE2000-U inverted microscope, equipped with Hoechst, FITC and TRICT filter sets and connected with a DXM1200F digital camera (Nikon AG, Egg, Switzerland). Images were processed with Photoshop 7.0 (Adobe Systems Inc., Munich, Germany).

Results

Amniotic fluid derived cells

Mesenchymal cells from human amniotic fluid (amniocytes) were isolated, cultured and passaged several times. Upon 90–100 % confluence, the amniocytes (Fig. 1a) demonstrated a rather irregular arrangement as opposed to the one of human fibroblasts (Fig. 1b) that appeared to be more ‘‘streamlined’’. The amniocytes shared the spindle-shaped morphology with fibroblasts.

Amniocytes were incorporated into bovine collagen type I hydrogels and FdA staining was performed 3 days thereafter to assess the viability of the cells as well as their morphology in this 3D culture system. FdA staining revealed high cell viability with spindle-shaped, dendrite, or stellate morphology of the cells (Fig. 1c), similar to fibroblasts in collagen hydrogel (Fig. 1d).

Macroscopic appearance of epidermis development on transplanted grafts

At transplantation of the three types of skin substitutes (amniocytes in the dermis, fibroblasts in the dermis, or, acellular dermis) on the back of immuno-incompetent rats, no macroscopic difference between the three types of transplants could be observed (Fig. 2a–c). Seven days post transplantation, complete take of all grafts in all animals was observed (Fig. 2d–f). The presence or absence of an epidermis was difficult to asses macroscopically at this early stage, although the transplants with acellular dermis appeared to have a rather moist surface (Fig. 2f), usually indicating a missing or poorly developed epidermis. Twenty-one days post transplantation, grafts containing Amniocytes or fibroblasts showed a clearly epithelialised surface and seemed well integrated into the rat tissue (Fig. 2g, h). Grafts with an acellular dermis had a moist surface (Fig. 2i) and appeared smaller compared to the other transplants.

Histological analysis of the epidermis

Excised grafts were sectioned and stained with haematoxylin & eosin. Seven days post transplantation, skin substitutes with amniocytes (Fig. 3a) showed a stratified epidermis of 4–6 keratinocyte layers with near-normal anatomy and a stratum corneum. The dermal part of these grafts was clearly distinguishable from the underlying tissue, and evenly distributed cells could be detected in the dermis

(Fig. 3a). Similar features were observed in grafts with fibroblasts (Fig. 3b). Twenty-one days post transplantation, the neodermis in transplants with Amniocytes and with fibroblasts showed a higher cell number than 7 days post transplantation and the epidermis demonstrated about 6–8 layers on the amniocyte-grafts (Fig. 3c) and about 8–10 layers on the fibroblast-grafts (Fig. 3d). Twenty-one days post transplantation, a large part of the dermis in grafts with acellular dermis was devoid of any cells, and no epidermal elements were detectable (Fig. 3e).

Basal lamina deposition, epidermal homeostasis and proliferation

Grafts excised 21 days post transplantation were sectioned and immunofluorescence stainings were performed. Staining of the amniocyte-grafts with an antibody to the basal lamina component laminin 5 (Fig. 4a) demonstrated a deposition of a continuous basal lamina in all transplants and keratin 1 expression was not fully established in all suprabasal layers (Fig. 4a). In fibroblast-grafts in the dermis, laminin 5 staining revealed a continuous basal lamina and keratin 1 was expressed in all suprabasal layers (Fig. 4b). In amniocyte-grafts, keratin 16 was continuously expressed in all suprabasal layers (Fig. 4c). Amniocyte-grafts demonstrated more cells expressing the proliferation marker Ki67 in the basal layer (Fig. 4c), while the fibroblast-grafts demonstrated more Ki67 positive cells in the dermis (Fig. 4d). In fibroblast-grafts, keratin 16 expression was found in all suprabasal layers (Fig. 4d). In amniocytes-grafts, keratin 15 expression could be observed in most of the basal cells, whereas expression of keratin 19 was detected in most suprabasal cells (Fig. 4e). In fibroblast-grafts, keratin 15 expression was found in most basal cells, and a subpopulation of these basal cells was positive for keratin 19 (Fig. 4f).

Discussion

We describe here the generation of dermo-epidermal skin grafts containing human primary amniotic fluid derived cells in the dermis instead of human fibroblasts. These tissue-engineered skin substitutes were compared to tissue-engineered dermo-epidermal skin substitutes with human primary fibroblasts in the dermis and grafts with an acellular dermis. The key finding of our study is that the amniocytes can competently substitute for fibroblasts and successfully support epidermis stratification and survival. Some aspects deserve detailed consideration.

The interaction between epithelium and underlying mesenchyme was studied extensively for many years. It became clear that for successful epidermal stratification and survival, an underlying mesenchyme is absolutely mandatory. The mesenchyme provides essential growth factors to the epithelial cells and so stimulates the stratification of the epidermis [25–28].

It was therefore not surprising that we could not observe epidermis stratification, nor survival, in our skin grafts created with an acellular dermis. Interestingly, transplants with amniocytes in the dermis showed near-normal structure, comparable to control transplants with fibroblasts in the dermis. The epithelial cells in amniocyte-grafts stratified to a near-normal epidermis including a stratum corneum and deposited a continuous basal lamina. However, expression patterns for markers of epidermal homeostasis suggested that 21 days post transplantation the epidermis was not yet in a fully homeostatic state. This aspect was reinforced by the detection of many suprabasal cells that were positive for keratin 19 expression, compared to the fibroblast-grafts where keratin 19 expression was restricted to some basal cells. These findings indicate that the development of the epidermis within amniocyte containing grafts is basically physiological, but slightly slower than in those containing fibroblast. These results provide compelling evidence that amniocytes incorporated into the dermal part of a dermo-epidermal skin graft can efficiently substitute fibroblasts and correctly support epidermal survival and stratification.

Diagnostic amniocentesis is routinely offered, can be safely performed under ultrasound guidance, and is associated with a very low rate of spontaneous abortion of only 0.5 % [29]. The removal of an additional small aliquot of amniotic fluid does

not represent an additional risk to fetus or mother and also does not apparently constitute an ethical concern.

The present study can be seen as a first step toward tissue engineering of fetal skin without the necessity of harvesting a formal fetal skin biopsy. We demonstrate that prenatally harvested amniocytes can be successfully employed to competently assume the role of dermal fibroblasts in a fetal-postnatal hybrid skin substitute (amniocytes = fetal cells, keratinocytes = postnatal cells). Of note, amniotic fluid also contains fetal epidermal cells that, hypothetically, might also be harvested, isolated, cultured, so as to form a fetal epidermis. Taken together, in a best case future scenario, autologous ‘‘fetal skingineering’’ could be accomplished by the sole use of amniotic fluid.

What are then, theoretically, possible applications for such laboratory-grown fetal skin? Human fetal surgery for spina bifida is a reality today and represents a novel standard of care for select fetuses suffering from that devastating malformation [30] (also at our centre [31]). Quite often, the back lesions of these fetal patients are very big for successful primary skin closure. In those situations, an ‘‘off-the-shelf’’ autologous fetal skin substitute might represent an ideal way to guarantee adequate skin coverage. Another hypothetical application might be the use of amniotic fluid derived bioengineered fetal skin to treat chronic skin wounds, particularly in polymorbid elderly patients which often demonstrate notorious wound healing problems. It is in fact conceivable that fetal skin (even if allogenic) harbours more wound healing power [8] than postnatal skin substitutes used for the same purpose [32, 33]. Finally, one could even think of harvesting and cryopreserving amniotic fluid for any potential use later in life. It was in fact shown that stored amniocytes remain viable and functional over decades of cryopreservation [10]. If the same holds true for amniotic fluid derived epidermal cells, then autologous skin might be engineered at any age of the patient for a number of possible indications (giant nevi, burns, scar revisions, chronic wounds, and other conditions where larger areas of skin are lost).

In summary and conclusion, we demonstrate here that amniocytes can competently assume the role of dermal fibroblasts in the context of bioengineering a full-thickness skin analog. This novel finding has fundamental implications on the emerging field of tissue engineering and harbours considerable potential regarding in vitro fabrication of both fetal and adult skin.

Conflict of interest

The authors declare that they have no conflict of interest.

Acknowledgements

This work was financially supported by the EUFP6 project EuroSTEC (soft tissue engineering for congenital birth defects in children: contract: LSHB-CT-2006-037409), by the EUFP7 project EuroSkinGraft (FP7/2007-2013: grant agreement n° 279024), and by the University of Zurich. We are particularly grateful to the Fondation Gaydoul and the sponsors of ‘‘DonaTissue’’ (Thérèse Meier and Robert Zingg) for their generous financial support and interest in our work.

Figures

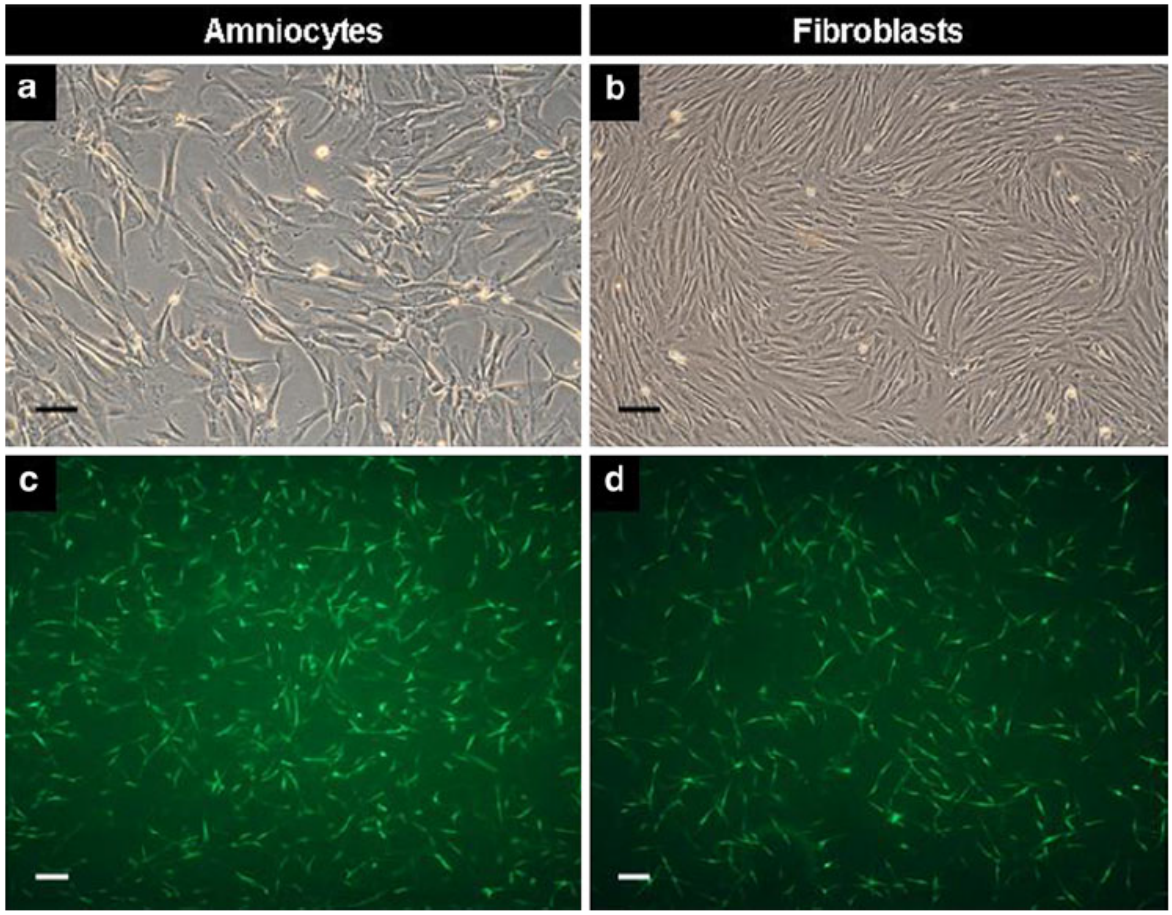

Fig. 1: Comparison of morphology of human primary amniocytes and human primary fibroblasts on cell culture plastic (2D) and in a collagen hydrogel (3D). **a** Phase contrast microscopy of Amniocytes shows cell morphology similar to spindle-shape morphology of fibroblasts (**b**). **c** Positive fluorescein diacetate staining of amniocytes in collagen hydrogel shows dendrite morphology and good viability of the cells. **d** Fluorescein diacetate staining of fibroblasts indicating high viability as seen by the mainly dendrite or stellate morphology. Scale bars 40 µm

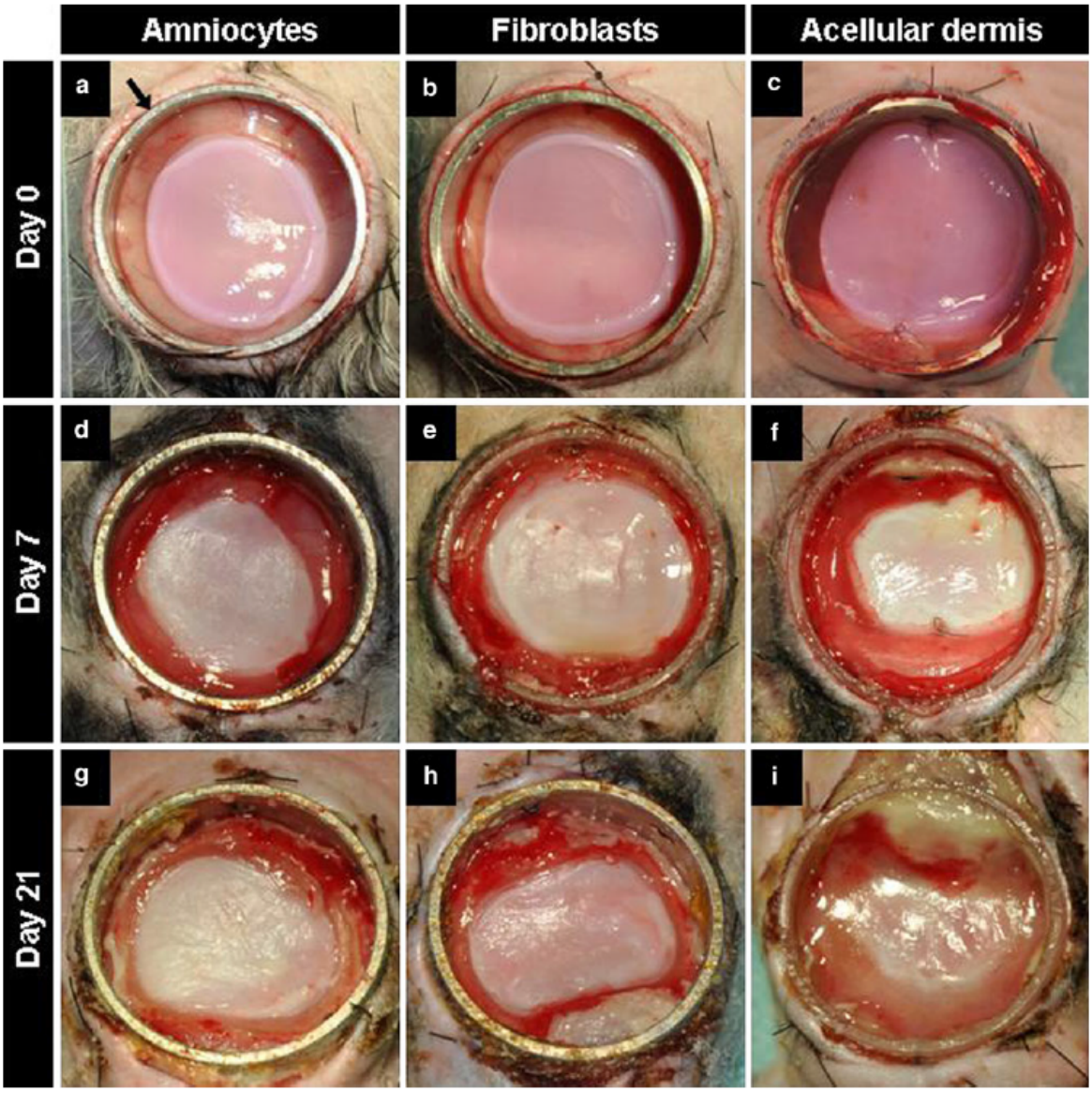

Fig. 2: Macroscopic views of grafts at time point of transplantation (day 0), 7 and 21 days post transplantation. **a–c** Transplants show similar appearance at the day of transplantation. **d, e** Seven days post transplantation, the surface of both amniocyte- and fibroblast-grafts is similar and looks rather dull and dry. **f** Grafts with acellular dermis appear more shiny and moist. **g, h** Twenty-one days post transplantation, grafts with amniocytes and with fibroblasts look similar as shown in **d, e. i** Twenty-one days post transplantation, grafts with acellular dermis look similar as described in **f**. Diameter of the ring (arrow in **a**) 26 mm (**a–i**)

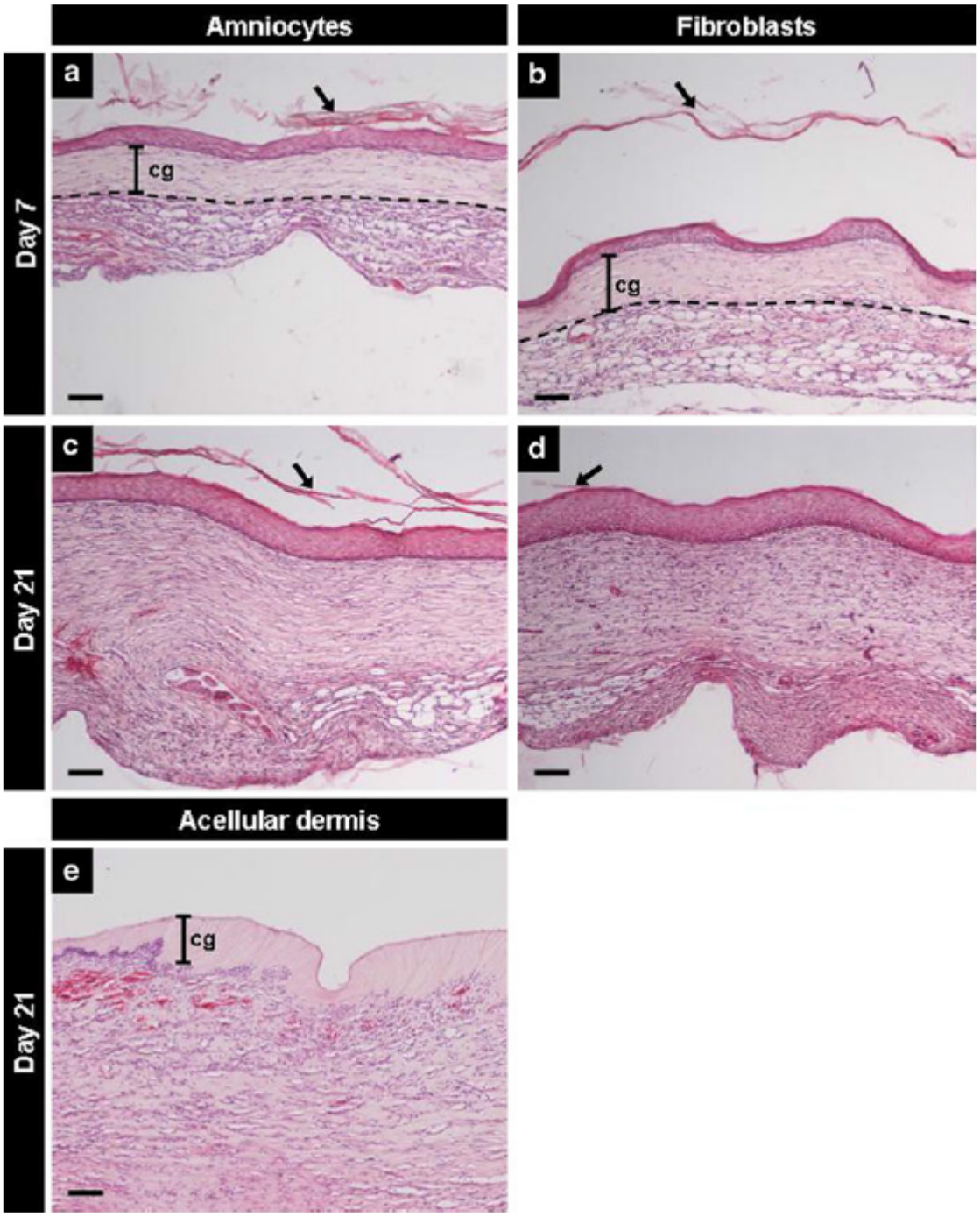

Fig. 3: Histological evaluation of the excised grafts (haematoxylin & eosin staining). **a** Seven days post transplantation, amniocyte grafts show a correctly stratified epidermis with 4–6 cell layers and a stratum corneum. The collagen gel is easily discernable. **b** Seven days post transplantation, fibroblast-grafts look similar as described in **a**. The collagen gel is similar as in **a**. **c** Twenty-one days post transplantation, the epidermis of amniocyte-grafts is near physiological and has 6–8 cell layers. The dermis is markedly populated by cells. **d** Twenty-one days post transplantation, the epidermis of fibroblast grafts is up to 8–10 cell layers thick including stratum corneum, and the dermis is densely populated by cells. **e** Twenty-one days post transplantation, grafts with acellular dermis show neither epidermis nor single epidermal cells. The collagen gel is easily detectable and a large part of it does not contain cells. The *dotted line* indicates the border between graft and underlying tissue. *Arrows* point at stratum corneum. *cg* Collagen gel. *Scale bars* 100 µm (**a–e**)

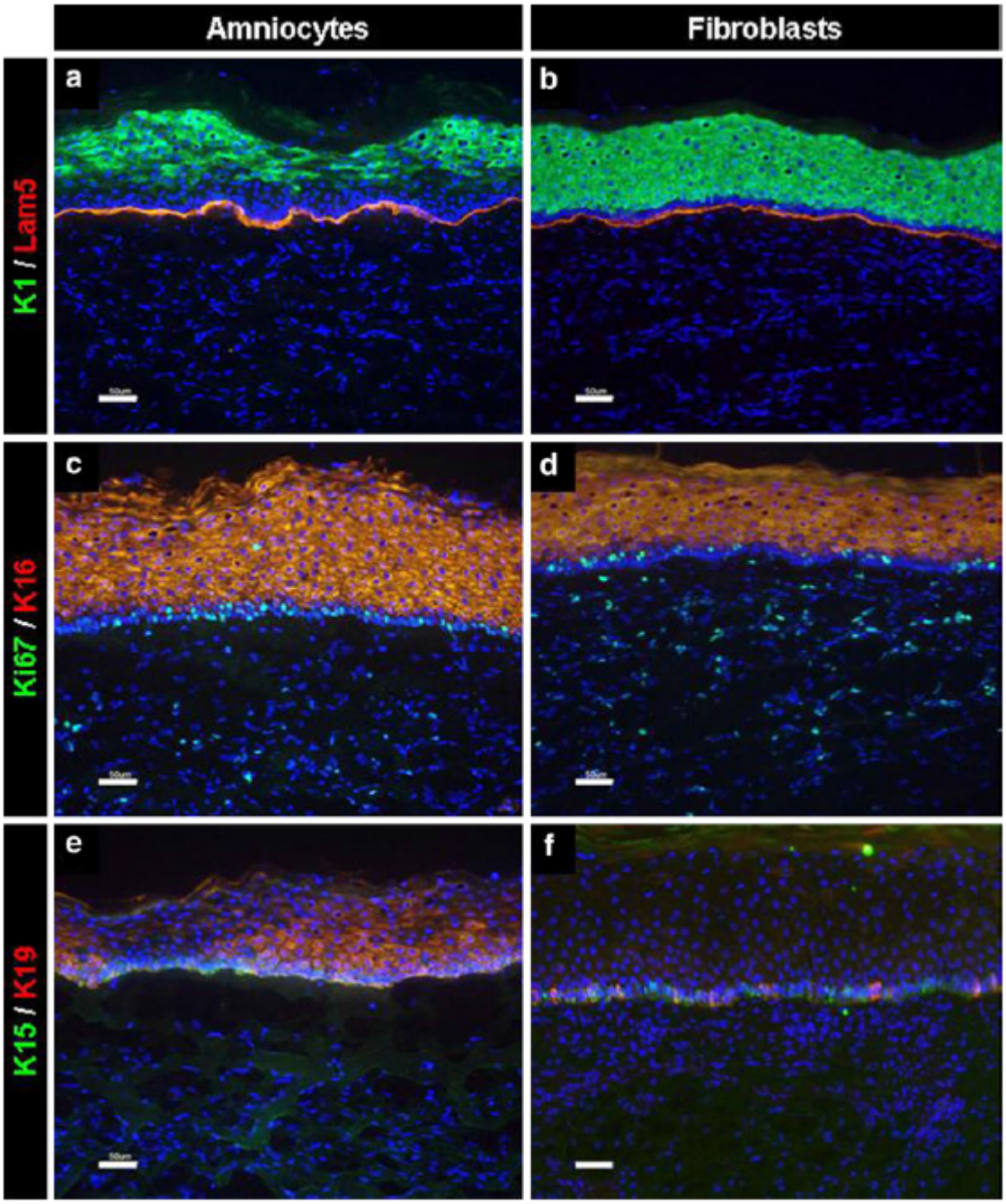

Fig. 4: Immunofluorescence stainings of grafts with amniocytes or with fibroblasts in the dermis 21 days after transplantation. **a, b** Staining of the basement membrane component laminin 5 (*red*) reveals the deposition of a continuous basement membrane in both types of transplants. Expression of keratin 1 (*green*) is not fully established in all suprabasal layers in amniocyte grafts, whereas in fibroblast grafts, all suprabasal layers express keratin 1. **c, d** In both types of transplants, keratin 16 (*red*) is expressed in all suprabasal layers. Proliferation as indicated by expression of Ki67 (*green*) in the basal cell layer of amniocyte-grafts is more pronounced compared to fibroblast-grafts. Proliferation of cells in the dermal part is lower in amniocyte-grafts than in fibroblast-grafts. **e, f** In amniocyte-grafts, keratin 19 (*red*) expression is detected in most suprabasal cells, whereas in fibroblast-grafts keratin 19 expression is restricted to some basal cells. In both types of grafts, keratin 15 expression (*green*) is detected in some basal cells. *Scale bars* 50 µm

References

1. Kunisaki SM, Jennings RW, Fauza DO (2006) Fetal cartilage engineering from amniotic mesenchymal progenitor cells. Stem ells Dev 15:245–253

2. Dobreva MP, Pereira PN, Deprest J, Zwijsen A (2010) On the origin of amniotic stem cells: of mice and men. Int J Dev Biol 54:761–777

3. Pappa KI, Anagnou NP (2009) Novel sources of fetal stem cells: where do they fit on the developmental continuum? Regen Med 4:423–433

4. Fauza D (2004) Amniotic fluid and placental stem cells. Best Pract Res Clin Obstet Gynaecol 18:877–891

5. Kaviani A, Perry TE, Dzakovic A, Jennings RW, Ziegler MM, Fauza DO (2001) The amniotic fluid as a source of cells for fetal tissue engineering. J Pediatr Surg 36:1662–1665

6. Mihu CM, Mihu D, Costin N, Rus Ciuca D, Susman S, Ciortea R (2008) Isolation and characterization of stem cells from the placenta and the umbilical cord. Rom J Morphol Embryol 49:441–446

7. In ‘t Anker PS, Scherjon SA, Kleijburg-van der Keur C et al (2003) Amniotic fluid as a novel source of mesenchymal stem cells for therapeutic transplantation. Blood 102:1548–1549

8. Yoon BS, Moon JH, Jun EK et al (2010) Secretory profiles and wound healing effects of human amniotic fluid-derived mesenchymal stem cells. Stem Cells Dev 19:887–902

9. Kim J, Lee Y, Kim H et al (2007) Human amniotic fluid-derived stem cells have characteristics of multipotent stem cells. Cell Prolif 40:75–90

10. Woodbury D, Kramer BC, Reynolds K, Marcus AJ, Coyne TM, Black IB (2006) Long-term cryopreserved amniocytes retain proliferative capacity and differentiate to ectodermal and mesodermal derivatives in vitro. Mol Reprod Dev 73:1463–1472

11. Fauza DO, Fishman SJ, Mehegan K, Atala A (1998) Videofetoscopically assisted fetal tissue engineering: bladder augmentation. J Pediatr Surg 33:7–12

12. Fauza DO, Marler JJ, Koka R, Forse RA, Mayer JE, Vacanti JP (2001) Fetal tissue engineering: diaphragmatic replacement. J Pediatr Surg 36:146–151

13. Fuchs JR, Terada S, Ochoa ER, Vacanti JP, Fauza DO (2002) Fetal tissue engineering: in utero tracheal augmentation in an ovine model. J Pediatr Surg 37:1000–1006 discussion 1000–1006

14. Fauza DO, Fishman SJ, Mehegan K, Atala A (1998) Videofetoscopically assisted fetal tissue engineering: skin replacement. J Pediatr Surg 33:357–361

15. Pontiggia L, Biedermann T, Meuli M et al (2009) Markers to evaluate the quality and self-renewing potential of engineered human skin substitutes in vitro and after transplantation. J Invest Dermatol 129:480–490

16. Biedermann T, Pontiggia L, Bottcher-Haberzeth S et al (2010) Human eccrine sweat gland cells can reconstitute a stratified epidermis. J Invest Dermatol 130:1996–2009

17. Böttcher-Haberzeth S, Biedermann T, Pontiggia L, et al. (2012) Human eccrine sweat gland cells turn into melanin-uptaking keratinocytes in dermo-epidermal skin substitutes. J Invest Dermatol. doi:10.1038/jid.2012.290

18. Costea DE, Loro LL, Dimba EAO, Vintermyr OK, Johannessen AC (2003) Crucial effects of fibroblasts and keratinocyte growth factor on morphogenesis of reconstituted human oral epithelium. J Invest Dermatol 121:1479–1486

19. Braziulis E, Diezi M, Biedermann T et al (2012) Modified plastic compression of collagen hydrogels provides an ideal matrix for clinically applicable skin substitutes. Tissue Eng Part C Methods 18:464–474

20. Armour AD, Powell HM, Boyce ST (2008) Fluorescein diacetate for determination of cell viability in tissue-engineered skin. Tissue Eng Part C 14:89–96

21. Bottcher-Haberzeth S, Biedermann T, Schiestl C et al (2012) Matriderm((R)) 1 mm versus Integra((R)) Single Layer 1.3 mm for one-step closure of full thickness skin defects: a comparative experimental study in rats. Pediatr Surg Int 28:171–177

22. Kiowski G, Biedermann T, Widmer DS et al (2012) Engineering melanoma progression in a humanized environment in vivo. J Invest Dermatol 132:144–153

23. Fusenig NE, Breitkreutz D, Dzarlieva RT, Boukamp P, Bohnert A, Tilgen W (1983) Growth and differentiation characteristics of transformed keratinocytes from mouse and human skin in vitro and in vivo. J Invest Dermatol 81:168s–175s

24. Lammers G, Verhaegen PD, Ulrich MM et al (2011) An overview of methods for the in vivo evaluation of tissue-engineered skin constructs. Tissue Eng Part B Rev 17:33–55

25. Rheinwald JG, Green H (1975) Serial cultivation of strains of human epidermal keratinocytes: the formation of keratinizing colonies from single cells. Cell 6:331–343

26. Leary T, Jones PL, Appleby M, Blight A, Parkinson K, Stanley M (1992) Epidermal keratinocyte self-renewal is dependent upon dermal integrity. J Invest Dermatol 99:422–430

27. Botchkarev VA, Kishimoto J (2003) Molecular control of epithelial-mesenchymal interactions during hair follicle cycling. J Investig Dermatol Symp Proc 8:46–55

28. Schultz GS, Wysocki A (2009) Interactions between extracellular matrix and growth factors in wound healing. Wound Repair Regen 17:153–162

29. Jauniaux E, Rodeck C (1995) Use, risks and complications of amniocentesis and chorionic villous sampling for prenatal diagnosis in early pregnancy. Early Pregnancy 1:245–252

30. Adzick NS, Thom EA, Spong CY et al (2011) A randomized trial of prenatal versus postnatal repair of myelomeningocele. N Engl J Med 364:993–1004

31. Meuli M, Moehrlen U, Flake AW, et al. (2012) Fetal Surgery in Zurich: Key Features of our First Open In Utero Repair of Myelomeningocele. Eur J Pediatr Surg (in press)

32. Zaulyanov L, Kirsner RS (2007) A review of a bi-layered living cell treatment (Apligraf) in the treatment of venous leg ulcers and diabetic foot ulcers. Clin Interv Aging 2:93–98

33. Marston WA (2004) Dermagraft, a bioengineered human dermal equivalent for the treatment of chronic nonhealing diabetic foot ulcer. Expert Rev Med Devices 1:21–31

4.3 A new model for preclinical testing of dermal substitutes for human skin reconstruction

Pediatr Surg Int (2013) 29:479–488
DOI 10.1007/s00383-013-3267-y

ORIGINAL ARTICLE

A new model for preclinical testing of dermal substitutes for human skin reconstruction

Fabienne Hartmann-Fritsch · Thomas Biedermann · Erik Braziulis · Martin Meuli · Ernst Reichmann

Accepted: 16 January 2013 / Published online: 1 February 2013

Abstract

Background/Purpose Currently, acellular dermal substitutes used for skin reconstruction are usually covered with split-thickness skin grafts.

The goal of this study was to develop an animal model in which such dermal substitutes can be tested under standardized conditions using a bioengineered dermo-epidermal skin graft for coverage.

Methods Bioengineered grafts consisting of collagen type I hydrogels with incorporated human fibroblasts and human keratinocytes seeded on these gels were produced. Two different dermal substitutes, namely Matriderm®, and an acellular collagen type I hydrogel, were applied onto full-thickness skin wounds created on the back of immuno-incompetent rats. As control, no dermal substitute was used. As coverage for the dermal substitutes either the bioengineered grafts were used, or, as controls, human split-thickness skin or neonatal rat epidermis were used. Grafts were excised 21 days post transplantation. Histology and immunofluorescence was performed to investigate survival, epidermis formation, and vascularization of the grafts.

Results The bioengineered grafts survived on all tested dermal substitutes. Epidermis formation and vascularization were comparable to the controls.

Conclusion We could successfully use human bioengineered grafts to test different dermal substitutes. This novel model can be used to investigate newly designed dermal substitutes in detail and in a standardized way.

Introduction

The today's gold standard to treat full-skin defects such as burns, giant nevi, or avulsion injuries is the transplantation of autologous split-thickness skin [1, 2]. Split-thickness skin can be applied directly on the wound bed, or it can be transplanted onto different acellular dermal substitutes such as Integra® (Integra) [1, 3-7] or Matriderm® (Matriderm) [8-13]. Dermal substitutes improve wound healing, impede scar contraction, and the cosmetic outcome compared to transplanted split-thickness skin alone [1, 14, 15]. A newly designed dermal substitute needs to be tested pre-clinically for its biological behavior and compatibility with split-thickness skin. For most dermal substitutes, tests are performed in a pig animal model with porcine split-thickness skin [16-19].

The aim of this experimental study was to test whether a human bioengineered skin graft can be used to replace human split-thickness skin for the pre-clinical testing of acellular dermal substitutes used for skin reconstruction.

Materials and Methods

Cell isolation and culture

Human skin samples were obtained after informed consent from patients and/or parents; all described studies were approved by the Medical Ethical Committee of the Kanton Zurich. Human primary fibroblasts and keratinocytes were isolated as previously described [20].

Engineered dermal substitutes (acellular collagen hydrogels)

To engineer acellular dermal substitutes, a solution of bovine collagen type I was neutralized with a NaOH containing buffer [21] and poured into cell culture inserts with a pore size of 3 µm (BD Falcon, Basel, Switzerland). After incubation for 2h at 37°C, the acellular dermal substitutes were plastically compressed as previously described [22]. The acellular collagen hydrogels were incubated for five days in Rheinwald and Green medium (RGM) [20], before transplantation, with medium changes performed every 2-3 days.

Matriderm

Matriderm 1 mm (Dr. Suwelack Skin & Health Care AG, Billerbeck, Germany) was cut into round pieces of 26 mm diameter and incubated in RGM for three minutes immediately before transplantation.

Human bioengineered skin grafts (bioengineered grafts)

Human bioengineered skin grafts based on collagen type I hydrogels with incorporated human dermal fibroblasts and human keratinocytes seeded on these hydrogels were created as previously described [23]. Briefly, 10^5 human primary dermal fibroblasts were mixed with bovine collagen type I (BD Biosciences, Basel, Switzerland) and neutralized with a buffer containing NaOH. The solution was poured into cell culture inserts with a pore size of 3 µm (BD Falcon, Basel, Switzerland). After incubation of 2h at 37°C and 5% CO_2, the hydrogels were plastically compressed [22]. The hydrogels were cultivated in DMEM supplemented with 10% FCS, and media changes were performed every 2-3 days. $7.5x10^5$ human primary keratinocytes were seeded onto the complete surface of the hydrogels five days thereafter. After three days of submerged cultivation in RGM, hydrogels were

cultivated for additional three days at the air-liquid interface, before transplantation onto immuno-incompetent rats.

Human split-thickness skin

Human split-thickness skin (leftovers from split-thickness skin transplantations) was received from patients from the University Children's Hospital Zurich after informed consent from patients and/or parents. Split-thickness skin was stored in DMEM at 4 °C until transplantation.

Neonatal rat epidermis

Neonatal rat epidermis of appropriate size was obtained from full-thickness skin samples from newborn Wistar rats (University of Zurich animal breeding program). Full-thickness skin samples were treated overnight in dispase (BD Biosciences) diluted 1:1 in Hank's balanced salt solution (Invitrogen) containing 5 mg/ml gentamicin (Invitrogen) at 4 ºC. To obtain an epidermis free of dermal components, the epidermis was peeled off the dermis immediately before transplantation.

Transplantation

All animal experiments were approved by the local Committee for Experimental Animal Research. The preparation of immuno-incompetent nu/nu rats (age 8-10 weeks, Harlan, Horst, The Netherlands) was performed as previously described [24]. Steel rings with a diameter for 26 mm were implanted into full-thickness skin defects on the back of the rats to prevent wound closure by ingrowth of rat skin into the wound area. Two different dermal substitutes, namely Matriderm and engineered acellular collagen hydrogels, were placed onto the wounds. The dermal substitutes were immediately covered with a) human bioengineered graft, b) human split-thickness skin, or, c) neonatal rat epidermis. Controls were performed without any dermal substitute, where the coverage grafts were transplanted directly on the fascia (Fig. 1). Sample sizes for each group are summarized in table 1. Transplants were covered with a silicon foil (Silon-SES, BMS, Allentown, PA, USA). Once a week, wound dressing changes and photographic documentations were performed. Animals were sacrificed 21 days post transplantation. Grafts were excised, halved, and embedded in O.C.T compound (Tissue-Tek®, Sakura Finetek,

Japan) or fixed in 4% paraformaldehyde (Medite Medizintechnik AG, Nunningen, Switzerland) and then embedded in paraffin (McCormick, Richmond, USA).

Histology

For haematoxylin & eosin staining, 10 µm thick paraffin sections were cut and stainings were imaged by light microscopy (Nikon Eclipse TE2000-U inverted microscope connected with a DXM1200F digital camera (Nikon AG, Egg, Switzerland).

For immunofluorescence stainings, O.C.T embedded tissue was frozen at -20 °C, and sectioned at 10 µm. Permeabilisation was performed in ice-cold acetone for 5 minutes, thereafter sections were air-dried, and washed three times in phosphate buffered saline (PBS). After blocking with PBS containing 2% bovine serum albumin (Sigma, Buchs, Switzerland) for 30 minutes at room temperature, sections were incubated with the pre-labeled antibodies for 1 hour at room temperature. Sections were washed three times with PBS, then nuclei were stained with 1 µg/ml Hoechst 33341 (Sigma, Buchs, Switzerland) in PBS for 5 minutes at room temperature. Sections were washed two times with PBS, and finally mounted with Dako fluorescent mounting solution (Dako, Baar, Switzerland).

Antibodies

The following antibodies were used: K1 (clone LHK1, 1:200, Novus Biologicals, Littleton, USA); Lam5α3 (clone P3H9-2, 1:100, Santa Cruz, Labforce AG, Nunningen, Switzerland); CD31 (clone TDL-3A12, 1:50, BD Biosciences Pharmingen, Basel, Switzerland) ; CD90 (clone AS02, 1:100, Dianova, Hamburg, Germany).

For immunofluorescence stainings, primary antibodies were pre-labeled with either Alexa488 or Alexa555 conjugated polyclonal goat F(ab')2 fragments, according to the manufacturer's instructions (Zenon Mouse IgG Labelling Kit, Molecular Probes, Invitrogen, Basel, Switzerland).

Fluorescence microscopy

The immunofluorescence stainings were analyzed with a Nikon Eclipse TE2000-U inverted microscope, equipped with Hoechst, FITC and TRICT filter sets and connected with a DXM1200F digital camera (Nikon AG, Egg, Switzerland).

Results

Macroscopic appearance of epidermis on transplanted grafts

Immediate after transplantation, the human bioengineered grafts macroscopically appeared similar in all groups (transplanted either directly on the fascia, on Matriderm, or, on an engineered acellular collagen hydrogel) (Fig. 2a-c). At time point of transplantation, human split-thickness skin macroscopically looked similar in all three groups, the underlying dermal substitute was not visible through the split-thickness skin (Fig. 2d-e). At time point of transplantation, neonatal rat epidermis appeared very thin and transparent (Fig. 2g-i) and the underlying dermal substitute was visible. Matriderm seemed red and dull, as a result from its incubation in RGM prior to transplantation (Fig. 2h). The engineered acellular collagen hydrogel shined white through the neonatal rat epidermis (Fig. 2i).

21 days post transplantation, a complete take of the bioengineered grafts in all three groups was observed (Fig. 3a-c). Grafts showed an epithelialised surface and seemed well integrated into the rat tissue. 21 days post transplantation, the split-thickness skins seemed well integrated into the rat tissue and in all three groups good take was observed with epidermis covering the complete surface (Fig. 3d-f). 21 days post transplantation, neonatal rat epidermis transplanted directly onto the fascia (Fig. 3g) macroscopically showed a better take rate compared to neonatal rat epidermis transplanted on Matriderm (Fig. 3h) and on engineered acellular collagen gel (Fig. 3i).

Histological analysis of grafts excised 21 days post transplantation

Grafts excised 21 days post transplantation were sectioned and stained with haematoxylin & eosin. Human bioengineered grafts showed a stratified epidermis of 6-9 layers that was similar in all three groups (Fig. 4a-c). Remnants of Matriderm could be detected between the bioengineered graft and the underlying rat tissue (Fig. 4b). The bioengineered graft could be distinguished from the engineered acellular collagen hydrogel, which was partially populated by rat cells (Fig. 4c).

Human split-thickness skin showed similar appearance in all three groups, with a multi-layered epidermis, prominent rete ridges, and a very prominent stratum corneum (Fig. 4d-f).

Transplantation of neonatal rat epidermis was partially successful when transplanted directly on the fascia, where a 2-3 layered epidermis could be detected (Fig. 4g). When transplanted on Matriderm (Fig. 4h) or on engineered acellular collagen gel (Fig. 4i), the epidermis did not survive, and only some single epidermal cells could be detected. The Matriderm material could not be clearly distinguished from the underlying rat tissue (Fig. 4h). The engineered acellular collagen hydrogel was clearly detectable and was only partially colonized by ingrown rat cells (Fig. 4i).

Basal lamina deposition and epidermis stratification

Grafts excised 21 days post transplantation were sectioned and immunofluorescence stainings were performed. Staining with an antibody to the basal lamina component laminin 5 revealed the deposition of a continuous basal lamina in human bioengineered grafts in all three groups (Fig. 5a-c). In bioengineered grafts, all suprabasal keratinocyte layers expressed keratin 1 (Fig. 5a-c). Similar expression patterns for laminin 5 and keratin 1 were observed in transplanted human split-thickness skin in all three groups (Fig. 5d-f). In the specimens where neonatal rat epidermis was transplanted, neither basal lamina deposition nor keratin 1 expression was detected in either group (Fig. 5g-i).

In human bioengineered grafts, the ingrowth of rat blood vessels, as detected by staining with CD31, was similar in all three groups (Fig. 6a-c). The human fibroblasts of the bioengineered graft could be detected by staining with CD90 in all groups (Fig. 6a-c). Similarly, in specimens covered with human split-thickness skin, rat blood vessels were found in proximity to the epidermis (Fig. 6d-f). The human origin was confirmed by CD90 staining, which was expressed by human fibroblasts in the split-thickness skin (Fig. 6d-f). In specimens covered with neonatal rat epidermis, the ingrowth of rat blood vessels was similar in all three groups (Fig. 6g-i). No human fibroblasts expressing CD90 were detected (Fig. 6d-i).

Discussion

The goal of this experimental study was to test whether a human bioengineered skin graft can be used to replace human split-thickness skin for the pre-clinical testing of acellular dermal substitutes used for skin reconstruction. These bioengineered grafts were compared to the current standard coverage of dermal substitutes, i.e. split-thickness skin, and to neonatal rat epidermis. In the global picture, human bioengineered grafts demonstrated a very similar biological behavior as split-thickness skin, while neonatal rat epidermis performed significantly poorer.

Several points deserve a detailed comment: Split-thickness skin was used as positive control for the new model, as split-thickness skin transplantation is the gold standard for complex dermo-epidermal skin reconstruction in clinical practice since more than 10 years [1, 25, 26]. Interestingly, we found that the human bioengineered graft behaved as well as split-thickness skin. When transplanted on Matriderm as well as on engineered acellular collagen hydrogel, the bioengineered skin grafts show similar biological performance as seen with transplantation of split-thickness skin. A continuous basal lamina was deposited as evidenced by staining for the basal lamina component laminin 5, and all suprabasal cells expressed keratin 1 as is seen in normal homeostatic skin. Rat blood vessels grew into the dermal part of the bioengineered grafts and so ensured sufficient oxygen and nutrient supply for the epidermis. The presence of human fibroblasts, which are indispensable key players regarding skin architecture and functionality, in the bioengineered skin grafts could be confirmed by the detection of human CD90-specific cells.

In sharp contrast, the performance of neonatal rat epidermis alone was significantly poorer. The most tenable explanation for the good performance of the bioengineered graft and split-thickness skin as opposed to rat epidermis is the presence of dermal components in the former and a complete lack of those elements in the latter. It is well documented in the literature that viable and functional dermal elements are crucial for epidermal viability and functionality [27-31].

The almost identical biological behavior of the bioengineered grafts compared to split-thickness skin indicates that human bioengineered grafts might be used in the future instead of split-thickness skin as standard dermo-epidermal coverage to test any newly designed dermal substitutes. Of note, human bioengineered grafts can be prepared in a very standardized way in terms of cell numbers, cell types, and

thickness of the graft. The use of a humanized model represents an additional advantage, given the fact that the mentioned preclinical testing procedures may lead to applications in human patients.

In summary and conclusion, this series of experiments provides evidence that human bioengineered skin grafts can successfully be employed to test different acellular dermal substitutes designed for skin reconstruction. Such testing is indispensable before new products can be applied clinically.

Conflict of interest

The authors declare that they have no conflict of interest.

Acknowledgements

This work was financially supported by the EU-FP6 project EuroSTEC (soft tissue engineering for congenital birth defects in children: contract: LSHB-CT-2006-037409), by the EU-FP7 project EuroSkinGraft (FP7/2007-2013: grant agreement n° 279024), and by the University of Zurich. We are particularly grateful to the Fondation Gaydoul and the sponsors of “Dona Tissue” (Thérèse Meier and Robert Zingg) for their financial support and interest in our work.

Figures and Tables

Table 1: Summary of the sample sizes for each group.

	On fascia	On Matriderm	On acellular collagen
Human bioengineered graft	10	3	4
Human split-thickness skin	1	1	1
Neonatal rat epidermis	4	4	4

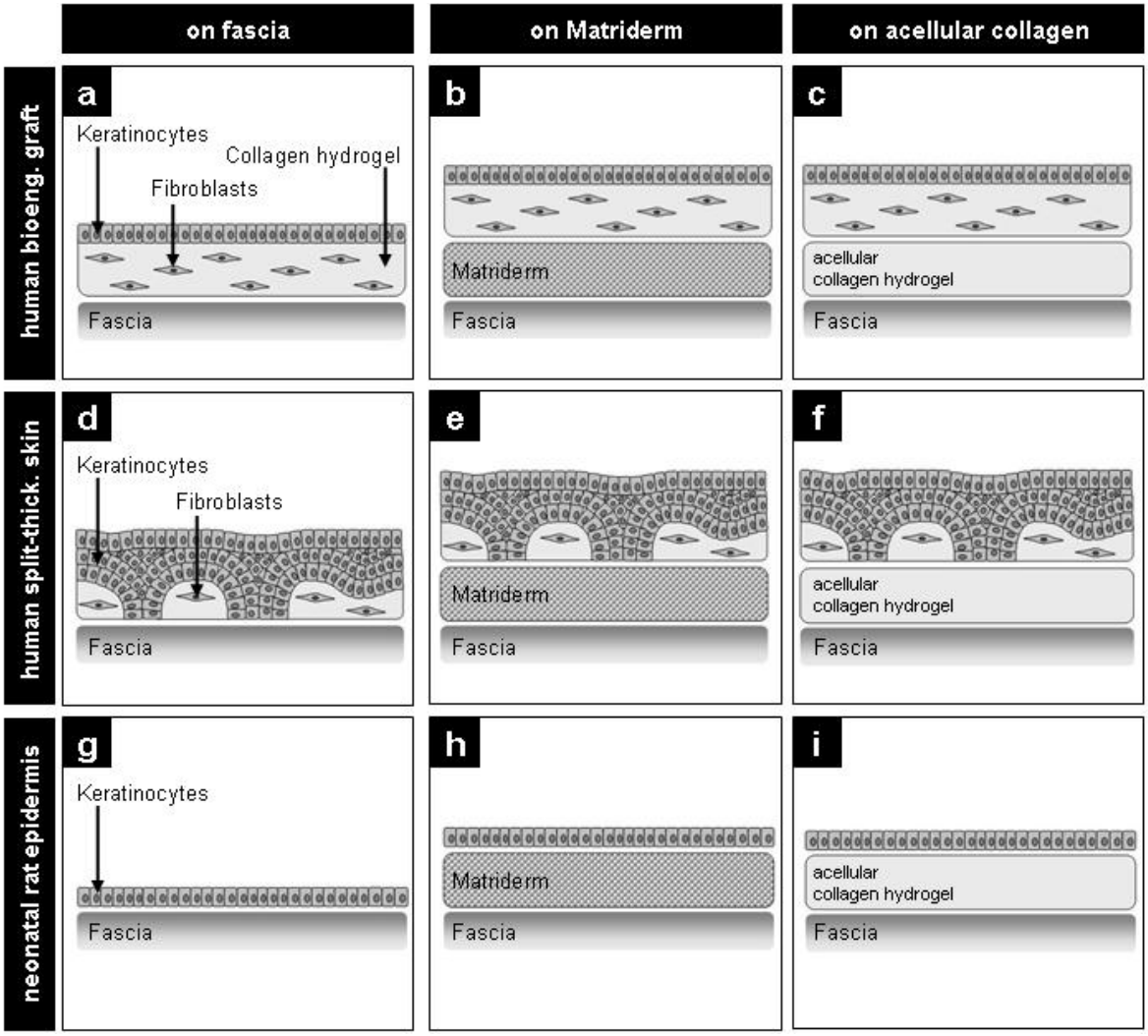

Fig. 1 Schematic overview on the different combinations of dermal substitutes and coverage used in this study. **a-c** Human bioengineered graft transplanted onto the fascia (**a**), on Matriderm (**b**), or, on engineered acellular collagen hydrogel (**c**). **d-f** Human split-thickness skin transplanted onto the fascia (**d**), on Matriderm (**e**), or, on engineered acellular collagen hydrogel (**f**). **g-i** Neonatal rat epidermis transplanted onto the fascia (**g**), on Matriderm (**h**), or, on engineered acellular collagen hydrogel (**i**).

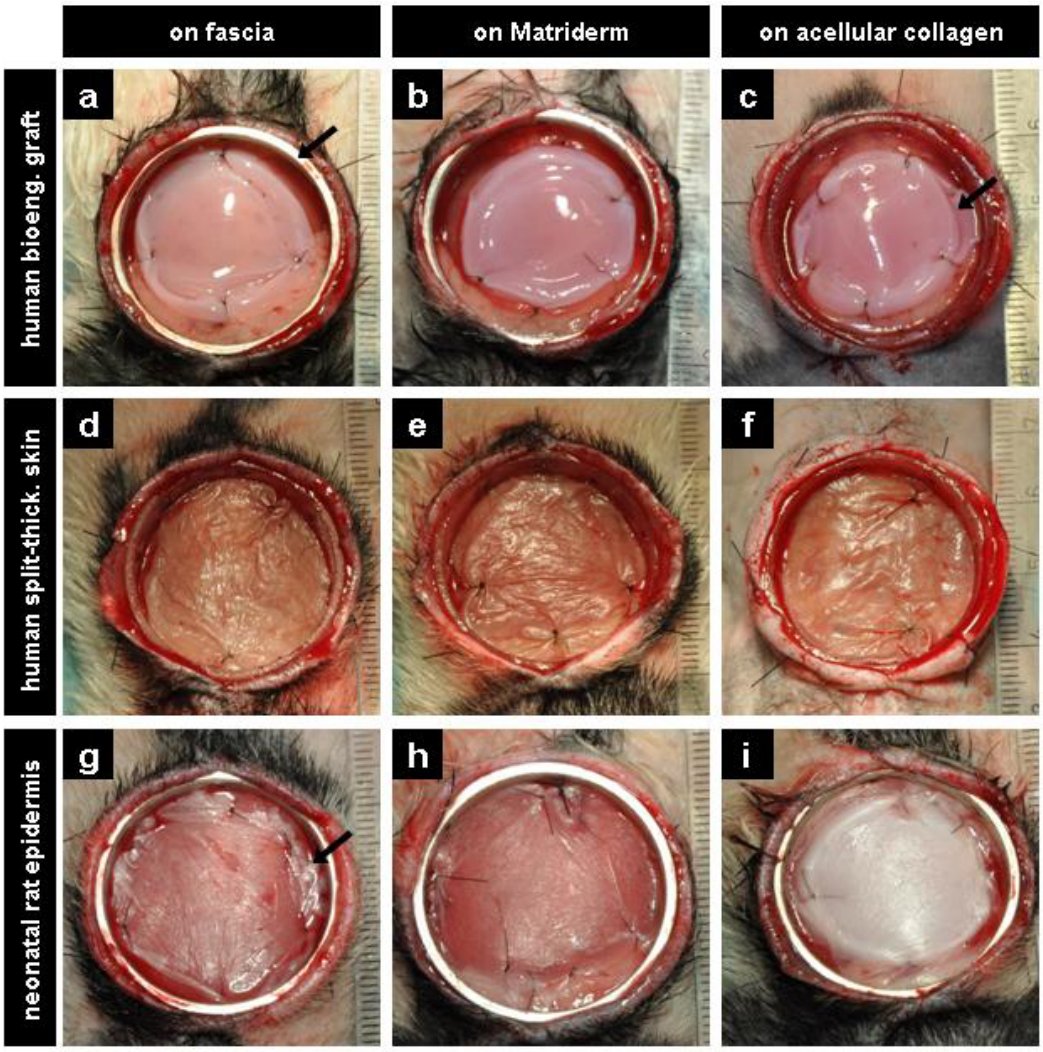

Fig. 2 Macroscopic view of grafts at time point of transplantation. **a-c** Human bioengineered graft appearance is similar in all three groups. The underlying engineered acellular collagen hydrogel is detectable in **c** (*arrow*). **d-f** Human split-thickness skin shows similar appearance in all three groups. **g-h** Neonatal rat epidermis looks similar when transplanted onto fascia and Matriderm. **i** Neonatal rat epidermis looks pale when transplanted onto engineered acellular collagen hydrogels. Diameter of the ring (*arrow* in **a**) 26 mm (**a-i**)

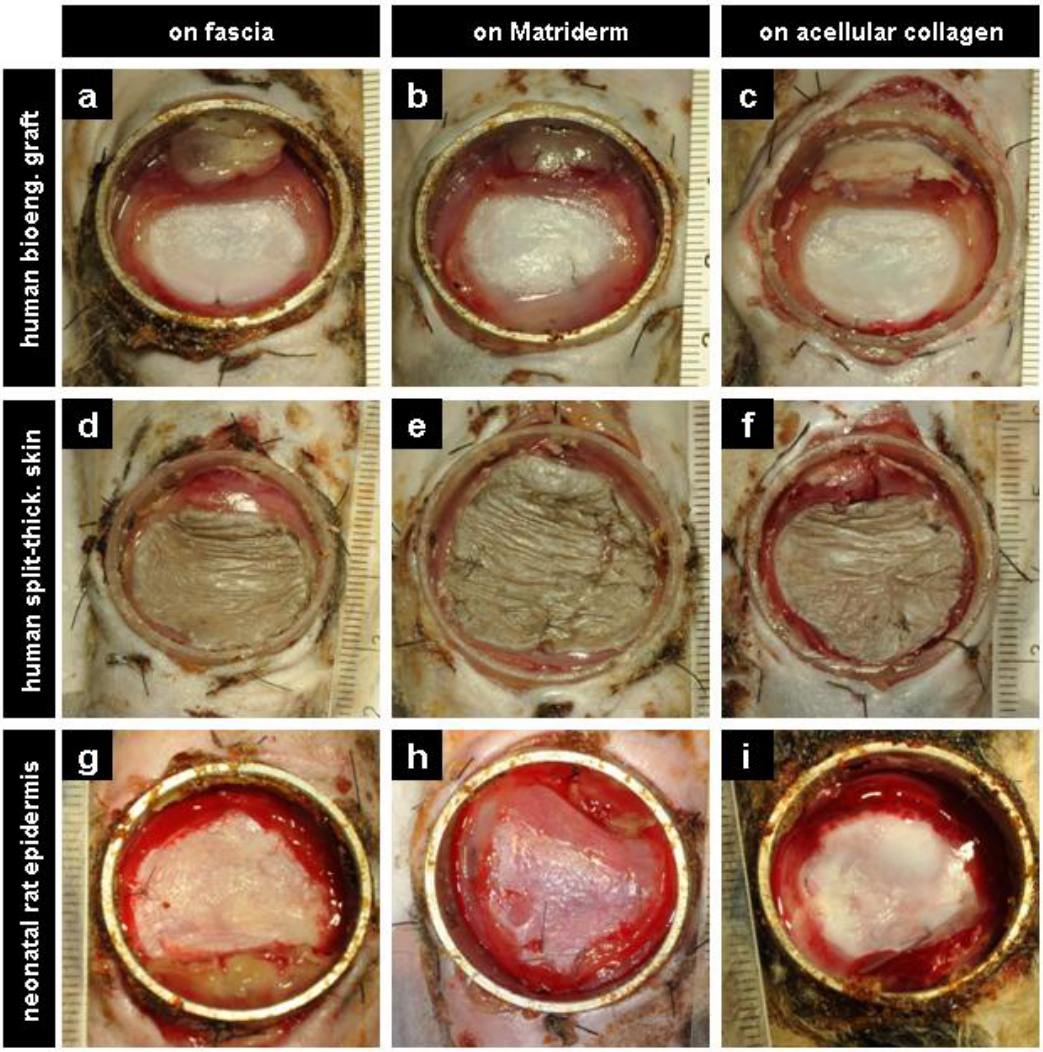

Fig. 3 Macroscopic view of grafts 21 days post transplantation. **a-c** Human bioengineered grafts show complete take in all three groups. Grafts look almost identical in all three groups. **d-f** Human split-thickness skin show complete take in all three groups. Grafts look almost identical in all three groups. **g-i** Neonatal rat epidermis show only partial take that is similar in all three groups. The surviving epidermal islets look very fragile and do not seem to be firmly attached to the wound bed.

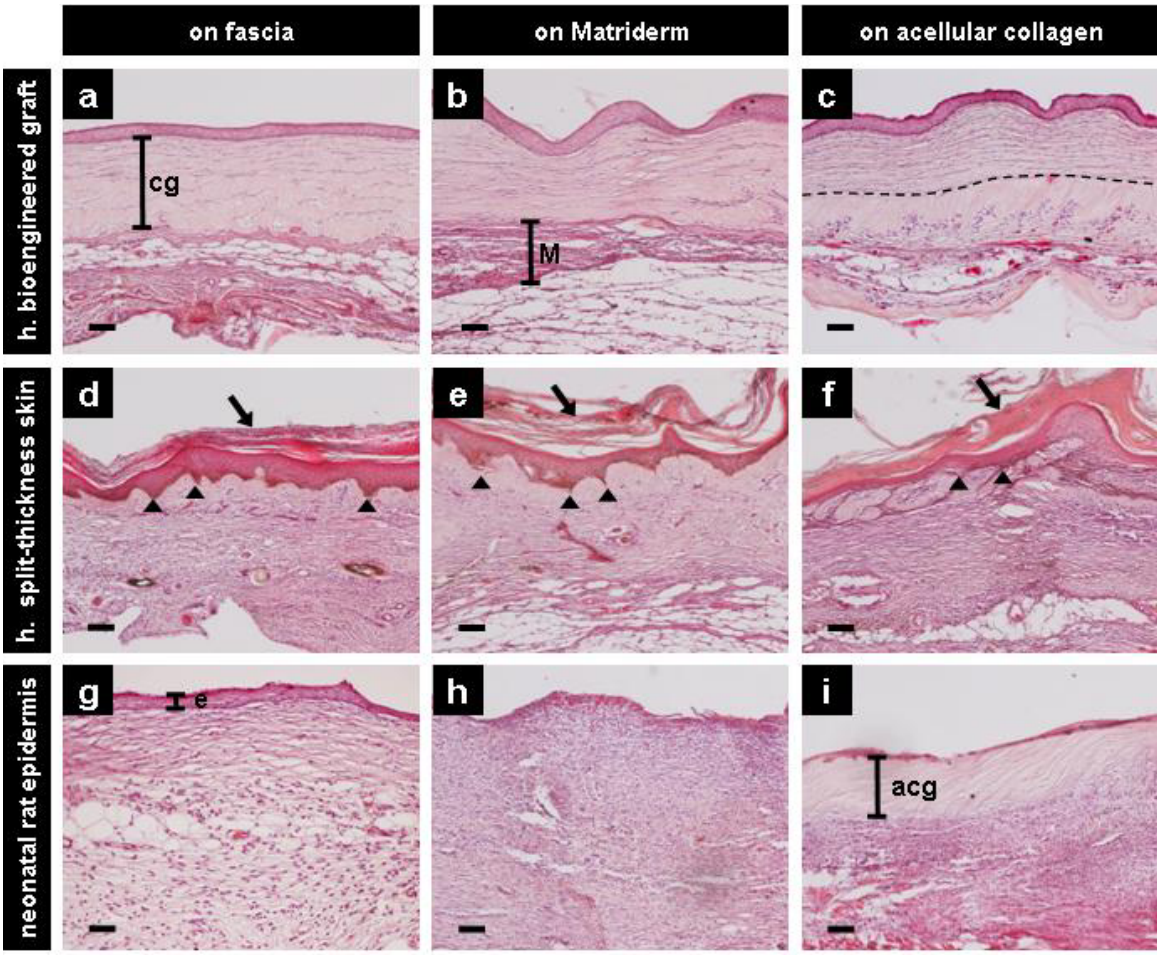

Fig. 4 Histological evaluation of grafts (haematoxylin & eosin staining) excised 21 days post transplantation. **a** Human bioengineered grafts transplanted onto the fascia show 6-9 keratinocyte layers and the dermal part of the bioengineered graft can be clearly distinguished from the underlying tissue (*cg* = collagen gel). **b** Human bioengineered grafts transplanted on Matriderm show similar appearance as in **a**. Remnants of Matriderm are detectable between the bioengineered graft and the underlying rat tissue (*M* = Matriderm). **c** Human bioengineered grafts transplanted on acellular collagen show similar appearance as in **a**. The border between graft and engineered acellular collagen hydrogel can be discerned (*dotted line*). **d-f** Human split-thickness skin look similar in all three groups. The normally configured epidermis shows a stratum corneum (*arrows*) and rete ridges (*arrow heads*). **g** Neonatal rat epidermis transplanted onto the fascia is very thin and unstratified (*black line*). **h** Neonatal rat epidermis transplanted onto Matriderm does not survive, no epidermis is detectable. **i** Neonatal rat epidermis transplanted on engineered acellular collagen hydrogel does not survive, only single epidermal cells are occasionally detectable. The collagen gel is easily discernable and there are almost no cells. (*acg* = engineered acellular collagen hydrogel). *Scale bars* 100 µm (**a**-**i**).

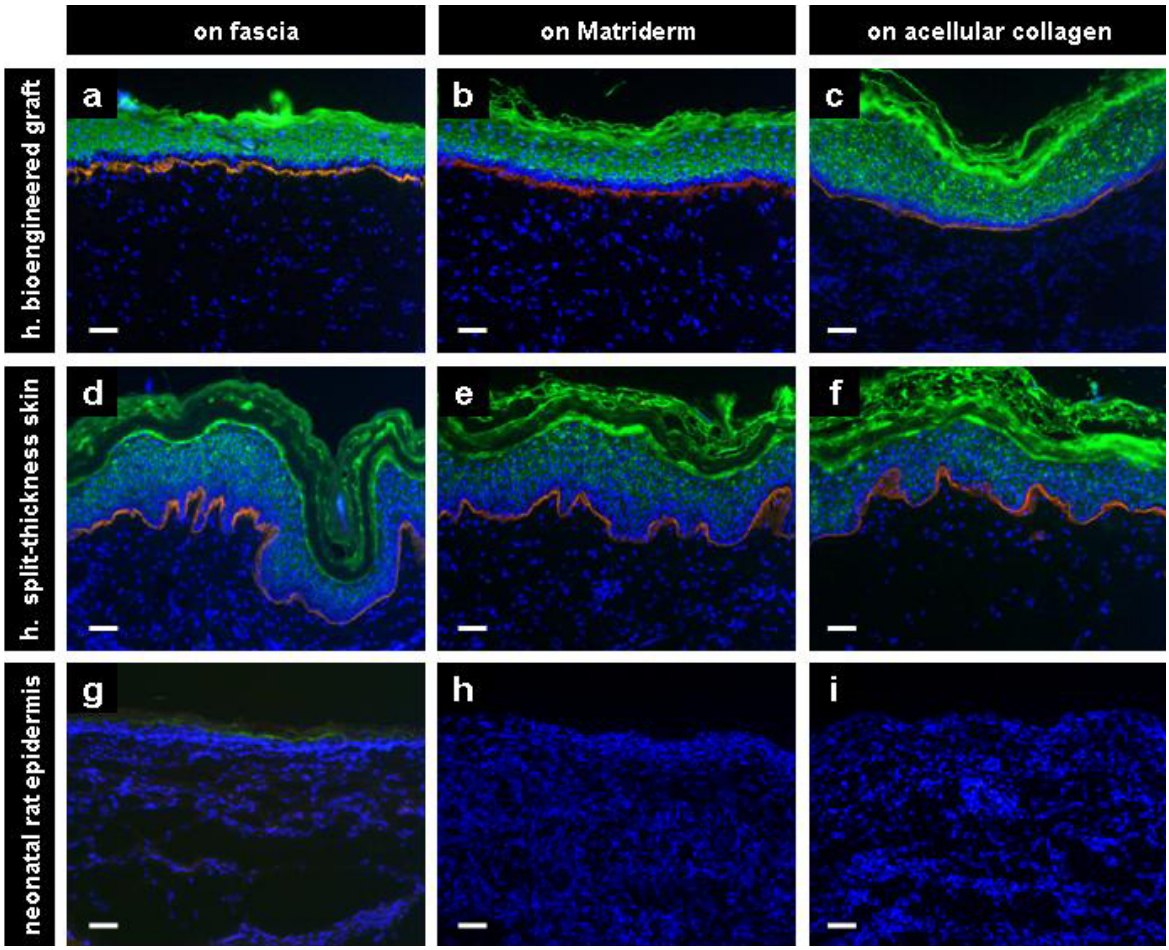

Fig. 5 Immunofluorescence stainings (laminin 5 and keratin 1) of grafts excised 21 days post transplantation. **a-c** In human bioengineered grafts in all three groups, staining of the basement membrane component laminin 5 (*red*) reveals the deposition of a continuous basement membrane. In all three groups, all suprabasal cells express keratin 1 (*green*). **d-f** Human split-thickness skin in all three groups shows similar expression of laminin 5 (*red*) and keratin 1 (*green*) as described for **a-c**. **g-i** In all three groups with neonatal rat epidermis transplantation, there is no laminin 5 (*red*) nor keratin 1 (*green*) expression. *Scale bars* 50 µm.

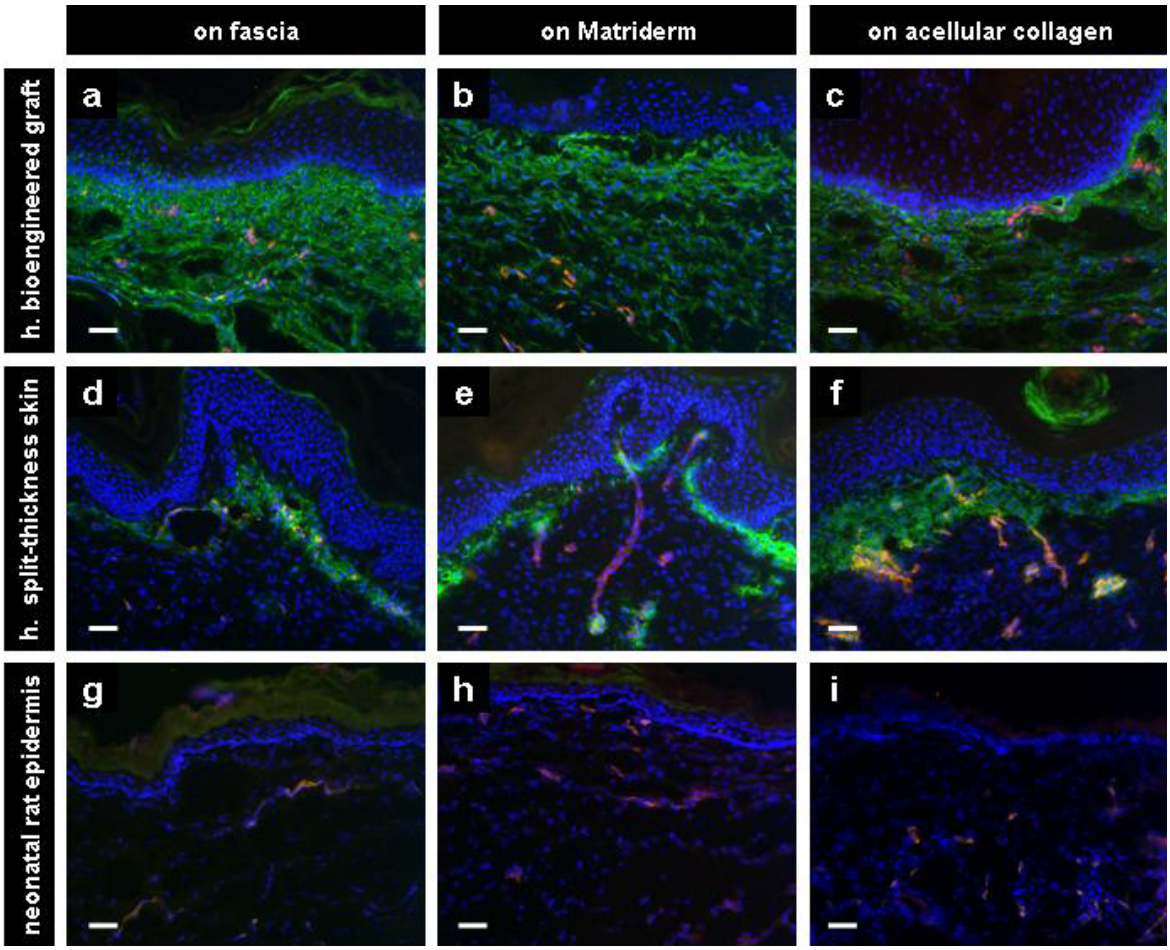

Fig. 6 Immunofluorescence stainings (CD31 and CD90) of grafts excised 21 days post transplantation. **a-c** In human bioengineered grafts in all three groups, staining with CD31 (*red*) reveals the ingrowth of rat blood vessels into the dermal part of the coverage graft. Also, human fibroblasts expressing CD90 (*green*) are detected in all groups. **d-f** In human split-thickness skin, rat blood vessels grew into the dermal part as detected by CD31 staining (*red*). Human fibroblasts are detected by staining with CD90 (*green*). **g-i** In neonatal rat epidermis in all three groups, staining with CD31 (*red*) reveals the ingrowth of rat blood vessels into the transplants. In all three groups, no human fibroblasts expressing CD90 (*green*) are detected. *Scale bars* 50 µm.

References

1. Schiestl C, Stiefel D, Meuli M (2010) Giant naevus, giant excision, eleg(i)ant closure? Reconstructive surgery with Integra Artificial Skin to treat giant congenital melanocytic naevi in children. J Plast Reconstr Aesthet Surg Apr;63(4):610-5

2. Schiestl C, Neuhaus K, Biedermann T, Böttcher-Haberzeth S, Reichmann E, Meuli M (2011) Novel treatment for massive lower extremity avulsion injuries in children: slow, but effective with good cosmesis. Eur J Pediatr Surg Mar;21(2):106-10

3. Stiefel D, Schiestl CM, Meuli M (2009) The positive effect of negative pressure: vacuum-assisted fixation of Integra artificial skin for reconstructive surgery. J Pediatr Surg Mar;44(3):575-80

4. Stiefel D, Schiestl C, Meuli M (2010) Integra Artificial Skin for burn scar revision in adolescents and children. Burns Feb;36(1):114-20

5. Böttcher-Haberzeth S, Biedermann T, Reichmann E (2010) Tissue engineering of skin. Burns Jun;36(4):450-60

6. Heitland A, Piatkowski A, Noah EM, Pallua N (2004) Update on the use of collagen/glycosaminoglycate skin substitute-six years of experiences with artificial skin in 15 German burn centers. Burns Aug;30(5):471-5

7. Branski LK, Herndon DN, Pereira C, Mlcak RP, Celis MM, Lee JO, Sanford AP, Norbury WB, Zhang XJ, Jeschke MG (2007) Longitudinal assessment of Integra in primary burn management: a randomized pediatric clinical trial. Crit Care Med Nov;35(11):2615-23

8. Schneider J, Biedermann T, Widmer D, Montano I, Meuli M, Reichmann E, Schiestl C (2009) Matriderm versus Integra: a comparative experimental study. Burns Feb;35(1):51-7

9. Cervelli V, Lucarini L, Cerretani C, Spallone D, Palla L, Brinci L, De Angelis B (2010) The use of Matriderm and autologous skin grafting in the treatment of diabetic ulcers: a case report. Int Wound J Aug;7(4):291-6

10. Böttcher-Haberzeth S, Biedermann T, Schiestl C, Hartmann-Fritsch F, Schneider J, Reichmann E, Meuli M (2012) Matriderm® 1 mm versus Integra® Single Layer 1.3 mm for one-step closure of full thickness skin defects: a comparative experimental study in rats. Pediatr Surg Int Feb;28(2):171-7

11. Keck M, Haluza D, Lumenta DB, Burjak S, Eisenbock B, Kamolz LP, Frey M (2011) Construction of a multi-layer skin substitute: Simultaneous cultivation of keratinocytes and preadipocytes on a dermal template. Burns Jun;37(4):626-30

12. Haslik W, Kamolz LP, Nathschläger G, Andel H, Meissl G, Frey M (2007) First experiences with the collagen-elastin matrix Matriderm as a dermal substitute in severe burn injuries of the hand. Burns May;33(3):364-8

13. Shakespeare PG (2005) The role of skin substitutes in the treatment of burn injuries Clin Dermatol Jul-Aug;23(4):413-8

14. Kearney JN (2001) Clinical evaluation of skin substitutes. Burns Aug;27(5):545-51

15. Cervelli V, Brinci L, Spallone D, Tati E, Palla L, Lucarini L, De Angelis B (2011) The use of MatriDerm® and skin grafting in post-traumatic wounds. Int Wound J Aug;8(4):400-5

16. Lamme EN, van Leeuwen RT, Mekkes JR, Middelkoop E (2002) Allogeneic fibroblasts in dermal substitutes induce inflammation and scar formation. Wound Repair Regen May-Jun;10(3):152-60

17. Middelkoop E, van den Bogaerdt AJ, Lamme EN, Hoekstra MJ, Brandsma K, Ulrich MM (2004) Porcine wound models for skin substitution and burn treatment. Biomaterials Apr;25(9):1559-67

18. van den Bogaerdt AJ, Ulrich MM, van Galen MJ, Reijnen L, Verkerk M, Pieper J, Lamme EN, Middelkoop E (2004) Upside-down transfer of porcine keratinocytes from a porous, synthetic dressing to experimental full-thickness wounds. Wound Repair Regen Mar-Apr;12(2):225-34

19. Philandrianos C, Andrac-Meyer L, Mordon S, Feuerstein JM, Sabatier F, Veran J, Magalon G, Casanova D (2012) Comparison of five dermal substitutes in full-thickness skin wound healing in a porcine model. Burns Sep;38(6):820-9

20. Pontiggia L, Biedermann T, Meuli M, Widmer D, Böttcher-Haberzeth S, Schiestl C, Schneider J, Braziulis E, Montaño I, Meuli-Simmen C, Reichmann E (2009) Markers to evaluate the quality and self-renewing potential of engineered human skin substitutes in vitro and after transplantation. J Invest Dermatol Feb;129(2):480-90

21. Costea DE, Loro LL, Dimba EA, Vintermyr OK, Johannessen AC (2003) Crucial effects of fibroblasts and keratinocyte growth factor on morphogenesis of reconstituted human oral epithelium. J Invest Dermatol Dec;121(6):1479-86

22. Braziulis E, Diezi M, Biedermann T, Pontiggia L, Schmucki M, Hartmann-Fritsch F, Luginbühl J, Schiestl C, Meuli M, Reichmann E (2012) Modified plastic compression of collagen hydrogels provides an ideal matrix for clinically applicable skin substitutes. Tissue Eng Part C Methods Jun;18(6):464-74

23. Biedermann T, Pontiggia L, Böttcher-Haberzeth S, Tharakan S, Braziulis E, Schiestl C, Meuli M, Reichmann E (2010) Human eccrine sweat gland cells can reconstitute a stratified epidermis. J Invest Dermatol Aug;130(8):1996-2009

24. Böttcher-Haberzeth S, Biedermann T, Pontiggia L, Braziulis E, Schiestl C, Hendriks B, Eichhoff OM, Widmer DS, Meuli-Simmen C, Meuli M, Reichmann E (2012) Human eccrine sweat gland cells turn into melanin-uptaking keratinocytes in dermo-epidermal skin substitutes. J Invest Dermatol in press

25. Meuli M, Raghunath M (1997) Burns (Part 2) Tops and flops using cultured epithelial autografts in children. Pediatr Surg Int Sep;12(7):471-7

26. Gobet R, Raghunath M, Altermatt S, Meuli-Simmen C, Benathan M, Dietl A, Meuli M (1997) Efficacy of cultured epithelial autografts in pediatric burns and reconstructive surgery. Surgery Jun;121(6):654-61

27. Rheinwald JG, Green H (1975) Serial cultivation of strains of human epidermal keratinocytes: the formation of keratinizing colonies from single cells. Cell Nov;6(3):331-43

28. Leary T, Jones PL, Appleby M, Blight A, Parkinson K, Stanley M (1992) Epidermal keratinocyte self-renewal is dependent upon dermal integrity. J Invest Dermatol Oct;99(4):422-30

29. Botchkarev VA, Kishimoto J (2003) Molecular control of epithelial-mesenchymal interactions during hair follicle cycling. J Investig Dermatol Symp Proc Jun;8(1):46-55

30. Schultz GS, Wysocki A (2009) Interactions between extracellular matrix and growth factors in wound healing. Wound Repair Regen Mar-Apr;17(2):153-62

31. Helary C, Zarka M, Giraud-Guille MM (2012) Fibroblasts within concentrated collagen hydrogels favour chronic skin wound healing. J Tissue Eng Regen Med Mar;6(3):225-37

4.4 Skingineering I: engineering porcine dermo-epidermal skin analogues for autologous transplantation in a large animal model

Pediatr Surg Int (2011) 27:241–247
DOI 10.1007/s00383-010-2777-0

ORIGINAL ARTICLE

Skingineering I: engineering porcine dermo-epidermal skin analogues for autologous transplantation in a large animal model

Erik Braziulis · Thomas Biedermann · Fabienne Hartmann-Fritsch · Clemens Schiestl · Luca Pontiggia · Sophie Böttcher-Haberzeth · Ernst Reichmann · Martin Meuli

Published online: 18 November 2010

Abstract

Background Extended full thickness skin defects still represent a considerable therapeutic challenge as ideal strategies for definitive autologous coverage are still not available. Tissue engineering of whole skin represents an equally attractive and ambitious novel approach. We have recently shown that laboratory-grown human skin analogues with near normal skin anatomy can be successfully transplanted on immuno-incompetent rats. The goal of the present study was to engineer autologous porcine skin grafts for transplantation in a large animal model (pig study = intended preclinical study). Materials and methods Skin biopsies were taken from the pig's abdomen. Epidermal keratinocytes and dermal fibroblasts were isolated and then expanded on culture dishes. Subsequently, highly concentrated collagen hydrogels and collagen/fibrin hydrogels respectively, both containing dermal fibroblasts, were prepared. Fibroblast survival, proliferation, and morphology were monitored using fluorescent labelling and laser scanning confocal microscopy. Finally, keratinocytes were seeded onto this dermal construct and allowed to proliferate. The resulting *in vitro* generated porcine skin substitutes were analysed by H&E staining and immunofluorescence.

Results Dermal fibroblast proliferation and survival in pure collagen hydrogels was poor. Also, the cells were mainly round-shaped and they did not develop 3D networks. In collagen/fibrin hydrogels, dermal fibroblast survival was significantly higher. The cells proliferated well, were spindle-shaped, and formed 3D-networks. When these latter dermal constructs were seeded with keratinocytes, a multilayered and partly stratified epidermis readily developed.

Conclusion This study provides compelling evidence that pig cell-derived skin analogues with near normal skin anatomy can be engineered *in vitro*. These tissue-engineered skin substitutes are needed to develop a large animal model to establish standardized autologous transplantation procedures for those studies that must be conducted before ''skingineering'' can eventually be clinically applied.

Introduction

Large full thickness skin defects typically result from burns, massive avulsion injuries, septic skin necroses, or from extended excision of scars or nevi [1–10]. The coverage of such lesions still poses a very significant challenge: the functionally and cosmetically best therapeutic option is transplanting full thickness autologous skin, however, donor sites are limited in a prohibitive way when there is extensive demand [11–14]. On the other end of the therapeutical spectrum stands the almost unlimited supply of cultured autologous epithelial autografts (CEA) (in numerous variations) that, despite enormous basic science and clinical research efforts, still requires 2–3 weeks of cultivation time and still yields far from ideal results [15–23].

Clearly, the clinical introduction of nowadays widely used dermal regeneration templates (e.g. Integra DRT® and Matriderm®) and the development of more sophisticated laboratory-grown skin substitutes containing keratinocytes, fibroblasts, extracellular matrix components, growth factors, and other cytokines have pushed the frontiers further [8, 16, 17, 24–29].

Yet, these techniques are still plagued with considerable problems including intricate and time consuming laboratory processes, fragility of grafts, staged operative procedures, susceptibility to infection, poor graft take, and, finally and most importantly, not really satisfactory long term results in terms of both functionality and cosmetic appearance of the reconstituted skin [30–32].

We have, therefore, invested over 10 years of laboratory research into the ambitious project of engineering an anatomically near normal skin analogue. Briefly summarized, we have managed to grow a hydrogel-based dermo-epidermal construct featuring a correctly stratified epidermis, a basement membrane, the characteristic structures of the dermo-epidermal junction, and a close to normal, prevascularised dermis [33]. These grafts, cultured from human cells, were then successfully grafted onto immuno-incompetent rats [34–36].

Theoretically, this progress may be seen as the indispensable evidence required before an eventual clinical application in human patients can be envisioned. Practically, however, we are facing the problem that the above mentioned human tissue grafts used in our rat model are way too small and ill-configured (round grafts, 2.5 cm diameter, covering about 4 cm^2) when looking at grafts suitable for large scale

transplantation in human patients. Ideally, such transplants should be rectangular and large (covering 50–100 cm^2).

Consequently, we have embarked on culturing skin substitutes with near normal anatomical architecture, mechanical properties allowing standard surgical handling, and appropriate size matching the prerequisites for large scale autologous transplantation in a large animal model (=immunocompetent setting). This article describes *in vitro* engineering of such grafts to be later used in pigs.

Materials and methods

In view of the envisioned animal model for large scale autologous transplantation, we have chosen the pig (Schweizer Edelschwein). Biopsies were taken as outlined in detail in the companion paper published in the same issue (Skingineering II).

Isolation and culture of keratinocytes and fibroblasts

Porcine skin samples (3x1 cm) were cut to 2–3 mm^2pieces and incubated for 15-18 h at 4°C in 12 U/ml dispase in HBSS containing 5 µg/ml gentamycin. The epidermis was then separated from the dermis using forceps. Epidermal cells were isolated by incubation in1% trypsin, 5 mM EDTA for 3 min at 37°C. After centrifugation, the cell pellet was resuspended in CT57keratinocyte medium containing 5 µg/ml gentamycin (CELLnTEC Advanced Cell Systems AG, Bern, Switzerland), then seeded on collagen type I-coated cell culture dishes (BD Falcon, Basel, Switzerland). Medium was changed every 2–3 days.

The dermal tissue was digested in 2 mg/ml Collagenase for about 60 min at 37°C. Isolated cells were seeded on 10 cm cell culture dishes containing fibroblast growth medium (DMEM supplemented with 10% FCS, 4 mM alanyl-L-glutamine, 1 mM sodium pyruvate, and 5 µg/ml gentamycin) and allowed to attach overnight, before dead cells and erythrocytes were removed by three washes in phosphate buffered saline (PBS). Collagenase was from Sigma (Buchs, Switzerland), and all other compounds were from Invitrogen (Basel, Switzerland).

Organotypic skin cultures

Organotypic cultures were prepared using a previously established transwell system (4.2 $cm^2$6-well cell culture inserts with membranes of 3.0 µm pore-size, BD Falcon, Basel, Switzerland). A highly concentrated acidic solution of bovine collagen type I (5 mg/ml, Symatese Biomatériaux, 69630 Chaponost, France) was neutralized on ice by drop wise addition of 0.5 M NaOH and immediately mixed with $5x10^4$human primary dermal fibroblasts (passage 1–2) suspended in fibroblast growth medium. For the fibrin-containing preparations, fibrinogen was added to the collagen before neutralization, thrombin was added after neutralization, and mixed thoroughly. All components were chilled on ice during gel preparation. The mixture was transferred

into 6-well culture inserts immediately and allowed to gel for 10 min at room temperature before being transferred into a cell culture incubator.

The fibroblast-containing gels were grown in fibroblast growth medium for 3–7 days before $7.5x10^5$keratinocytes were seeded onto the entire surface of each gel. After initial submersed cultivation in Rheinwald and Green keratinocyte differentiation medium (RGM) [37] for 3–7 days, the medium level was lowered to 1.5 ml to expose the developing epidermis to air (air–liquid interface) for additional 7–10 days. Medium changes were performed every 2–3 days.

Fluorescein diacetate (FdA) vital cell staining

Fluorescein diacetate (FdA) staining was performed as published and proven to be suitable for the determination of cell viability in tissue-engineered skin [38, 39]. In short, cell culture medium was replaced for 2 min with the equal volume of 5 µM FdA in PBS, freshly prepared from a stock solution of 5 mM FdA in acetone. The FdA was removed by washing twice in PBS before fresh culture medium was applied.

Actin and nuclear staining

Gels were fixed in 4% paraformaldehyde and permeabilised in acetone/methanol (1:1) for 20 min at -20°C, air dried, and washed 3x in PBS. Then they were blocked in PBS containing 2% BSA (Sigma) for 30 min. Cytoskeletal actin was stained with phalloidin-TRITC in blocking buffer for 1 h at room temperature. Slides were washed twice for 5 min in PBS. Thereafter sections were incubated for 5 min in PBS containing 1 mg/ml Hoechst 33342 (Sigma) and then washed twice for 5 min in PBS. Finally, the samples were mounted with Dako fluorescent mounting solution (Dako, Baar, Switzerland).

Fluorescence microscopy

Fluorescence microscopy pictures were photographed using a DXM1200F digital camera connected to a Nikon Eclipse TE2000-U inverted microscope, equipped with Hoechst 33342, FITC, and TRITC filter sets or Nikon SMZ1500 stereo microscope with FITC filters (Nikon AG, Egg, Switzerland), (Software: Nikon ACT-1 vers. 2.70).

For confocal imaging, a Nikon C1 Laser Scanning Microscope upgrade on the Eclipse TE2000-U was used. A helium–neon laser with 543-nm excitation was used

for tetramethylrhodamineiso-thiocyanate (TRITC) and 408- nm excitation was used for Hoechst 33342. With the Plan Apo 40 c/N.A.0.95 objective 50 optical sections were captured. Images were processed with Imaris 6.4.0 (Bitplane, Zurich, Switzerland) and Photoshop 7.0 (Adobe Systems Inc, Munich, Germany).

Results

Cell isolation

Porcine dermal fibroblasts could be isolated efficiently from the dermis according to the protocol and media established for the isolation of human dermal fibroblasts [35]. Starting from a 3x1 cm skin biopsy, we received approximately one million fibroblasts within 2–3 days that could be further expanded and passaged. This efficiency as well as proliferation rate is comparable to that of human fibroblasts. Importantly, the morphology of porcine fibroblasts was typical and similar to human fibroblasts (Fig. 1a) [40]. Most cells were viable as shown by viability assay using FdA (Fig. 1b).

Trypsinisation of the porcine epidermis resulted in rapid release of keratinocytes that attached within 2 h to bovine collagen type I-coated cell culture dishes. Within 5–8 days the keratinocytes could be expanded to six million cells in a medium optimised for human keratinocyte precursor enrichment. The morphology of confluent keratinocytes resembled the typical cobblestone pattern of epithelial cells with some interspersed large cells (Fig. 1c). By staining with FdA we could show that the majority of cells were vital (Fig. 1d). Therefore our procedure used for human skin cell isolation and cultivation could be applied for porcine cells without any changes [35].

Fibroblast behaviour in collagen

When porcine fibroblasts were cultivated in highly concentrated collagen type I hydrogels (3 mg/ml), FdA staining revealed that only few vital cells were present 2 days after gel preparation. Furthermore, the majority of cells were round and did not show dendritic or stellate morphology typical for human fibroblasts in collagen gels and in normal dermis [40]. After prolonged cultivation in collagen gels (10 days), some porcine fibroblasts started to proliferate and acquired stellate morphology (data not shown). Porcine fibroblasts seeded in fibrin gels however, were fastly proliferating and showed dendritic or stellate morphology already 1 day after gel preparation (data not shown). We therefore included increasing fibrin concentrations from 0.2 to 1.0 mg/ml in collagen gels to stimulate porcine fibroblasts. Confocal scanning laser microscopy of actin-stained fibroblasts showed a clear effect of fibrin on cell density and morphology. Already 3 days after gel preparation, this effect was detectable and

it intensified over the ensuing days. As little as 0.2 mg/ml fibrin in collagen increased the number of vital cells with mainly stellate or dendritic morphology (Fig. 2a, b). This effect was slightly more pronounced with 0.5 and 1.0 mg/ml fibrin (Fig. 2c, d).

Porcine in vitro skin model

Already one day after seeding porcine keratinocytes on the fibroblast containing gels, a confluent keratinocyte layer was established, indicating that porcine keratinocytes can attach and survive on collagen gels (data not shown). This keratinocyte layer was stable during the initial submersed cultivation phase. During the following air-exposed cultivation phase, a partly stratified epidermis developed (Fig. 3a): a distinct basal layer, 5–7 suprabasal layers, and a well developed stratum corneum (conjunctum and disjunctum) were present. Notably, a stratum granulosum and spinosum could not be distinguished morphologically at this stage. Also, the dermo-epidermal junction was not yet fully established, resulting in an apparently accidental separation of epidermis and dermis in histological sections (cutting artefact). Fibroblasts were present within the dermal component (Fig. 3b). In summary, these features of the engineered porcine skin were typical for *in vitro* generated skin at early stages that will develop further after transplantation [35].

Discussion

This is the first report on *in vitro* engineering of a pig cell derived skin analogue consisting of a multilayered epidermis, a preformed dermo-epidermal junction, and a collagen gel-based dermis-like structure containing fibroblasts and essential extracellular matrix components. In other words, the desirable basic graft profile is basically matched. The following crucial aspects deserve a detailed comment.

First, and most importantly, the graft does exhibit the most essential anatomical hallmarks of skin, although not fully developed. For instance, the epidermis is not yet normally stratified and differentiated. Also, the dermo-epidermal junction is still weak in that cutting for histology easily leads to disruption between epidermis and dermis which is not the case in normal skin. Similarly, the dermal compartment of the construct is, in reality, to be seen as a competent template for the later establishment of a mature dermis. Although abundant dermal fibroblasts, viewed as the key effector cells of the dermis [41], are present, and although certain crucial ECM components are part of the template, the physiological inventory of components and spatial arrangement of these is not yet accomplished. Moreover, certain morphologic characteristics like rete ridges and dermal vasculature are absent at this stage. Obviously, skin appendages are absent.

This ‘‘set of imperfections’’ is mostly identical to what we found when engineering small human cell-derived skin analogues [34, 35]. Interestingly, after transplantation onto immuno-incompetent rats, we observed maturation and differentiation processes finally leading to a near normal skin anatomy (apart from missing skin appendages) [34, 35]. It is, therefore, reasonable to assume that similar mechanisms will also take place after autologous transplantation of the described grafts in the pig model.

Second, since the planned transplantation of the skin substitutes described here in a pig model is intended to be the last preclinical evaluation, it is imperative that all laboratory procedures (cell isolation, expansion, and Organotypic culture system) should be identical or at least very similar to our already established human cell-based system [34, 35]. This is in fact the case for most aspects. In particular, we used the identical cell isolation technique as well as media and growth conditions as we did for our human cell-derived experiments [34, 35]. The only initial lack of correspondence was that porcine fibroblasts did not develop as well in highly

concentrated collagen gels as human fibroblasts did. By addition of fibrin, however, this problem could be solved effectively in that porcine fibroblasts were stimulated to behave like human fibroblasts. This observation is interesting in two ways. It raises the questions why porcine fibroblasts do not tolerate high collagen concentrations and whether the already favourable growth conditions for human fibroblasts could be further improved by adding fibrin to the collagen matrix.

In summary, this study shows that pig cell-derived skin analogues closely approaching normal skin anatomy can be engineered *in vitro*. Evidently, the next experimental step is the development of an appropriate pig model in order to establish a standardized transplantation procedure for further studies.

Acknowledgments

This work was financially supported by EU-FP6project EuroSTEC (soft tissue engineering for congenital birth defects in children: contract: LSHB-CT-2006-037409) and by the University of Zurich. We are particularly grateful to the Fondation Gaydoul and the sponsors of ‘‘DonaTissue’’ (Thérèse Meier, Robert Zingg, the Vontobel Foundation, and the Werner Spross Foundation) for their generous financial support and interest in our work.

Figures

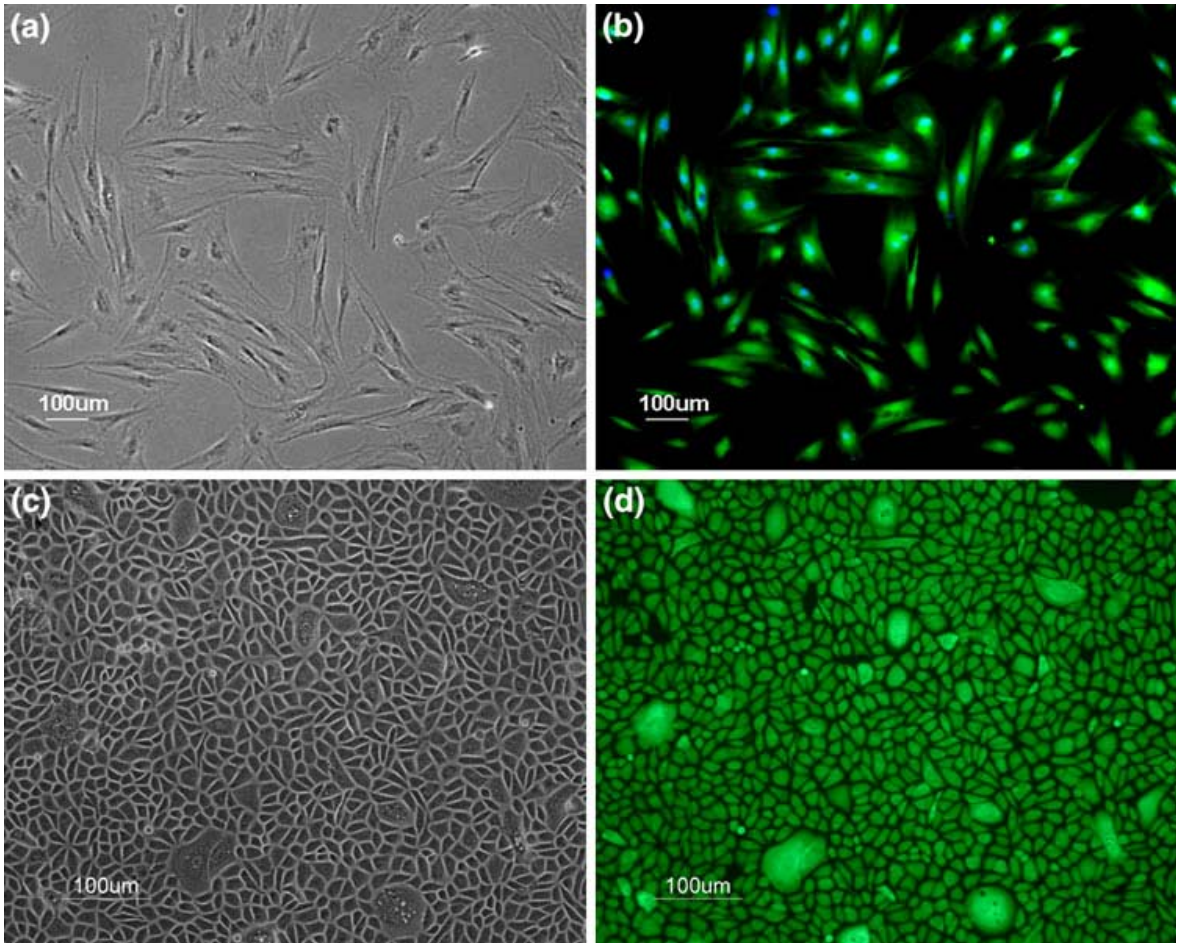

Fig. 1: Two-dimensional cell culture of primary porcine fibroblasts and keratinocytes. **a** Phase contrast microscopy shows typical spindle like morphology of fibroblasts in two-dimensional culture. **b** Positive FdA labelling indicates the viability of all adherent fibroblasts. **c** The majority of confluent porcine primary keratinocytes display typical epithelial cobblestone morphology, while few cells are significantly larger and round. **d** FdA staining reveals that both, the large and the small keratinocytes, are vital. Scale bars 50 µm (a + b); 100 µm (c + d)]

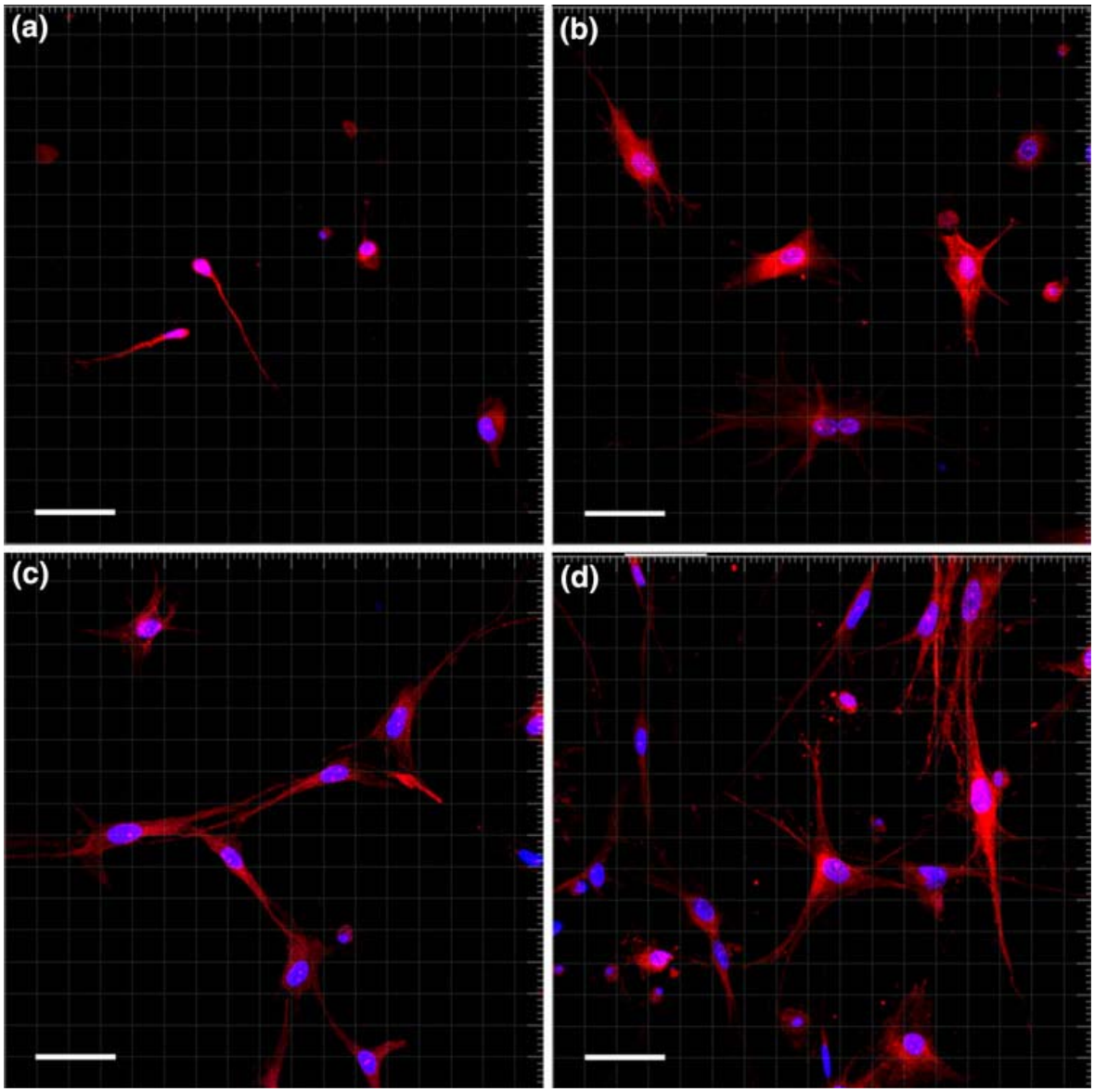

Fig. 2: Laser scanning confocal microscopy of porcine fibroblasts in three-dimensional collagen gels, 7 days after preparation. Actin cytoskeleton staining (red) and nuclear staining (blue).**a** In highly concentrated collagen gels, only few porcine fibroblasts survive and most cells are round or have few extensions. **b–d** By adding increasing fibrin concentrations, more fibroblasts are present and the prevailing morphology is stellate or dendritic. Fibrin concentrations were **(b)** 0.2 mg/ml, **(c)** 0.5 mg/ml, **(d)** 1.0 mg/ml. (scale bars 50 µm, grids 20 µm)

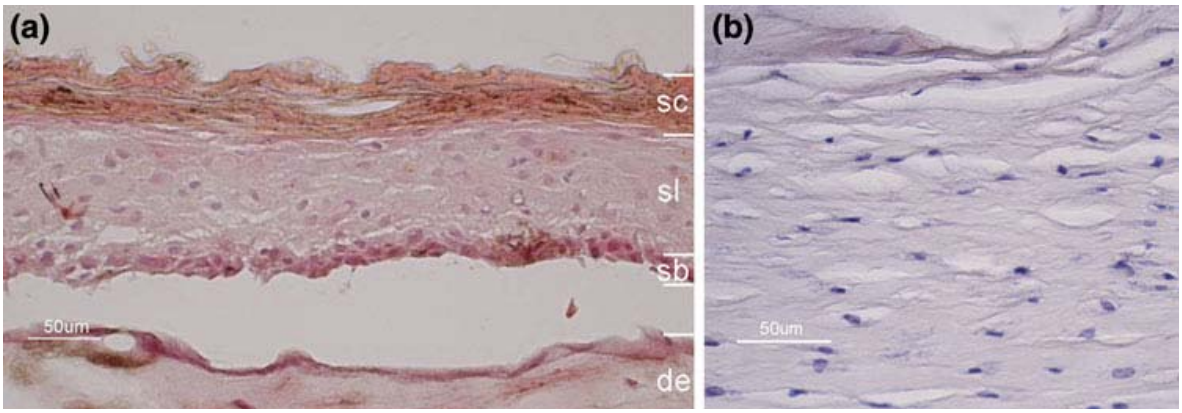

Fig. 3: Histological evaluation of *in vitro* engineered porcine skin, 20 days in culture, H&E staining. **a** A partly stratified epidermis with a well defined stratum corneum (sc), 5–7 suprabasal layers (sl), and a dense stratum basale (sb) have developed on the dermal equivalent (de). Of note, the junction between epidermis and dermis is still weak and disrupted when preparing sections. **b** Fibroblasts were present within the dermal component (gel). (scale bars 50 µm)

References

1. Aarabi S, LongakerMT, Gurtner GC (2007) Hypertrophic scar formation following burns and trauma: new approaches to treatment. PLoS Med 4(9):e234

2. Arneja JS, GosainAK (2007) Giant congenital melanocytic nevi. PlastReconstrSurg 120(2):26e–40e

3. Bauer BS, Corcoran J (2005) Treatment of large and giant nevi. ClinPlastSurg 32(1):11–8, vii

4. Berman B, Viera MH, Amini S, Huo R, Jones IS (2008) Prevention and management of hypertrophic scars and keloids after burns in children. J CraniofacSurg 19(4):989–1006

5. Bittencourt FV, Marghoob AA, Kopf AW, Koenig KL, Bart RS (2000) Large congenital melanocytic nevi and the risk for development of malignant melanoma and neurocutaneousmelanocytosis. Pediatrics 106(4):736–741

6. Earle SA, Marshall DM (2005) Management of giant congenital nevi with artificial skin substitutes in children. J CraniofacSurg 16(5):904–907

7. Kryger ZB, Bauer BS (2008) Surgical management of large and giant congenital pigmented nevi of the lower extremity. PlastReconstrSurg 121(5):1674–1684

8. Schiestl C, Stiefel D, Meuli M (2010) Giant naevus, giant excision, eleg(i)ant closure? reconstructive surgery with integra artificial skin to treat giant congenital melanocytic naevi in children. J PlastReconstrAesthetSurg 63(4):610–615

9. Tannous ZS, Mihm MC Jr, Sober AJ, Duncan LM (2005) Congenital melanocytic nevi: clinical and histopathologic features, risk of melanoma, and clinical management. J Am Acad Dermatol 52(2):197–203

10. Zaal LH, Mooi WJ, SillevisSmitt JH, van der Horst CM (2004) Classification of congenital melanocytic naevi and malignant transformation: a review of the literature. Br J PlastSurg 57(8):707–719

11. Andreassi A, Bilenchi R, Biagioli M, D'Aniello C (2005) Classification and pathophysiology of skin grafts. Clin Dermatol 23(4):332–337

12. Loss M, Wedler V, Kunzi W, Meuli-Simmen C, Meyer VE (2000) Artificial skin, split-thickness autograft and cultured autologous keratinocytes combined to treat a severe burn injury of 93% of TBSA. Burns 26(7):644–652

13. Sheridan R (2009) Closure of the excised burn wound: autografts, semipermanent skin substitutes, and permanent skin substitutes. ClinPlastSurg 36(4):643–651

14. Lochbühler H, Meuli M (1992) Current concepts in pediatric burn care: surgery of severe burns. Eur J PediatrSurg 2(4): 201–204

15. Meuli M, Raghunath M (1997) Burns (Part 2). Tops and flops using cultured epithelial autografts in children. PediatrSurgInt 12(7):471–477

16. Wood FM, Kolybaba ML, Allen P (2006) The use of cultured epithelial autograft in the treatment of major burn injuries: a critical review of the literature. Burns 32(4):395–401

17. Atiyeh BS, Costagliola M (2007) Cultured epithelial autograft (CEA) in burn treatment: three decades later. Burns 33(4): 405–413

18. Raghunath M, Bachi T, Meuli M, Altermatt S, Gobet R, Bruckner-Tuderman L, Steinmann B (1996) Fibrillin and elastin expression in skin regenerating from cultured keratinocyte autografts:

morphogenesis of microfibrils begins at the dermo-epidermal junction and precedes elastic fiber formation. J Invest Dermatol 106(5):1090–1095

19. Raghunath M, Hopfner B, Aeschlimann D, Luthi U, Meuli M, Altermatt S, Gobet R, Bruckner-Tuderman L, Steinmann B (1996) Cross-linking of the dermo-epidermal junction of skin regenerating from keratinocyte autografts. Anchoring fibrils are a target for tissue transglutaminase. J Clin Invest 98(5):1174–1184

20. Raghunath M, Meuli M (1997) Cultured epithelial autografts: diving from surgery into matrix biology. PediatrSurgInt 12(7): 478–483

21. Raghunath M, Tschodrich-Rotter M, Sasaki T, Meuli M, Chu ML, Timpl R (1999) Confocal laser scanning analysis of the association of fibulin-2 with fibrillin-1 and fibronectin define different stages of skin regeneration. J Invest Dermatol 112(1): 97–101

22. Raghunath M, Unsold C, Kubitscheck U, Bruckner-Tuderman L, Peters R, Meuli M (1998) The cutaneous microfibrillar apparatus contains latent transforming growth factor-beta binding protein-1 (LTBP-1) and is a repository for latent TGF-beta1. J Invest Dermatol 111(4):559–564

23. Gobet R, Raghunath M, Altermatt S, Meuli-Simmen C, Benathan M, Dietl A, Meuli M (1997) Efficacy of cultured epithelial autografts in pediatric burns and reconstructive surgery. Surgery 121(6):654–661

24. Carsin H, Ainaud P, Le Bever H, Rives J, Lakhel A, Stephanazzi J, Lambert F, Perrot J (2000) Cultured epithelial autografts in extensive burn coverage of severely traumatized patients: a five year single-center experience with 30 patients. Burns 26(4): 379–387

25. Hernon CA, Dawson RA, Freedlander E, Short R, Haddow DB, Brotherston M, MacNeil S (2006) Clinical experience using cultured epithelial autografts leads to an alternative methodology for transferring skin cells from the laboratory to the patient. Regen Med 1(6):809–821

26. Munster AM (1996) Cultured skin for massive burns. A prospective, controlled trial. Ann Surg 224(3):372–375 (discussion 375–7)

27. Ronfard V, Rives JM, Neveux Y, Carsin H, Barrandon Y (2000) Long-term regeneration of human epidermis on third degree burns transplanted with autologous cultured epithelium grown on a fibrin matrix. Transplantation 70(11):1588–1598

28. Stiefel D, Schiestl C, Meuli M (2010) Integra artificial skin for burn scar revision in adolescents and children. Burns 36(1):114–120

29. Schneider J, Biedermann T, Widmer D, Montano I, Meuli M, Reichmann E, Schiestl C (2009) Matriderm versus Integra: a comparative experimental study. Burns 35(1):51–57

30. Böttcher-Haberzeth S, Biedermann T, Reichmann E (2010) Tissue engineering of skin. Burns 36(4):450–460

31. Boyce ST (2001) Design principles for composition and performance of cultured skin substitutes. Burns 27(5):523–533

32. Shakespeare PG (2005) The role of skin substitutes in the treatment of burn injuries. Clin Dermatol 23(4):413–418

33. Montaño I, Schiestl C, Schneider J, Pontiggia L, Luginbuhl J, Biedermann T, Böttcher-Haberzeth S, Braziulis E, Meuli M, Reichmann E (2010) Formation of human capillaries in vitro: the engineering of prevascularized matrices. Tissue Eng Part A 16(1):269–282

34. Biedermann T, Pontiggia L, Böttcher-Haberzeth S, Tharakan S, Braziulis E, Schiestl C, Meuli M, Reichmann E (2010) Human eccrine sweat gland cells can reconstitute a stratified epidermis. J Invest Dermatol 130(8):1996–2009

35. Pontiggia L, Biedermann T, Meuli M, Widmer D, Böttcher- Haberzeth S, Schiestl C, Schneider J, Braziulis E, Montaño I, Meuli-Simmen C, Reichmann E (2009) Markers to evaluate the quality and self-renewing potential of engineered human skin substitutes in vitro and after transplantation. J Invest Dermatol 129(2):480–490

36. Tharakan S, Pontiggia L, Biedermann T, Böttcher-Haberzeth S, Schiestl C, Reichmann E, Meuli M (2010) Transglutaminases, involucrin, and loricrin as markers of epidermal differentiation in skin substitutes derived from human sweat gland cells. PediatrSurgInt 26(1):71–77

37. Rheinwald JG, Green H (1975) Serial cultivation of strains of human epidermal keratinocytes: the formation of keratinizing colonies from single cells. Cell 6(3):331–343

38. Armour AD, Powell HM, Boyce ST (2008) Fluorescein diacetate for determination of cell viability in tissue-engineered skin. Tissue Eng Part C Methods 14(1):89–96

39. Jones KH, Senft JA (1985) An improved method to determine cell viability by simultaneous staining with fluorescein diacetatepropidium iodide. J HistochemCytochem 33(1):77–79

40. Grinnell F, Ho CH, Tamariz E, Lee DJ, Skuta G (2003) Dendritic fibroblasts in three-dimensional collagen matrices. MolBiol Cell 14(2):384–395

41. Rinn JL, Wang JK, Liu H, Montgomery K, van de Rijn M, Chang HY (2008) A systems biology approach to anatomic diversity of skin. J Invest Dermatol 128(4):776–782

4.5 Skingineering II: transplantation of large-scale laboratory-grown skin analogues in a new pig model

Pediatr Surg Int (2011) 27:249–254
DOI 10.1007/s00383-010-2792-1

ORIGINAL ARTICLE

Skingineering II: transplantation of large-scale laboratory-grown skin analogues in a new pig model

Clemens Schiestl · Thomas Biedermann · Erik Braziulis · Fabienne Hartmann-Fritsch · Sophie Böttcher-Haberzeth · Margarete Arras · Nikola Cesarovic · Flora Nicolls · Carsten Linti · Ernst Reichmann · Martin Meuli

Published online: 11 November 2010

Abstract

Background Tissue engineering of skin with near-normal anatomy is an intriguing novel strategy to attack the still unsolved problem of how to ideally cover massive full-thickness skin defects. After successful production of large, pig cell-derived skin analogues, we now aim at developing an appropriate large animal model for transplantation studies.

Materials and methods In four adult Swiss pigs, full-thickness skin defects, measuring 7.5x7.5 cm, were surgically created and then shielded against the surrounding skin by a new, self-designed silicone chamber. In two animals each, Integra dermal regeneration templates or cultured autologous skin analogues, respectively, were applied onto the wound bed. A sophisticated shock-absorbing dressing was applied for the ensuing 3 weeks. Results were documented photographically and histologically.

Results All animals survived uneventfully. Integra healed in perfectly, while the dermo-epidermal skin analogues showed complete take of the dermal compartment but spots of missing epidermis. The chamber proved effective in precluding (''false positive'') healing from the wound edges and the special dressing efficiently kept the operation site intact and clean for the planned 3 weeks.

Conclusion We present a novel and valid pig model permitting both transplantation of large autologous, laboratory-engineered skin analogues and also keeping the site of intervention undisturbed for at least three postoperative weeks. Hence, the model will be used for experiments testing whether such large skin analogues can restore near normal skin, particularly in the long term. If so, clinical application can be envisioned.

Introduction

In the preceding companion paper [1] (‘‘Skingineering I’’, published in this issue) we have provided detailed information concerning the notorious clinical problems when large or massive full-thickness skin defects have to be covered. Moreover, we have outlined the rationale for tissue engineering of skin with near normal architecture as a potential novel strategy to overcome the mentioned problem.

As a matter of fact, the successful transplantation of small human cell-derived skin analogues on athymic rats [2–4] represents an important step forward with regard to eventual clinical application of this technique, and it led us to design a further experimental series where autologous large scale transplantation of such constructs should be tested in a large animal model. In the aforementioned companion paper [1] we report on the engineering of pig cell-derived skin substitutes suitable for transplantation in a pig model.

The goal of the present study was to create such a pig model that allows standardised large-scale transplantation of laboratory-engineered autologous skin analogues. This model, if valid, would then be used for additional preclinical experiments looking in detail at various critical aspects including particularly functional and cosmetic long-term outcomes of the so reconstituted skin.

Materials and methods

Animals

Adolescent female Swiss pigs (Edelschwein), aged between 2 and 3 months, weighing between 30 and 35 kg were housed in a group of 4, received adequate quantities of pellet food, yoghurt, and they had access to water ad libitum. They were provided with natural day–night cycles. For the purpose of acclimatisation, housing began 2 weeks before the start of the experimental phase. Following skin biopsy, they were again housed in a group of 4 for another 3 weeks until the formal operative procedure. In order to minimise the risk of peer-inflicted damage to the operation site, they were thereafter housed individually in neighbouring stalls for the ensuing three postoperative weeks until they were killed (details see below).

Silicone chamber

In order to prevent any spontaneous healing processes from the wound edges, a silicone chamber was sutured to the wound edges after creation of the skin defect. This device was newly designed (by first author CS) and fabricated (by Carsten Linti, ITV Denkendorf, Germany; Fig. 1).

The transplantation chamber consists of two parts: the chamber, and the cover plate. Both parts are made from silicone rubber using a special cast procedure. The elastic chamber has hardness (shore A) of 80 after curing and removal from the mould. The cover plate is casted from a two-part silicone rubber that cures at room temperature. The flexible cover has hardness (shore A) of 25.

The moulded silicone rubber parts are biocompatible, biostable, and heat resistant (200°C) and thus amenable to standard sterilisation processes, e.g. steam sterilisation.

Anaesthesia and pain management

The study protocol was approved by the local Committee for Experimental Animal Research (Kantonales Veterinäramt des Kantons Zürich, permission number 172/2009).

Prior to all surgical procedures, the pigs were fasted overnight to avoid vomiting and aspiration. At first, all animals were sedated by an intramuscular injection of a mixture of ketamine 20 mg/kg (Narketan®10 ad us. vet., Vétoquinol AG,

Switzerland), azaperone 1.25 mg/kg (StresnilTMad us. vet., Biokema SA, Switzerland) and atropine 0.03 mg/kg (Atropine 0.1%: Kantonsapotheke Zürich, Switzerland). A venous catheter was placed at the ear to apply propofol (20 mg i.v.) (Disoprivan®1% Astra Zeneca, Switzerland) to facilitate intubation. Animals were then intubated with an endotracheal tube 8 mm in diameter (AireCufTM, Veterinary Endotracheal Tube, all Silicone, Bivona Inc., Indiana, USA) and artificial respiration was applied. Anaesthesia was maintained with 2.5% isoflurane (AttaneTMisoflurane ad us. vet., Minrad Inc., New York, USA) in oxygen (4.5 l/min). The operation field was shaved and the skin was disinfected.

Anaesthesia was terminated by leaving the animal on oxygen alone. When breathing normally, the animal was extubated. Intraoperative analgesia was provided by buprenorphine, 0.01 mg/kg (Temgesic®, Essex Chemie AG, Switzerland). Post-operative analgesia was provided by a transdermal fentanyl matrix patch (50 µg/h) (Durogesic® Matrix, Janssen-Cilag AG, Switzerland). Antimicrobial prophylaxis was intraoperatively provided by augmentin (600 mg i.v.) (Augmentin®, GlaxoSmithKline AG, Switzerland) and continued for 5 days (2x625 mg p.o.).

Operative procedures:

Biopsy

Animals were anaesthetised as described above, placed in a left lateral position, and disinfected. A strip-shaped (1x10 cm) full-thickness skin biopsy was harvested from the right hemiabdomen, and the wound was sutured closed. The specimen was then processed as detailed in the twin paper [1].

Creation of full-thickness skin defect, chamber implantation, and transplantation of skin substitutes

Three weeks post biopsy, animals were again anaesthetised as described, placed in prone position, shaved, and disinfected. A square-shaped, 7.5x7.5 cm, full-thickness skin defect over the midline lumbar area was created. Particular care was taken to excise a tissue plate including the entire subcutaneous fat layer so as to ascertain all epithelial elements that could have contributed to later epithelialisation were removed (Fig. 2a).

The silicone chamber was then implanted and fixed to the skin edges as outlined above (Fig. 2b; n = 4).

In two animals, the wound was covered with Integra dermal regeneration template (IDRT) in order to obtain immediate and reliable wound protection [5] a setting that allows studying the behaviour and the biologic effects of the chamber over time. In two other animals, a cultured skin substitute [1] was transplanted in order to phenomenologically test graft take (Fig. 2c). All wound sites were covered with a soft silver foam dressing. The chamber was closed with a 2-mm-thick silicone cover plate (Fig. 2d). With the purpose of protecting the operation sites in an optimal way against any sort of potential mechanical trauma over the ensuing 3 weeks, a multilayer shock absorber device was installed comprising elements attenuating direct as well as sheering forces (Fig. 3) and held in place by a customized garment (Fig. 4).

Postoperative management, euthanasia: harvesting and processing of samples

All animals were individually housed for 3 weeks postoperatively with weekly dressing changes and wound site documentations. Thereafter, they were killed by intravenous administration of pentobarbital (40–60 mg/kg i.v., Esconarkon, ad us. vet., Streuli Pharma AG, Switzerland). After chamber removal, all wound sites were completely excised and processed for histology (H&E staining).

Results

All pigs survived all experimental procedures and the postoperative phase without any significant complications.

The silicone chambers could be inserted into the wound and sewed in place according to the outlined specifications in all animals. Both IDRT and skin analogue placement onto the chamber-sheltered wound bed could be performed without any problem. Over the ensuing 3 weeks (formal dressing changes after 1 and 2 weeks), all the dressings and shock absorber devices remained in place and intact. No adverse events, especially bleeding, infection, or traumatic damage, were observed. Macroscopically, the chamber did not cause any particular reaction within the surrounding tissues like, e.g. a pronounced inflammatory response or excessive granulation tissue production, nor did it exhibit any obvious signs of material damage like, e.g. deformation, frailty, altered consistency, surface erosion, rust, or colour change.

The IDRT implantation yielded a take of 100% after 1 week and the usually encountered peach colour after 3 weeks indicating correct ingrowth and vascularization in both animals [6]. No signs of infection and no obvious findings indicating any kind of unfavourable interaction of surrounding skin and/or IDRT with the chamber were identified (Fig. 5a, b). Histologically, the Integra demonstrated the expected and well-documented architecture of a neodermis 3 weeks post implantation [6, 7] (Fig. 5c).

Cultured dermo-epidermal skin substitutes showed a take (determined also 1 week after transplantation) of the dermal part of nearly 100%, whereas the epidermal coverage was estimated between 50 and 60% (Fig. 6a). Histologically (3 weeks post transplantation), the dermal compartment demonstrated the well-known features characterising a neodermis while the epidermis was well established and correctly stratified in some areas (Fig. 6b), whereas in other areas, it was missing.

Discussion

The study reported here provides compelling evidence that we have established a valid pig model that allows transplantation of large autologous skin analogues and also warrants the site of operation be kept undisturbed for at least 3 weeks after transplantation. The following pivotal profile properties of this large animal model deserve to be addressed in more detail.

First, the model permits transplantation of sizeable grafts measuring 7 9 7 cm. This size is suitable for large scale transplantation as it equals for instance the usual size of commercially available cultured epidermal autografts for clinical use [8]. Also, it has similar dimensions as conventional split thickness skin grafts applied on human patients, especially on children [9].

Second, autologous transplantation as performed in this experiment parallels the future clinical situation where, obviously, only autologous skin analogue-coverage of full-thickness skin defects can potentially provide definitive repair in human patients.

Third, the silicone chamber insertion was done for scientific reasons alone: we wanted, particularly in view of the future experiments, to explicitly and reliably shield the area of interest from any (even partial) false-positive results through healing from the wound edges. Overall, the chamber seems to be a valid device in that its handling proved to be easy, and it granted the wanted strict compartmentalisation of the operation field from the surrounding skin. Moreover, there were no macroscopically detectable adverse effects, in particular impaired healing, coming from the chamber itself. Of note, IDRT healed in promptly and uneventfully as was to be expected, while the much more delicately engineered skin analogues healed with spotty epidermal deficits. The random pattern epidermal lack, however, speaks against a chamber-associated problem as then, the non-epithelialised areas would most likely lay adjacent to the chamber. Yet, the graft healing observed must not be over-interpreted in any direction. The goal of this experiment was the establishment of a large animal/large graft transplantation model, not the in-depth investigation of results after grafting. The latter will be looked at specifically in a next series of formal experiments.

It is noteworthy that our chamber is by far the largest and first rectangular such device ever published. All other chambers used for similar purposes were round in

shaped and had a maximum diameter or 4 cm [10–12]. In terms of an outlook, we figure that the size of this chamber can easily be enlarged, or, alternatively, two or more adjacent chambers could be jointly used in the same animal if large enough.

Fourth, an obligatory requirement of the model is maximum graft protection for the first postoperative weeks, when the graft is most vulnerable, and when the animal is presumably most annoyed and therefore prone to get rid of the irritation in any way possible. Therefore, we chose the back as operation site since the animal cannot reach this area with mouth or extremities. Also, rubbing is, even though not entirely impossible, rather challenging. Clearly, adequate pain management and individual housing, the combination of a closed-up chamber, and a sophisticated overlying shock-absorbing dressing proved effective in all animals alike. This aspect cannot be overemphasised since all envisioned future experiments rely on long-term observation (up to 6–12 months), so grafts must definitely survive the initial phase until, when stable enough, they can eventually be left without dressing.

Finally, pig skin is the closest relative with regard to human skin in terms of anatomy and physiology [13, 14]. Therefore, a pig model as the one presented here appears to be the most appropriate choice for a preclinical setting in view of future skin analogue transplantations in human patients.

In conclusion, we devised a practicable new pig model allowing transplantation of large autologous, laboratory-engineered skin analogues and that, importantly, allows keeping the site of intervention clean and intact for the first three postoperative weeks. This model appears suitable to reliably conduct those experiments that will investigate in detail whether large tissue-engineered skin analogues can consistently reconstitute near-normal skin also in the long run. If so, this strategy may eventually be introduced into clinical practice.

Acknowledgments

This work was financially supported by EU-FP6 project EuroSTEC (soft tissue engineering for congenital birth defects in children: contract: LSHB-CT-2006-037409) and by the University of Zurich. We are particularly grateful to the Foundation Gaydoul and the sponsors of ‘‘DonaTissue’’ (Thérèse Meier, Robert Zingg, the Vontobel Foundation, and the Werner Spross Foundation) for their generous financial support and interest in our work. We thank Edy Meyer from BalgristTec AG for his precious help with the animal garments.

Figures

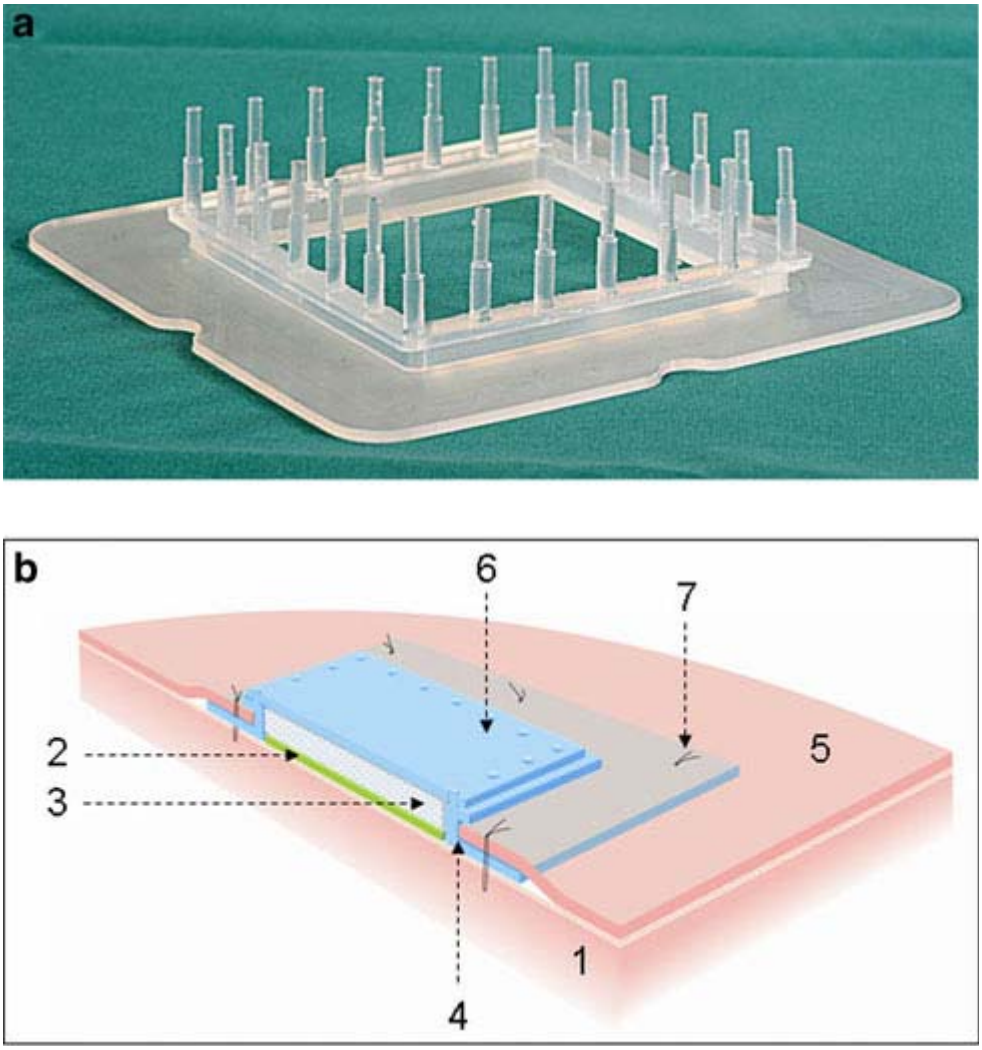

Fig. 1: Silicone chamber. **a** Silicone chamber designed to prevent spontaneous healing from the surrounding skin. The area inside the chamber measures 7x7 cm. **b** Schematic drawing showing the organisation of the wound area with the implanted silicone chamber: *1)* muscle including overlying fascia, *2)* skin analogue, *3)* soft silver foam, *4)* silicone chamber, *5)* pig skin, *6)* 2 mm thick silicone cover plate to close the chamber, *7)* Fixation sutures

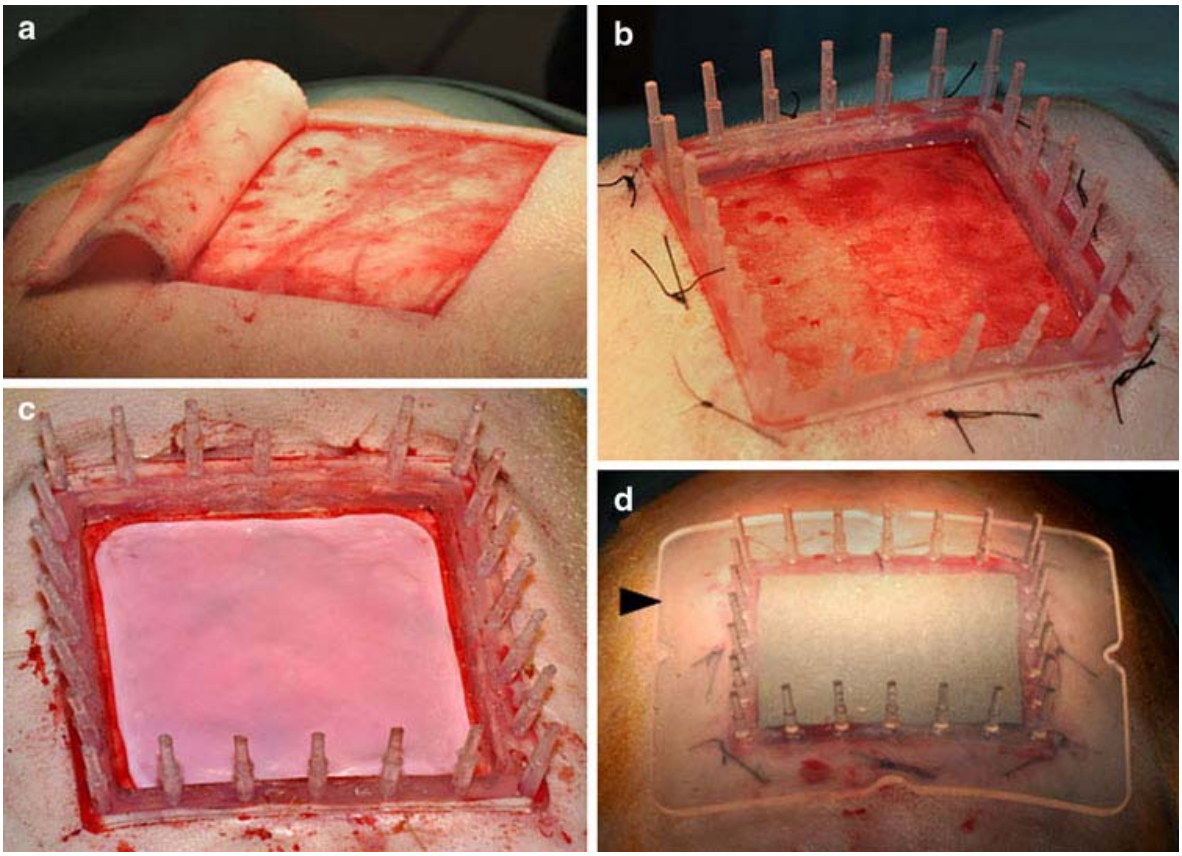

Fig. 2: Surgical procedure of skin substitute transplantation. **a** A full-thickness skin defect of 7.5x7.5 cm, located over the lumbar area is created. **b** The silicone chamber is implanted and secured by fixation sutures. **c** The cultured skin substitute is transplanted onto the full-thickness wound. **d** The wound is covered with soft silver foam (grey) and a 2-mm-thick silicone cover plate (*arrowhead*)

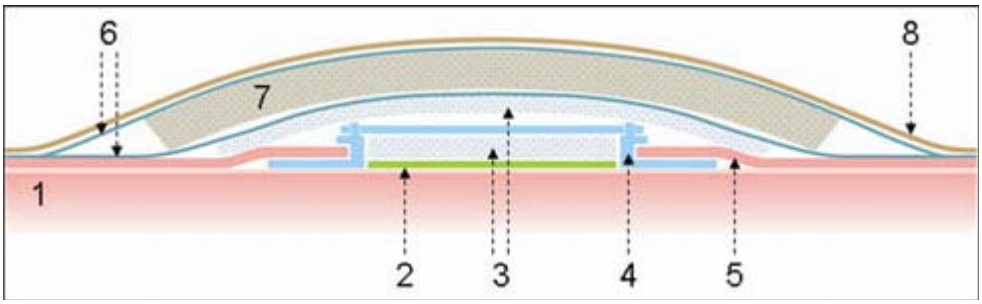

Fig. 3: Multilayered shock absorber device. Schematic drawing showing the architecture of the device: 1 muscle including overlying fascia, 2 skin analogue, 3 soft silver foam, 4 silicone chamber, 5 pig skin, 6 fixation tapes encasing the foam, 7 foam, 8 customized garment

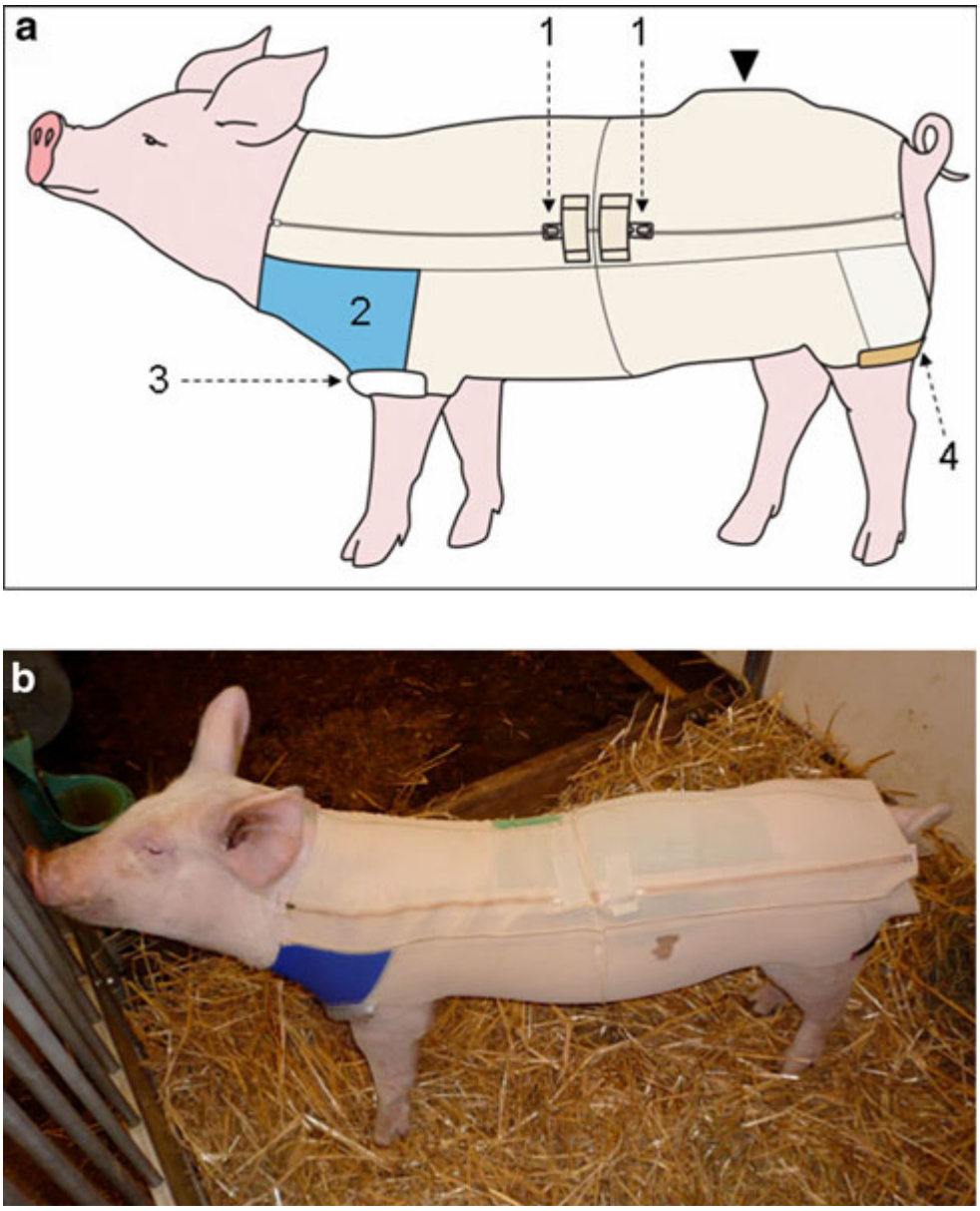

Fig. 4: Customized garment. **a** Schematic drawing of the customized garment for pigs, indicating the essential features: *1)* two separate zippers, *2)* neoprene insertion, *3)* border of lambskin upholstery, *4)* elastic fabric strip. *Arrowhead* indicates location of shock absorber device under garment. **b** Picture showing the ‘‘custom-made’’ garment on a pig

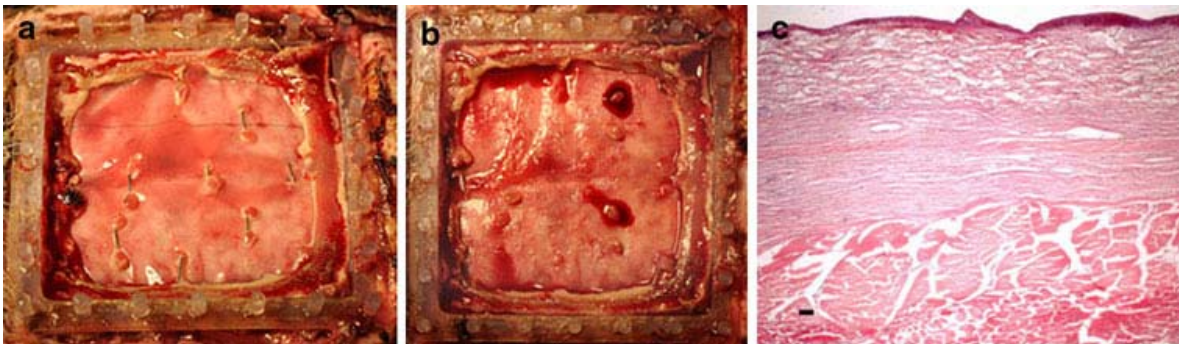

Fig. 5: Dermal substitute integra (IDRT) 3 weeks after transplantation. **a** Macroscopic view of the transplanted IDRT in place. **b** Macroscopic view of an IDRT-derived neodermis, silicone foil already removed. **c** Haematoxylin and Eosin staining of the excised IDRT (scale bar 100 µm)

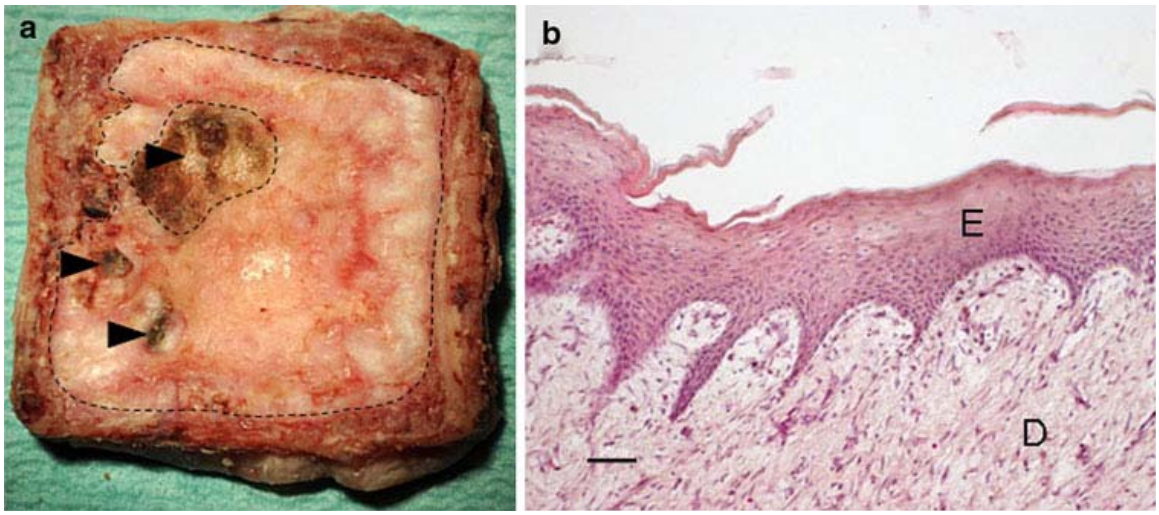

Fig. 6: Laboratory-grown skin substitute 3 weeks after transplantation. **a** Macroscopic view of the excised skin substitute. *Dotted line* indicates epithelialised area. *Arrowheads* indicate locations of previously taken punch biopsies. **b** Haematoxylin and Eosin staining of the excised skin substitute with close to normal epidermis (E) and dermis (D) (scale bar 50 µm)

References

1. Braziulis E, Biedermann T, Hartmann-Fritsch F, Schiestl C, Pontiggia L, Böttcher S, Reichmann E, Meuli M (2010) Skingineering I: engineering porcine dermo-epidermal skin analogues for autologous transplantation in a large animal model. PediatrSurgInt (intended to be published in same issue as this paper)

2. Pontiggia L, Biedermann T, Meuli M, Widmer D, Böttcher-Haberzeth S, Schiestl C, Schneider J, Braziulis E, Montaño, Meuli-Simmen C, Reichmann E (2009) Markers to evaluate the quality and self-renewing potential of engineered human skin substitutes in vitro and after transplantation. J Invest Dermatol 129(2):480–490

3. Tharakan S, Pontiggia L, Biedermann T, Böttcher-Haberzeth S, Schiestl C, Reichmann E, Meuli M (2010) Transglutaminases, involucrin, and loricrin as markers of epidermal differentiation in skin substitutes derived from human sweat gland cells. PediatrSurgInt 26(1):71–77

4. Biedermann T, Pontiggia L, Böttcher-Haberzeth S, Tharakan S, Braziulis E, Schiestl C, Meuli M, Reichmann E (2010) Human eccrine sweat gland cells can reconstitute a stratified epidermis. J Invest Dermatol 130(8):1996–2009

5. Melendez MM, Martinez RR, Dagum AB, McClain SA, Simon M, Sobanko J, Zimmerman T, Wetterau M, Muller D, Xu X, Singer AJ, Arora B (2008) Porcine wound healing in full-thickness skin defects using Integra with and without fibrin glue with keratinocytes. Can J PlastSurg 16(3):147–152

6. Moiemen NS, Staiano JJ, Ojeh NO, Thway Y, Frame JD (2001) Reconstructive surgery with Integra dermal regeneration template: histologic study, clinical evaluation, and current practice. PlastReconstrSurg 108(1):93–103

7. Stern R, McPherson M, LongakerMT (1990) Histologic study of artificial skin used in the treatment of full-thickness thermal injury. J Burn Care Rehabil 11(1):7–13

8. Böttcher-Haberzeth S, Biedermann T, Reichmann E (2010) Tissue engineering of skin. Burns 36(4):450–460

9. Lochühler H, Meuli M (1992) Current concepts in pediatric burn care: surgery of severe burns. Eur J PediatrSurg 2(4):201–204

10. Hinrichsen N, Birk-Sørensen L, Gottrup F, Hjortdal V (1998) Wound contraction in an experimental porcine model. Scand J PlastReconstrSurg Hand Surg 32(3):243–248

11. Grant I, Warwick K, Marshall J, Green C, Martin R (2002) The co-application of sprayed cultured autologous keratinocytes and autologous fibrin sealant in a porcine wound model. Br J PlastSurg 55(3):219–227

12. Shevchenko RV, Sibbons PD, Sharpe JR, James SE (2008) Use of a novel porcine collagen paste as a dermal substitute in fullthickness wounds. Wound Repair Regen 16(2):198–207

13. Sullivan TP, Eaglstein WH, DavisSC, Mertz P (2001) The pig as a model for human wound healing. Wound Repair Regen 9(2): 66–76

14. Zhu KQ, Carrougher GJ, Gibran NS, Isik FF, Engrav LH (2007) Review of the female Duroc/Yorkshire pig model of human fibroproliferative scarring. Wound Repair Regen 15(Suppl 1): S32–S39

5. CONCLUSIONS

In the first publication presented in this work (182) I showed the successful combination of collagen type I hydrogels and biodegradable meshes to generate dermo-epidermal skin substitutes. Several aspects deserve a detailed comment. Both mesh types that were tested in this study did not hamper the survival and proliferation of the dermal fibroblasts and epidermal keratinocytes, neither *in vitro* nor *in vivo* after the transplantation of the skin substitutes onto the back of immuno-incompetent rats. *In vivo*, a continuous basement membrane was deposited and several suprabasal layers and a stratum corneum were detectable. In addition, ingrown blood vessels were observed, ensuring nutrients supply for the skin graft. The handling properties of the mesh-reinforced hydrogels were markedly better than the handling of non-reinforced hydrogels. This might be an important advantage for clinical application. The mesh-reinforced skin substitutes show high potential for the treatment of severe full-thickness skin injuries.

Further studies could evaluate a mesh similar to the knitted mesh but with decreased fibre thickness. The mesh tested in this study showed a relatively high total fibre volume, which probably could be reduced for skin reconstruction. Moreover, it has been shown that resorption of the fibres of the knitted mesh is reached after 36 months (183). For the application in skin reconstruction, it might be interesting to test the incorporation of a modified version of the knitted mesh with a lower fraction of lactide, which would reduce the degradation time. Another point to address in subsequent studies is the behaviour of skin substitutes with the incorporated meshes in long-term experiments. As the process of wound healing and subsequent remodelling of the newly formed tissue takes several months up to years (96-99), it would be advantageous to study the *in vivo* degradation of the meshes over a long period and to evaluate the quality of the new skin tissue after this time.

Another aspect was addressed in the second publication of this work (184), in which I could show that human amniotic fluid derived cells can substitute for fibroblasts and support epidermal growth and stratification in a dermo-epidermal skin substitute. This represents the first step towards engineered fetal skin, but without the need for harvesting an actual skin biopsy of the fetus. The approach for

engineering fetal skin from cells obtained from the amniotic fluid is very appealing, as the amniotic fluid is an easily accessible cell source already during pregnancy and not only after birth. The human amniocytes integrated into a collagen type I hydrogel, instead of the usually used human dermal fibroblasts, were able to substitute for fibroblast function with regard to proliferation and differentiation of the epidermis. Interestingly, this finding was especially highlighted as skin substitutes with an acellular dermal compartment showed poor epidermis survival. This result reinforces the need for a mesenchymal compartment that supports the survival, proliferation and differentiation of the epidermal keratinocytes and the importance of the cross-talk between mesenchyme and epithelium (71,143,185-186).

After this successful first step towards engineered fetal skin, the next step will be to also include fetal keratinocytes. One possibility would be to differentiate amniocytes into an epithelial lineage. Alternatively, one could think about isolating fetal keratinocytes directly from the human amniotic fluid. If this could be achieved, a truly fetal skin analogue could be generated. In addition to the application of a fetal engineered skin for the closure of a fetal spina bifida defect, engineered fetal skin might also have a potential in the autologous treatment of chronic wounds, as it has been shown that fetal skin has an increased wound healing power to adult skin and that human amniocytes remain viable and functional over decades of cryopreservation (187-188).

Tissue engineering of a dermo-epidermal skin substitute not only has great potential and importance in the direct treatment of full-thickness skin injuries; an engineered dermo-epidermal skin analogue also has potential applications in the pre-clinical field. This aspect I investigated in publication III of this thesis (189). The development of new medicinal products for the treatment of skin defects requires intensive pre-clinical testing. To mimic the clinical application of products designed for dermal regeneration as close as possible (100,119,190), we established a model that imitates human split-thickness skin and allows for the pre-clinical testing in a humanised animal model. The engineered grafts showed very similar characteristics and behaviour as human split-thickness skin. One clear difference to split-thickness skin was observed regarding the presence of rete ridges in the original human split-thickness skin, whereas the engineered grafts showed a more flattened dermo-epidermal junction. The advantage of this new model is its preparation method and

easy availability. The preparation can be standardised with regard to cell number, cell types, and thickness. This represents an advantage over the original split-thickness skin, in which for example the thickness shows high variations even when same settings for the dermatome are used, depending on the age of the patient, body location but also the executing surgeon. With this model, newly designed products for dermal reconstruction can easily be tested in a setting with a human skin substitute, but without the need for human split-thickness skin.

It is a major goal of the TBRU to perform clinical trials for the bio-engineered dermo-epidermal skin substitute denovoSkin and the bio-engineered dermal substitute denovoDerm. For the approval of phase I clinical trials by the federal authorities, sufficient and conclusive pre-clinical data on the two products are essential requirements. Initially, the *in vivo* studies with the product (denovoSkin) were performed in the immuno-incompetent rat model. This model allows the transplantation of round grafts with a diameter of ~3 cm. For additional pre-clinical evaluation, *in vivo* studies on a large animal model, using products exhibiting clinical relevant sizes and shapes and applying them in an autologous context, are required. Therefore we established a new porcine model in which larger square-shaped grafts up of 49 cm^2 (7x7 cm) were transplanted. The corresponding results are presented in this work in publications IV and V (191-192). Several points deserve detailed comments. The pig was chosen as large animal model as it has been shown that the porcine skin is the animal skin with most similarities to human skin (180-181). Pigs are immuno-competent animals, therefore skin substitutes needed to be generated with autologous porcine dermal fibroblasts and epidermal keratinocytes for each individual animal in the experiments. Consequently, protocols for the isolation of dermal fibroblasts and epidermal keratinocytes had to be adapted to the special characteristics of porcine skin, for example the thickness of the skin. Additionally, we found that although porcine skin is thought to be the closest to human skin, the porcine dermal fibroblasts behaved differently in a collagen type I hydrogel than human dermal fibroblasts. The survival and proliferation of the fibroblasts could markedly be increased when fibrin was added to the collagen hydrogel. In the rat model a modified Fusenig chamber was used to prevent ingrowth of rat tissue over the transplanted skin substitute. Similar to this, also for the porcine model a chamber was needed that protects the graft. Only with such a chamber it was possible to

prove that the wound closed because of the skin substitute and not due to wound healing by cells migrating to the wound from the wound borders. The final step for the establishment of the new pig model concerned the appropriate wound dressing for these animals. Therefore a special dressing garment was developed, customised for each animal, to ensure maximal protection for the transplanted skin substitutes. The proof of principle of this newly established model was successful, and in the meanwhile this model also was used for the transplantation of different variations of large, square dermo-epidermal skin substitutes.

The series of publications presented in this work covers different aspects of the bio-engineering of autologous human skin grafts and of their clinical application. In this sense my work has contributed to the applied (translational) side of cell and tissue biology, and to the ultimate goal of developing a complex dermo-epidermal skin graft that closely resembles normal human skin and that can be safely and conveniently applied on severe full thickness skin wounds, by the surgeon.

6. REFERENCES

1. Kanitakis J. (2002). Anatomy, histology and immunohistochemistry of normal human skin. Eur J Dermatol 12:390-9; quiz 400-1.

2. Groeber F, M Holeiter, M Hampel, S Hinderer and K Schenke-Layland. (2011). Skin tissue engineering--in vivo and in vitro applications. Clin Plast Surg 39:33-58.

3. Freinkel RK and DT Woodley. (2001). The biology of the skin. The Parthenon Publishing Group.

4. Cummings B. (2004). Pearson Education Inc.

5. Ishida-Yamamoto A and H Iizuka. (1998). Structural organization of cornified cell envelopes and alterations in inherited skin disorders. Exp Dermatol 7:1-10.

6. Alonso L and E Fuchs. (2003). Stem cells of the skin epithelium. Proc Natl Acad Sci U S A 100 Suppl 1:11830-5.

7. Kanitakis J. (1998). Immunohistochemistry of normal human skin. In: *Diagnostic Immunohistochemistry of the Skin. An illustrated text*. Chapman & Hall Med, London. p 38-51.

8. Girolomoni G, C Caux, S Lebecque, C Dezutter-Dambuyant and P Ricciardi-Castagnoli. (2002). Langerhans cells: still a fundamental paradigm for studying the immunobiology of dendritic cells. Trends Immunol 23:6-8.

9. Lacour JP, D Dubois, A Pisani and JP Ortonne. (1991). Anatomical mapping of Merkel cells in normal human adult epidermis. Br J Dermatol 125:535-42.

10. Bragulla HH and DG Homberger. (2009). Structure and functions of keratin proteins in simple, stratified, keratinized and cornified epithelia. J Anat 214:516-59.

11. Magin TM, P Vijayaraj and RE Leube. (2007). Structural and regulatory functions of keratins. Exp Cell Res 313:2021-32.

12. Vijayaraj P, C Kroger, U Reuter, R Windoffer, RE Leube and TM Magin. (2009). Keratins regulate protein biosynthesis through localization of GLUT1 and -3 upstream of AMP kinase and Raptor. J Cell Biol 187:175-84.

13. Ku NO, DM Toivola, P Strnad and MB Omary. (2010). Cytoskeletal keratin glycosylation protects epithelial tissue from injury. Nat Cell Biol 12:876-85.

14. Moll R, M Divo and L Langbein. (2008). The human keratins: biology and pathology. Histochem Cell Biol 129:705-33.

15. Windoffer R and RE Leube. (1999). Detection of cytokeratin dynamics by time-lapse fluorescence microscopy in living cells. J Cell Sci 112 (Pt 24):4521-34.

16. Kolsch A, R Windoffer, T Wurflinger, T Aach and RE Leube. (2009). The keratin-filament cycle of assembly and disassembly. J Cell Sci 123:2266-72.

17. Windoffer R, M Beil, TM Magin and RE Leube. (2011). Cytoskeleton in motion: the dynamics of keratin intermediate filaments in epithelia. J Cell Biol 194:669-78.

18. Fuchs E. (1995). Keratins and the skin. Annu Rev Cell Dev Biol 11:123-53.

19. Alberts B, A Johnson, J Lewis, M Raff, K Roberts and P Walter. (2004). Molekularbiologie der Zelle. Wiley-VCH.

20. Fuchs E and K Weber. (1994). Intermediate filaments: structure, dynamics, function, and disease. Annu Rev Biochem 63:345-82.

21. Pontiggia L, T Biedermann, M Meuli, D Widmer, S Bottcher-Haberzeth, C Schiestl, J Schneider, E Braziulis, I Montano, C Meuli-Simmen and E Reichmann. (2009). Markers to evaluate the quality and self-renewing potential of engineered human skin substitutes in vitro and after transplantation. J Invest Dermatol 129:480-90.

22. Green KJ and CA Gaudry. (2000). Are desmosomes more than tethers for intermediate filaments? Nat Rev Mol Cell Biol 1:208-16.

23. Drugline. (2012). Drugs Information Online.

24. Tsuruta D, T Hashimoto, KJ Hamill and JC Jones. (2011). Hemidesmosomes and focal contact proteins: functions and cross-talk in keratinocytes, bullous diseases and wound healing. J Dermatol Sci 62:1-7.

25. Fuchs E and C Byrne. (1994). The epidermis: rising to the surface. Curr Opin Genet Dev 4:725-36.

26. Ishida-Yamamoto A, M Simon, M Kishibe, Y Miyauchi, H Takahashi, S Yoshida, TJ O'Brien, G Serre and H Iizuka. (2004). Epidermal lamellar granules transport different cargoes as distinct aggregates. J Invest Dermatol 122:1137-44.

27. McGrath JA, RA Eady and FM Pope. (2004). Rook's Textbook of Dermatology. Blackwell Publishing.

28. Marks R, S Barton and R Marshall. (1983). Aspects of the physiology and pathophysiology of desquamation. Curr Probl Dermatol 11:195-205.

29. Elias PM. (1983). Epidermal lipids, barrier function, and desquamation. J Invest Dermatol 80:44s-9s.

30. Ya-Xian Z, T Suetake and H Tagami. (1999). Number of cell layers of the stratum corneum in normal skin - relationship to the anatomical location on the body, age, sex and physical parameters. Arch Dermatol Res 291:555-9.

31. Wertz PW and B van den Bergh. (1998). The physical, chemical and functional properties of lipids in the skin and other biological barriers. Chem Phys Lipids 91:85-96.

32. Schaefer H and TE Redelmeier. (1996). Skin Barrier: Principles of Percutaneous Absorption. Basel: Karger.

33. Harding CR. (2004). The stratum corneum: structure and function in health and disease. Dermatol Ther 17 Suppl 1:6-15.

34. Chapman SJ and A Walsh. (1990). Desmosomes, corneosomes and desquamation. An ultrastructural study of adult pig epidermis. Arch Dermatol Res 282:304-10.

35. Simon M, N Jonca, M Guerrin, M Haftek, D Bernard, C Caubet, T Egelrud, R Schmidt and G Serre. (2001). Refined characterization of corneodesmosin proteolysis during terminal differentiation of human epidermis and its relationship to desquamation. J Biol Chem 276:20292-9.

36. Watkinson A, C Harding, A Moore and P Coan. (2001). Water modulation of stratum corneum chymotryptic enzyme activity and desquamation. Arch Dermatol Res 293:470-6.

37. Hoath SB and HI Maibach. (2003). Neonatal Skin: Structure and function. Marcel Dekker, New York.

38. Wood F. (2012). Tissue engineering of skin. Clin Plast Surg 39:21-32.

39. Morrison KM, GR Miesegaes, EA Lumpkin and SM Maricich. (2009). Mammalian Merkel cells are descended from the epidermal lineage. Dev Biol 336:76-83.

40. Van Keymeulen A, G Mascre, KK Youseff, I Harel, C Michaux, N De Geest, C Szpalski, Y Achouri, W Bloch, BA Hassan and C Blanpain. (2009). Epidermal progenitors give rise to Merkel cells during embryonic development and adult homeostasis. J Cell Biol 187:91-100.

41. Fuchs E. (1998). Beauty is skin deep: the fascinating biology of the epidermis and its appendages. Harvey Lect 94:47-77.

42. Coolen NA, KC Schouten, E Middelkoop and MM Ulrich. (2010). Comparison between human fetal and adult skin. Arch Dermatol Res 302:47-55.

43. Cormack DH. (1987). The integumentary system. In: *Ham's Histology*.

44. Sorrell JM and AI Caplan. (2004). Fibroblast heterogeneity: more than skin deep. J Cell Sci 117:667-75.

45. Sorrell JM, MA Baber and AI Caplan. (2004). Site-matched papillary and reticular human dermal fibroblasts differ in their release of specific growth factors/cytokines and in their interaction with keratinocytes. J Cell Physiol 200:134-45.

46. Bruckner P. Suprastructures of extracellular matrices: paradigms of functions controlled by aggregates rather than molecules. Cell Tissue Res 339:7-18.

47. Ingber DE. (2003). Tensegrity I. Cell structure and hierarchical systems biology. J Cell Sci 116:1157-73.

48. Lee CH, A Singla and Y Lee. (2001). Biomedical applications of collagen. Int J Pharm 221:1-22.

49. Kolacna L, J Bakesova, F Varga, E Kostakova, L Planka, A Necas, D Lukas, E Amler and V Pelouch. (2007). Biochemical and biophysical aspects of collagen nanostructure in the extracellular matrix. Physiol Res 56 Suppl 1:S51-60.

50. Smith LT, KA Holbrook and JA Madri. (1986). Collagen types I, III, and V in human embryonic and fetal skin. Am J Anat 175:507-21.

51. Wong T, JA McGrath and H Navsaria. (2007). The role of fibroblasts in tissue engineering and regeneration. Br J Dermatol 156:1149-55.

52. Chipev CC and M Simon. (2002). Phenotypic differences between dermal fibroblasts from different body sites determine their responses to tension and TGFbeta1. BMC Dermatol 2:13.

53. Schafer IA, M Pandy, R Ferguson and BR Davis. (1985). Comparative observation of fibroblasts derived from the papillary and reticular dermis of infants and adults: growth kinetics, packing density at confluence and surface morphology. Mech Ageing Dev 31:275-93.

54. Sorrell JM, DA Carrino, MA Baber and AI Caplan. (1999). Versican in human fetal skin development. Anat Embryol (Berl) 199:45-56.

55. Moulin V, FA Auger, D Garrel and L Germain. (2000). Role of wound healing myofibroblasts on re-epithelialization of human skin. Burns 26:3-12.

56. Eyden B. (2001). The myofibroblast: an assessment of controversial issues and a definition useful in diagnosis and research. Ultrastruct Pathol 25:39-50.

57. Rubin JS, DP Bottaro, M Chedid, T Miki, D Ron, G Cheon, WG Taylor, E Fortney, H Sakata, PW Finch and et al. (1995). Keratinocyte growth factor. Cell Biol Int 19:399-411.

58. Werner S. (1998). Keratinocyte growth factor: a unique player in epithelial repair processes. Cytokine Growth Factor Rev 9:153-65.

59. Andreadis ST, KE Hamoen, ML Yarmush and JR Morgan. (2001). Keratinocyte growth factor induces hyperproliferation and delays differentiation in a skin equivalent model system. Faseb J 15:898-906.

60. Werner S and H Smola. (2001). Paracrine regulation of keratinocyte proliferation and differentiation. Trends Cell Biol 11:143-6.

61. Waelti ER, SP Inaebnit, HP Rast, T Hunziker, A Limat, LR Braathen and U Wiesmann. (1992). Co-culture of human keratinocytes on post-mitotic human dermal fibroblast feeder cells: production of large amounts of interleukin 6. J Invest Dermatol 98:805-8.

62. Breuhahn K, A Mann, G Muller, A Wilhelmi, P Schirmacher, A Enk and M Blessing. (2000). Epidermal overexpression of granulocyte-macrophage colony-stimulating factor induces both keratinocyte proliferation and apoptosis. Cell Growth Differ 11:111-21.

63. Rubin JS, DP Bottaro and SA Aaronson. (1993). Hepatocyte growth factor/scatter factor and its receptor, the c-met proto-oncogene product. Biochim Biophys Acta 1155:357-71.

64. Aumailley M and P Rousselle. (1999). Laminins of the dermo-epidermal junction. Matrix Biol 18:19-28.

65. Marinkovich MP, DR Keene, CS Rimberg and RE Burgeson. (1993). Cellular origin of the dermal-epidermal basement membrane. Dev Dyn 197:255-67.

66. Smola H, HJ Stark, G Thiekotter, N Mirancea, T Krieg and NE Fusenig. (1998). Dynamics of basement membrane formation by keratinocyte-fibroblast interactions in organotypic skin culture. Exp Cell Res 239:399-410.

67. Ghohestani RF, K Li, P Rousselle and J Uitto. (2001). Molecular organization of the cutaneous basement membrane zone. Clin Dermatol 19:551-62.

68. Breitkreutz D, N Mirancea and R Nischt. (2009). Basement membranes in skin: unique matrix structures with diverse functions? Histochem Cell Biol 132:1-10.

69. Masunaga T. (2006). Epidermal basement membrane: its molecular organization and blistering disorders. Connect Tissue Res 47:55-66.

70. Krieg T and M Aumailley. (2011). The extracellular matrix of the dermis: flexible structures with dynamic functions. Exp Dermatol 20:689-95.

71. Botchkarev VA and J Kishimoto. (2003). Molecular control of epithelial-mesenchymal interactions during hair follicle cycling. J Investig Dermatol Symp Proc 8:46-55.

72. Fuchs E and JA Nowak. (2008). Building epithelial tissues from skin stem cells. Cold Spring Harb Symp Quant Biol 73:333-50.

73. Gat U, R DasGupta, L Degenstein and E Fuchs. (1998). De Novo hair follicle morphogenesis and hair tumors in mice expressing a truncated beta-catenin in skin. Cell 95:605-14.

74. Hardy MH. (1992). The secret life of the hair follicle. Trends Genet 8:55-61.

75. Fuchs E. (2007). Scratching the surface of skin development. Nature 445:834-42.

76. Lyle S, M Christofidou-Solomidou, Y Liu, DE Elder, S Albelda and G Cotsarelis. (1998). The C8/144B monoclonal antibody recognizes cytokeratin 15 and defines the location of human hair follicle stem cells. J Cell Sci 111 (Pt 21):3179-88.

77. Weedon D and G Strutton. (1981). Apoptosis as the mechanism of the involution of hair follicles in catagen transformation. Acta Derm Venereol 61:335-9.

78. Cotsarelis G, TT Sun and RM Lavker. (1990). Label-retaining cells reside in the bulge area of pilosebaceous unit: implications for follicular stem cells, hair cycle, and skin carcinogenesis. Cell 61:1329-37.

79. Morris RJ, Y Liu, L Marles, Z Yang, C Trempus, S Li, JS Lin, JA Sawicki and G Cotsarelis. (2004). Capturing and profiling adult hair follicle stem cells. Nat Biotechnol 22:411-7.

80. Ohyama M, A Terunuma, CL Tock, MF Radonovich, CA Pise-Masison, SB Hopping, JN Brady, MC Udey and JC Vogel. (2006). Characterization and isolation of stem cell-enriched human hair follicle bulge cells. J Clin Invest 116:249-60.

81. Blanpain C, WE Lowry, A Geoghegan, L Polak and E Fuchs. (2004). Self-renewal, multipotency, and the existence of two cell populations within an epithelial stem cell niche. Cell 118:635-48.

82. Lavker RM, S Miller, C Wilson, G Cotsarelis, ZG Wei, JS Yang and TT Sun. (1993). Hair follicle stem cells: their location, role in hair cycle, and involvement in skin tumor formation. J Invest Dermatol 101:16S-26S.

83. Levy V, C Lindon, Y Zheng, BD Harfe and BA Morgan. (2007). Epidermal stem cells arise from the hair follicle after wounding. Faseb J 21:1358-66.

84. Tumbar T, G Guasch, V Greco, C Blanpain, WE Lowry, M Rendl and E Fuchs. (2004). Defining the epithelial stem cell niche in skin. Science 303:359-63.

85. Shibasaki M and CG Crandall. (2010). Mechanisms and controllers of eccrine sweating in humans. Front Biosci (Schol Ed) 2:685-96.

86. Groscurth P. (2002). Anatomy of sweat glands. Curr Probl Dermatol 30:1-9.

87. Barrandon Y. (2003). Developmental biology: A hairy situation. Nature 422:272-3.

88. Biedermann T, L Pontiggia, S Bottcher-Haberzeth, S Tharakan, E Braziulis, C Schiestl, M Meuli and E Reichmann. (2010). Human eccrine sweat gland cells can reconstitute a stratified epidermis. J Invest Dermatol 130:1996-2009.

89. Böttcher-Haberzeth S, T Biedermann, L Pontiggia, E Braziulis, C Schiestl, B Hendriks, OM Eichhoff, DS Widmer, C Meuli-Simmen, M Meuli and E Reichmann. (2013). Human Eccrine Sweat Gland Cells Turn Into Melanin-Uptaking Keratinocytes In Dermo-Epidermal Skin Substitutes. J Invest Dermatol 133:316-24

90. P&G. (2007-2012). Special Skin Structures. P&G.

91. Beise U. (2009). Verbrennungen und Verbrühungen. ARS Medici 22.

92. Enoch S, A Roshan and M Shah. (2009). Emergency and early management of burns and scalds. Bmj 338:b1037.

93. Tumbar T. (2006). Epithelial skin stem cells. Methods Enzymol 419:73-99.

94. Shevchenko RV, SL James and SE James. (2010). A review of tissue-engineered skin bioconstructs available for skin reconstruction. J R Soc Interface 7:229-58.

95. Martin P. (1997). Wound healing--aiming for perfect skin regeneration. Science 276:75-81.

96. Gurtner GC, S Werner, Y Barrandon and MT Longaker. (2008). Wound repair and regeneration. Nature 453:314-21.

97. Priya SG, H Jungvid and A Kumar. (2008). Skin tissue engineering for tissue repair and regeneration. Tissue Eng Part B Rev 14:105-18.

98. Midwood KS, LV Williams and JE Schwarzbauer. (2004). Tissue repair and the dynamics of the extracellular matrix. Int J Biochem Cell Biol 36:1031-7.

99. Seifert AW, JR Monaghan, SR Voss and M Maden. (2012). Skin regeneration in adult axolotls: a blueprint for scar-free healing in vertebrates. PLoS One 7:e32875.

100. Stiefel D, C Schiestl and M Meuli. (2010). Integra Artificial Skin for burn scar revision in adolescents and children. Burns 36:114-20.

101. Tomasek JJ, G Gabbiani, B Hinz, C Chaponnier and RA Brown. (2002). Myofibroblasts and mechano-regulation of connective tissue remodelling. Nat Rev Mol Cell Biol 3:349-63.

102. Brockes JP, A Kumar and CP Velloso. (2001). Regeneration as an evolutionary variable. J Anat 199:3-11.

103. Ferguson MW, DJ Whitby, M Shah, J Armstrong, JW Siebert and MT Longaker. (1996). Scar formation: the spectral nature of fetal and adult wound repair. Plast Reconstr Surg 97:854-60.

104. Mast BA, RF Diegelmann, TM Krummel and IK Cohen. (1992). Scarless wound healing in the mammalian fetus. Surg Gynecol Obstet 174:441-51.

105. Larson BJ, MT Longaker and HP Lorenz. (2010). Scarless fetal wound healing: a basic science review. Plast Reconstr Surg 126:1172-80.

106. Herndon DN, RE Barrow, RL Rutan, TC Rutan, MH Desai and S Abston. (1989). A comparison of conservative versus early excision. Therapies in severely burned patients. Ann Surg 209:547-52; discussion 552-3.

107. Schiestl C, D Stiefel and M Meuli. (2010). Giant naevus, giant excision, eleg(i)ant closure? Reconstructive surgery with Integra Artificial Skin to treat giant congenital melanocytic naevi in children. J Plast Reconstr Aesthet Surg 63:610-5.

108. Meuli M and M Raghunath. (1997). Burns (Part 2). Tops and flops using cultured epithelial autografts in children. Pediatr Surg Int 12:471-7.

109. Gobet R, M Raghunath, S Altermatt, C Meuli-Simmen, M Benathan, A Dietl and M Meuli. (1997). Efficacy of cultured epithelial autografts in pediatric burns and reconstructive surgery. Surgery 121:654-61.

110. Andreassi A, R Bilenchi, M Biagioli and C D'Aniello. (2005). Classification and pathophysiology of skin grafts. Clin Dermatol 23:332-7.

111. Stanton RA and DA Billmire. (2002). Skin resurfacing for the burned patient. Clin Plast Surg 29:29-51.

112. Supp DM and ST Boyce. (2005). Engineered skin substitutes: practices and potentials. Clin Dermatol 23:403-12.

113. Bottcher-Haberzeth S, T Biedermann and E Reichmann. (2010). Tissue engineering of skin. Burns 36:450-60.

114. Bottcher-Haberzeth S, S Kapoor, M Meuli, K Neuhaus, T Biedermann, E Reichmann and C Schiestl. Osmotic expanders in children: no filling--no control--no problem? Eur J Pediatr Surg 21:163-7.

115. Wood FM and SB McMahon. (1989). The response of the peripheral nerve field to controlled soft tissue expansion. Br J Plast Surg 42:682-6.

116. Cervelli V, L Lucarini, C Cerretani, D Spallone, L Palla, L Brinci and B De Angelis. (2011). The use of Matriderm and autologous skin grafting in the treatment of diabetic ulcers: a case report. Int Wound J 7:291-6.

117. Branski LK, DN Herndon, C Pereira, RP Mlcak, MM Celis, JO Lee, AP Sanford, WB Norbury, XJ Zhang and MG Jeschke. (2007). Longitudinal assessment of Integra in primary burn management: a randomized pediatric clinical trial. Crit Care Med 35:2615-23.

118. Heitland A, A Piatkowski, EM Noah and N Pallua. (2004). Update on the use of collagen/glycosaminoglycate skin substitute-six years of experiences with artificial skin in 15 German burn centers. Burns 30:471-5.

119. Stiefel D, CM Schiestl and M Meuli. (2009). The positive effect of negative pressure: vacuum-assisted fixation of Integra artificial skin for reconstructive surgery. J Pediatr Surg 44:575-80.

120. Bottcher-Haberzeth S, T Biedermann, C Schiestl, F Hartmann-Fritsch, J Schneider, E Reichmann and M Meuli. (2012). Matriderm((R)) 1 mm versus Integra((R)) Single Layer 1.3 mm for one-step closure of full thickness skin defects: a comparative experimental study in rats. Pediatr Surg Int. 28:171-7.

121. Haslik W, LP Kamolz, G Nathschlager, H Andel, G Meissl and M Frey. (2007). First experiences with the collagen-elastin matrix Matriderm as a dermal substitute in severe burn injuries of the hand. Burns 33:364-8.

122. Keck M, D Haluza, DB Lumenta, S Burjak, B Eisenbock, LP Kamolz and M Frey. Construction of a multi-layer skin substitute: Simultaneous cultivation of keratinocytes and preadipocytes on a dermal template. Burns 37:626-30.

123. Schneider J, T Biedermann, D Widmer, I Montano, M Meuli, E Reichmann and C Schiestl. (2009). Matriderm versus Integra: a comparative experimental study. Burns 35:51-7.

124. Shakespeare PG. (2005). The role of skin substitutes in the treatment of burn injuries. Clin Dermatol 23:413-8.

125. Cervelli V, L Brinci, D Spallone, E Tati, L Palla, L Lucarini and B De Angelis. (2011). The use of MatriDerm(R) and skin grafting in post-traumatic wounds. Int Wound J 8:400-5.

126. Kearney JN. (2001). Clinical evaluation of skin substitutes. Burns 27:545-51.

127. Hansen SL, DW Voigt, P Wiebelhaus and CN Paul. (2001). Using skin replacement products to treat burns and wounds. Adv Skin Wound Care 14:37-44; quiz 45-6.

128. Abai B, D Thayer and PM Glat. (2004). The use of a dermal regeneration template (Integra) for acute resurfacing and reconstruction of defects created by excision of giant hairy nevi. Plast Reconstr Surg 114:162-8.

129. Burke JF, IV Yannas, WC Quinby, Jr., CC Bondoc and WK Jung. (1981). Successful use of a physiologically acceptable artificial skin in the treatment of extensive burn injury. Ann Surg 194:413-28.

130. Soejima K, M Nozaki, K Sasaki, M Takeuchi and N Negishi. (1997). Reconstruction of burn deformity using artificial dermis combined with thin split-skin grafting. Burns 23:501-4.

131. van Zuijlen PP, AJ van Trier, JF Vloemans, F Groenevelt, RW Kreis and E Middelkoop. (2000). Graft survival and effectiveness of dermal substitution in burns and reconstructive surgery in a one-stage grafting model. Plast Reconstr Surg. 106:615-23.

132. Huang L, K Nagapudi, RP Apkarian and EL Chaikof. (2001). Engineered collagen-PEO nanofibers and fabrics. J Biomater Sci Polym Ed 12:979-93.

133. Clark RA, K Ghosh and MG Tonnesen. (2007). Tissue engineering for cutaneous wounds. J Invest Dermatol 127:1018-29.

134. Griffiths M, N Ojeh, R Livingstone, R Price and H Navsaria. (2004). Survival of Apligraf in acute human wounds. Tissue Eng 10:1180-95.

135. Apligraf. (2012). apligraf.com/patient/what_is_apligraf/how_is_apligraf_applied.html.

136. Integra. (2012). ilstraining.com/idrt/idrt/brs_it_01.html.

137. Matriderm. (2012). ideal-ms.com/healthcare-matriderm/.

138. Nerem RM. (1992). Tissue engineering in the USA. Med Biol Eng Comput. 30:CE8-12.

139. Bell E. (2000). Tissue engineering in perspective. In: *Principles of tissue enigeering*. San Diego: Academic Press.

140. Schmidt D, A Mol, JM Kelm and SP Hoerstrup. (2007). In vitro heart valve tissue engineering. Methods Mol Med. 140:319-30.

141. Guven S, A Mehrkens, F Saxer, DJ Schaefer, R Martinetti, I Martin and A Scherberich. (2011). Engineering of large osteogenic grafts with rapid engraftment capacity using mesenchymal and endothelial progenitors from human adipose tissue. Biomaterials 32:5801-9.

142. Drury JL and DJ Mooney. (2003). Hydrogels for tissue engineering: scaffold design variables and applications. Biomaterials 24:4337-51.

143. Rheinwald JG and H Green. (1975). Serial cultivation of strains of human epidermal keratinocytes: the formation of keratinizing colonies from single cells. Cell 6:331-43.

144. Carsin H, P Ainaud, H Le Bever, J Rives, A Lakhel, J Stephanazzi, F Lambert and J Perrot. (2000). Cultured epithelial autografts in extensive burn coverage of severely traumatized patients: a five year single-center experience with 30 patients. Burns 26:379-87.

145. Cuono C, R Langdon and J McGuire. (1986). Use of cultured epidermal autografts and dermal allografts as skin replacement after burn injury. Lancet 1:1123-4.

146. Hernon CA, RA Dawson, E Freedlander, R Short, DB Haddow, M Brotherston and S MacNeil. (2006). Clinical experience using cultured epithelial autografts leads to an alternative methodology for transferring skin cells from the laboratory to the patient. Regen Med 1:809-21.

147. Munster AM. (1996). Cultured skin for massive burns. A prospective, controlled trial. Ann Surg 224:372-5; discussion 375-7.

148. O'Connor N, JB Mulliken, S Banks-Schlegel, O Kehinde and H Green. (1981). Grafting of burns with cultured epithelium prepared from autologous epidermal cells. Lancet 1:75-8.

149. Ronfard V, JM Rives, Y Neveux, H Carsin and Y Barrandon. (2000). Long-term regeneration of human epidermis on third degree burns transplanted with autologous cultured epithelium grown on a fibrin matrix. Transplantation 70:1588-98.

150. Rue LW, 3rd, WG Cioffi, WF McManus and BA Pruitt, Jr. (1993). Wound closure and outcome in extensively burned patients treated with cultured autologous keratinocytes. J Trauma 34:662-7; discussion 667-8.

151. Wood FM, ML Kolybaba and P Allen. (2006). The use of cultured epithelial autograft in the treatment of major burn wounds: eleven years of clinical experience. Burns 32:538-44.

152. Bell E, HP Ehrlich, DJ Buttle and T Nakatsuji. (1981). Living tissue formed in vitro and accepted as skin-equivalent tissue of full thickness. Science 211:1052-4.

153. Boyce ST, MJ Goretsky, DG Greenhalgh, RJ Kagan, MT Rieman and GD Warden. (1995). Comparative assessment of cultured skin substitutes and native skin autograft for treatment of full-thickness burns. Ann Surg. 222:743-52.

154. Loss M, V Wedler, W Kunzi, C Meuli-Simmen and VE Meyer. (2000). Artificial skin, split-thickness autograft and cultured autologous keratinocytes combined to treat a severe burn injury of 93% of TBSA. Burns 26:644-52.

155. Papini R. (2004). Management of burn injuries of various depths. Bmj 329:158-60.

156. Deitch EA, TM Wheelahan, MP Rose, J Clothier and J Cotter. (1983). Hypertrophic burn scars: analysis of variables. J Trauma 23:895-8.

157. Berman B, MH Viera, S Amini, R Huo and IS Jones. (2008). Prevention and management of hypertrophic scars and keloids after burns in children. J Craniofac Surg 19:989-1006.

158. Falanga V. (1993). Chronic wounds: pathophysiologic and experimental considerations. J Invest Dermatol 100:721-5.

159. Phillips T, B Stanton, A Provan and R Lew. (1994). A study of the impact of leg ulcers on quality of life: financial, social, and psychologic implications. J Am Acad Dermatol 31:49-53.

160. MacNeil S. (2007). Progress and opportunities for tissue-engineered skin. Nature 445:874-80.

161. Yang S, KF Leong, Z Du and CK Chua. (2001). The design of scaffolds for use in tissue engineering. Part I. Traditional factors. Tissue Eng 7:679-89.

162. Ratner BD and SJ Bryant. (2004). Biomaterials: where we have been and where we are going. Annu Rev Biomed Eng 6:41-75.

163. Park JB and RS Lakes. (1992). Biomaterials: an introduction. Plenum Press, New York.

164. Park SN, JC Park, HO Kim, MJ Song and H Suh. (2002). Characterization of porous collagen/hyaluronic acid scaffold modified by 1-ethyl-3-(3-dimethylaminopropyl)carbodiimide cross-linking. Biomaterials 23:1205-12.

165. Lee CR, AJ Grodzinsky and M Spector. (2001). The effects of cross-linking of collagen-glycosaminoglycan scaffolds on compressive stiffness, chondrocyte-mediated contraction, proliferation and biosynthesis. Biomaterials 22:3145-54.

166. Vandenburgh HH, P Karlisch and L Farr. (1988). Maintenance of highly contractile tissue-cultured avian skeletal myotubes in collagen gel. In Vitro Cell Dev Biol 24:166-74.

167. von Heimburg D, S Zachariah, I Heschel, H Kuhling, H Schoof, B Hafemann and N Pallua. (2001). Human preadipocytes seeded on freeze-dried collagen scaffolds investigated in vitro and in vivo. Biomaterials 22:429-38.

168. Nerem RM and D Seliktar. (2001). Vascular tissue engineering. Annu Rev Biomed Eng 3:225-43.

169. Fishman JA. (2001). Infection in xenotransplantation. J Card Surg 16:363-73.

170. Thomson RC, MC Wake and MJ Yaszemski. (1995). Biodegradable polymer scaffolds to regenerate organs. Adv Polym Sci 122:245-74.

171. Makadia HK and SJ Siegel. (2011). Poly Lactic-co-Glycolic Acid (PLGA) as Biodegradable Controlled Drug Delivery Carrier. Polymers (Basel) 3:1377-1397.

172. Jain RA. (2000). The manufacturing techniques of various drug loaded biodegradable poly(lactide-co-glycolide) (PLGA) devices. Biomaterials 21:2475-90.

173. Wu XS. (1995). Synthesis and properties of biodegradable lactic/glycolic acid polymers. In: *Encyclopedic handbook of biomaterials and bioengineering*. Marcel Dekker, New York. p 1151-200.

174. Li WJ, CT Laurencin, EJ Caterson, RS Tuan and FK Ko. (2002). Electrospun nanofibrous structure: a novel scaffold for tissue engineering. J Biomed Mater Res 60:613-21.

175. Sahota PS, JL Burn, M Heaton, E Freedlander, SK Suvarna, NJ Brown and S Mac Neil. (2003). Development of a reconstructed human skin model for angiogenesis. Wound Repair Regen 11:275-84.

176. Braziulis E, M Diezi, T Biedermann, L Pontiggia, M Schmucki, F Hartmann-Fritsch, J Luginbuhl, C Schiestl, M Meuli and E Reichmann. (2012). Modified plastic compression of collagen hydrogels provides an ideal matrix for clinically applicable skin substitutes. Tissue Eng Part C Methods 18:464-74.

177. Brown RA, M Wiseman, CB Chuo, U Cheema and SN Nazhat. (2005). Ultrarapid Engineering of Biomimetic Materials and Tissues: Fabrication of Nano- and Microstructures by Plastic Compression. Adv Funct Mater 15:1762-1770.

178. Reichmann E. (2011). EuroSkinGraft. HEALTH-2011.1.4-1.

179. Kaviani A, TE Perry, A Dzakovic, RW Jennings, MM Ziegler and DO Fauza. (2001). The amniotic fluid as a source of cells for fetal tissue engineering. J Pediatr Surg 36:1662-5.

180. Sullivan TP, WH Eaglstein, SC Davis and P Mertz. (2001). The pig as a model for human wound healing. Wound Repair Regen 9:66-76.

181. Zhu KQ, GJ Carrougher, NS Gibran, FF Isik and LH Engrav. (2007). Review of the female Duroc/Yorkshire pig model of human fibroproliferative scarring. Wound Repair Regen 15 Suppl 1:S32-9.

182. Hartmann-Fritsch F, T Biedermann, E Braziulis, J Luginbuhl, L Pontiggia, S Bottcher-Haberzeth, TH van Kuppevelt, KA Faraj, C Schiestl, M Meuli and E Reichmann. (2012). Collagen hydrogels strengthened by biodegradable meshes are a basis for dermo-epidermal skin grafts intended to reconstitute human skin in a one-step surgical intervention. J Tissue Eng Regen Med.

183. Hjort H, T Mathisen, A Alves, G Clermont and JP Boutrand. (2011). Three-year results from a preclinical implantation study of a long-term resorbable surgical mesh with time-dependent mechanical characteristics. Hernia.

184. Hartmann-Fritsch F, N Hosper, J Luginbuhl, T Biedermann, E Reichmann and M Meuli. (2013). Human amniotic fluid derived cells can competently substitute dermal fibroblasts in a tissue-engineered dermo-epidermal skin analog. Pediatr Surg Int 29:61-9.

185. Leary T, PL Jones, M Appleby, A Blight, K Parkinson and M Stanley. (1992). Epidermal keratinocyte self-renewal is dependent upon dermal integrity. J Invest Dermatol 99:422-30.

186. Schultz GS and A Wysocki. (2009). Interactions between extracellular matrix and growth factors in wound healing. Wound Repair Regen 17:153-62.

187. Yoon BS, JH Moon, EK Jun, J Kim, I Maeng, JS Kim, JH Lee, CS Baik, A Kim, KS Cho, JH Lee, HH Lee, KY Whang and S You. (2010). Secretory profiles and wound healing effects of human amniotic fluid-derived mesenchymal stem cells. Stem Cells Dev 19:887-902.

188. Woodbury D, BC Kramer, K Reynolds, AJ Marcus, TM Coyne and IB Black. (2006). Long-term cryopreserved amniocytes retain proliferative capacity and differentiate to ectodermal and mesodermal derivatives in vitro. Mol Reprod Dev 73:1463-72.

189. Hartmann-Fritsch F, T Biedermann, E Braziulis, M Meuli and E Reichmann. (2013). A new model for preclinical testing of dermal substitutes for human skin reconstruction. Pediatr Surg Int 29:479-88

190. Schiestl C, K Neuhaus, T Biedermann, S Bottcher-Haberzeth, E Reichmann and M Meuli. (2011). Novel treatment for massive lower extremity avulsion injuries in children: slow, but effective with good cosmesis. Eur J Pediatr Surg 21:106-10.

191. Braziulis E, T Biedermann, F Hartmann-Fritsch, C Schiestl, L Pontiggia, S Bottcher-Haberzeth, E Reichmann and M Meuli. (2011). Skingineering I: engineering porcine dermo-epidermal skin analogues for autologous transplantation in a large animal model. Pediatr Surg Int 27:241-7.

192. Schiestl C, T Biedermann, E Braziulis, F Hartmann-Fritsch, S Bottcher-Haberzeth, M Arras, N Cesarovic, F Nicolls, C Linti, E Reichmann and M Meuli. (2011). Skingineering II: transplantation of large-scale laboratory-grown skin analogues in a new pig model. Pediatr Surg Int 27:249-54.

7. ABBREVIATIONS

BSA	Bovine serum albumin
CD	Cluster of differentiation
CK	Cytokeratin
DAPI	4',6-diamidino-2-phenylindole
DMEM	Dulbecco's Modified Eagle Medium
ECM	Extracellular matrix
FCS	Fetal calf serum
FDA	United States Food and Drug Administration
FdA	Fluorescein diacetate
FITC	Fluorescein iso-thiocyanate
GMP	Good manufacturing practice
H&E	Haematoxylin & Eosin
HMB45	Human melanoma black
IDRT	Integra dermal regeneration template®
K	Cytokeratin
KGF-1	Keratinocyte growth factor 1
PBS	Phosphate buffered saline
PLGA	Poly(lactic-*co*-glycolic acid)
TBSA	Total body surface area
TBRU	Tissue Biology Research Unit
TE	Tissue engineering
TRITC	Tetramethyl rhodamine iso-thiocyanate

8. CURRICULUM VITAE

Personal Data

Name	**Fabienne Hartmann-Fritsch**
Date of birth	**7. October 1983**
Place of birth	**Winterthur, ZH**
Citizen of	**Worb, BE**

Education

2008 – 2013	**PhD study** University Zürich, Switzerland Tissue Biology Research Unit, Department of Surgery, University Children's Hospital Zürich, Switzerland
2006 – 2008	**Master of Science ETH in Biology** Swiss Federal Institute of Technology (ETH) Zürich, Switzerland Elective major: Microbiology and Immunology Master thesis: *Characterization of FP-Sial, the sialyltransferase of green sea turtle herpes virus*. Supervision Prof. Dr. M. Ackermann
2002 – 2006	**Bachelor of Science ETH in Biology** Swiss Federal Institute of Technology (ETH) Zürich, Switzerland Elective major: Microbiology and Immunology
1998 – 2002	**Matura, mathematics and science focus** Kantonsschule Im Lee, Winterthur, Switzerland

Presentations and Posters

September 2012	**XXV International Symposium on Pediatric Surgical Research** London, United Kingdom Presentation: *Human amniotic fluid derived cells can competently substitute dermal fibroblasts in a tissue engineered dermo-epidermal skin analog*
September 2012	**XXV International Symposium on Pediatric Surgical Research** London, United Kingdom Presentation: *A new model for preclinical testing of dermal substitutes for human skin reconstruction*
October 2011	**XXXVIII Congress of the European Society for Artificial Organs (ESAO 2011) and IV Biennial Congress of the International Federation on Artificial Organs (IFAO 2011)** Porto, Portugal Poster: *Tissue Engineering of skin - Biodegradable scaffolds incorporated into laboratory grown skin substitutes*

November 2010 **Consortium Meeting European Program on Soft Tissue Engineering for Children (EuroSTEC)**
Berlin, Germany
Presentation: *Establishing an animal model for large skin substitute transplantations*

November 2009 **Consortium Meeting European Program on Soft Tissue Engineering for Children (EuroSTEC)**
Leuven, Belgium
Presentation: *Hydrogels with scaffolds in tissue engineering*

August 2009 **World Congress Tissue Engineering International & Regenerative Medicine Society (TERMIS)**
Seoul, South Korea
Poster: *Monitoring the self-renewing potential in engineered human skin substitutes*

April 2009 **Consortium Meeting European Program on Soft Tissue Engineering for Children (EuroSTEC)**
Groningen, The Netherlands
Presentation: *Combining degradable scaffolds and hydrogels*

Others

2009 – present **External expert examiner for Biology Matura exams**
Kantonsschule Im Lee
Winterthur, Switzerland
Annually, oral and written exams

September 2012 **World Congress Tissue Engineering International & Regenerative Medicine Society (TERMIS)**
Vienna, Austria
Participant

November 2011 **Consortium Meeting European Program on Soft Tissue Engineering for Children (EuroSTEC)**
Amsterdam, The Netherlands
Participant

August 2011 **6th World Congress on Pediatric Burns**
Zürich, Switzerland
Member of the local organising committee

October 2010 **Workshop 2010 European Club for Pediatric Burns**
Rome, Italy
Participant

September 2009 **XXII International Symposium on Pediatric Surgical Research**
Geneva, Italy
Participant

9. PUBLICATIONS

Hartmann-Fritsch F, Biedermann T, Braziulis E, Luginbühl J, Pontiggia L, Böttcher-Haberzeth S, van Kuppevelt TA, Faraj, K, Schiestl C, Meuli M, Reichmann E. Collagen hydrogels strengthened by biodegradable meshes are a basis for dermo-epidermal skin grafts intended to reconstitute human skin in a one-step surgical intervention. Tissue Eng Regen Med. Epub ahead of print, Dec 10. doi: 10.1002/term.1665.

Hartmann-Fritsch F, Hosper NA, Luginbühl J, Biedermann T, Reichmann E, Meuli M. Human amniotic fluid derived cells can competently substitute dermal fibroblasts in a tissue engineered dermo-epidermal skin analog. Pediatr Surg Int. 2013;29(1):61-9

Hartmann-Fritsch F, Biedermann T, Braziulis E, Meuli M, Reichmann E. A new model for preclinical testing of dermal substitutes for human skin reconstruction. Pediatr Surg Int. 2013;29(5):479-488

Ackermann M, Koriabine M, **Hartmann-Fritsch F**, de Jong PJ, Lewis TD, Schetle N, Work TM, Dagenais J, Balazs GH, Leong JAC. The genome of chelonidherpesvirus harbors atypical genes. PLoS One. 2012;7(10):e46623

Braziulis E, Diezi M, Biedermann T, Pontiggia L, Schmucki M, **Hartmann-Fritsch F**, Luginbühl J, Schiestl C, Meuli M, Reichmann E. Modified plastic compression of collagen hydrogels provide an ideal matrix for clinically applicable skin substitutes. Tissue Eng Part C Methods 2012;18(6):464-74

Böttcher-Haberzeth S, Biedermann T, Schiestl C, **Hartmann-Fritsch F**, Schneider J, Reichmann E, Meuli M. Matriderm® 1 mm versus Integra® Single Layer 1.3mm for one-step closure of full-thickness skin defects: a comparative experimental study in rats. Pediatr Surg Int 2012;28(2)

Schiestl C, Biedermann T, Braziulis E, **Hartmann-Fritsch F**, Böttcher-Haberzeth S, Arras M, et al. Skingineering II: transplantation of large-scale laboratory-grown skin analogues in a new pig model. PediatrSurgInt 2010;27(3):249-54.

Braziulis E, Biedermann T, **Hartmann-Fritsch F**, Schiestl C, Pontiggia L, Böttcher-Haberzeth S, et al. Skingineering I: engineering porcine dermo-epidermal skin analogues for autologous transplantation in a large animal model. PediatrSurgInt2011;27(3):241-7.

Schulz BL, Stirnimann CU, Grimshaw JP, Brozzo MS, **Fritsch F**, Mohorko E, et al. Oxidoreductase activity of oligosaccharyltransferase subunits Ost3p and Ost6p defines site-specific glycosylation efficiency. Proc Nat Acad Sci 2009;106(27):11061-6.

10. CONTRIBUTIONS

I contributed to the following publications as indicated:

Publication I:

Collagen hydrogels strengthened by biodegradable meshes are a basis for dermo-epidermal skin grafts intended to reconstitute human skin in a one-step surgical intervention

- Experimental outline
- Performance of experiments
- Figures
- Manuscript writing

Publication II:

Human amniotic fluid derived cells can competently substitute dermal fibroblasts in a tissue engineered dermo-epidermal skin analogue

- Experimental outline
- Performance of experiments
- Figures
- Manuscript writing

Publication III:

A new model for preclinical testing of dermal substitutes for human skin reconstruction

- Experimental outline
- Performance of experiments
- Figures
- Manuscript writing

Publication IV:

Skingineering I: Engineering porcine dermo-epidermal skin analogues for autologous transplantation in a large animal model

- Porcine keratinocyte and fibroblast isolation and cultivation (Figure 1a, c)
- Processing and staining of *in vitro* cultivated graft (Figure 3)

Publication V:

Skingineering II: transplantation of large-scale laboratory-grown skin analogues in a new pig model

- Assistant, surgical procedure of skin substitute transplantation (Figure 2)
- Dermal substitute Integra (IDRT) 3 weeks after transplantation. Processing and staining of transplanted graft (Figure 5)
- Laboratory-grown skin substitute 3 weeks after transplantation. Processing and staining of transplanted graft (Figure 6)
- Arrangement of figures 1-6

11. ACKNOWLEDGEMENTS

I would like to thank Prof. Dr. Ernst Reichmann for giving me the opportunity of doing my PhD studies in his group on such an interesting and fascinating field. Thank you for your support throughout these years.

I would like to thank Prof. Dr. Lukas Sommer for supervising my PhD thesis and Prof. Dr. Reinhard Dummer and Prof. Dr. Martin Hersberger for being committee members for my PhD thesis.

This work was financially supported by the EU-FP6 project EuroSTEC (soft tissue engineering for congenital birth defects in children: contract: LSHB-CT-2006-037409), by the EU-FP7 project EuroSkinGraft (FP7/2007-2013: grant agreement n° 279024), and by the University of Zurich. I am particularly grateful to the Fondation Gaydoul and the sponsors of “DonaTissue” (Thérèse Meier and Robert Zingg) for their generous financial support and interest in my work.

Many thanks to Prof. Dr. Martin Meuli and PD Dr. Clemens Schiestl for their support and providing me with insights into the fascinating field of fetal surgery, plastic and reconstructive surgery, and the treatment of burn injuries.

Great thanks to all present and former members of the TBRU for their tremendous support, scientific help and friendship throughout my PhD studies.

My most profound thanks go to my beloved ones, my family and my friends.